

# IMPLICIT REGULARIZATION AND MOMENTUM ALGORITHMS IN NONLINEAR ADAPTIVE CONTROL AND PREDICTION

**Nicholas M. Boffi**

John A. Paulson School of Engineering and Applied Sciences  
 Harvard University  
 Cambridge, MA 02138  
 boffi@g.harvard.edu

**Jean-Jacques E. Slotine**

Nonlinear Systems Laboratory  
 Massachusetts Institute of Technology  
 Cambridge, MA 02139  
 jjs@mit.edu

## ABSTRACT

Stable concurrent learning and control of dynamical systems is the subject of adaptive control. Despite being an established field with many practical applications and a rich theory, much of the development in adaptive control for nonlinear systems revolves around a few key algorithms. By exploiting strong connections between classical adaptive nonlinear control techniques and recent progress in optimization and machine learning, we show that there exists considerable untapped potential in algorithm development for both adaptive nonlinear control and adaptive dynamics prediction. We first introduce first-order adaptation laws inspired by natural gradient descent and mirror descent. We prove that when there are multiple dynamics consistent with the data, these non-Euclidean adaptation laws implicitly regularize the learned model. Local geometry imposed during learning thus may be used to select parameter vectors – out of the many that will achieve perfect tracking or prediction – for desired properties such as sparsity. We apply this result to regularized dynamics predictor and observer design, and as concrete examples consider Hamiltonian systems, Lagrangian systems, and recurrent neural networks. We subsequently develop a variational formalism based on the Bregman Lagrangian to define adaptation laws with momentum applicable to linearly parameterized systems and to nonlinearly parameterized systems satisfying monotonicity or convexity requirements. We show that the Euler Lagrange equations for the Bregman Lagrangian lead to natural gradient and mirror descent-like adaptation laws with momentum, and we recover their first-order analogues in the infinite friction limit. We illustrate our analyses with simulations demonstrating our theoretical results.

## 1 INTRODUCTION

Adaptation is an online learning problem concerned with control or prediction of the dynamics of an unknown nonlinear system. This task is accomplished by constructing an approximation to the true dynamics through the online adjustment of a vector of parameter estimates under the assumption that there exists a fixed vector of parameters that globally fits the dynamics. The overarching goal is provably safe, stable, and concurrent learning and control of nonlinear dynamical systems.

Adaptive control theory is a mature field, and many results exist tailored to specific system structures (Ioannou and Sun, 2012; Narendra and Annaswamy, 2005; Slotine and Li, 1991). An adaptive control algorithm typically consists of a parameter estimator coupled in feedback to the controlled system, and the parameter estimator is often strongly inspired by gradient-based optimization algorithms. A significant difference between standard optimization algorithms and adaptive control algorithms is that the parameter estimator must not only converge to a set of parameters that leads to perfect tracking of the desired trajectory, but the system must remain stable throughout adaptation. The additional requirement of stability prevents the immediate application of optimization algorithms as adaptive control algorithms, and stability must be proved by jointly analyzing the closed-loop system and estimator.

Significant progress has been made in adaptive control even for nonlinear systems in the *linearly parameterized* setting, where the dynamics approximation is of the form  $\hat{\mathbf{f}} = \mathbf{Y}(\mathbf{x}, t)\hat{\mathbf{a}}$  for some known regressor matrix  $\mathbf{Y}(\mathbf{x}, t)$  and vector of parameter estimates  $\hat{\mathbf{a}}(t)$ . Examples include the adaptive robot trajectory controller of Slotine and Li (1987) and the neural network-based controller of Sanner and Slotine (1992), which employs a mathematical expansion in physical nonlinear basis functions to uniformly approximate the unknown dynamics.

Unlike its linear counterpart, solutions to the adaptive control problem in the general nonlinearly parameterized setting  $\hat{\mathbf{f}} = \mathbf{f}(\mathbf{x}, \hat{\mathbf{a}}, t)$  have remained elusive. Intuitively, this is unsurprising: guarantees for gradient-based optimization algorithms typically rely on convexity, with a few notable exceptions such as the Polyak-Lojasiewicz condition (Polyak, 1963). In the linearly parameterized setting, the underlying optimization problem will be convex. When the parameters appear nonlinearly, the problem is in general nonconvex and difficult to provide guarantees for.

In this work, we provide new provably globally convergent algorithms for both the linearly and nonlinearly parameterized adaptive control problems, along with new insight into existing adaptive control algorithms for the linearly parameterized setting. Our results for nonlinearly parameterized systems are valid under the monotonicity assumptions of Tyukin et al. (2007) or the convexity assumptions of Fradkov (1980). These monotonicity assumptions are equivalent to those commonly satisfied by generalized linear models in statistics (Kakade et al., 2011).

### 1.1 DESCRIPTION OF PRIMARY CONTRIBUTIONS

Our contributions can be categorized into two main advances.

1. We further develop a class of natural gradient and mirror descent-like algorithms that have recently appeared in the literature in the context of physically consistent inertial parameter learning in robotics (Lee et al., 2018) and geodesically convex optimization (Wensing and Slotine, 2018). We prove that these algorithms implicitly regularize the learned system model in both the linearly parameterized and nonlinearly parameterized settings.
2. We construct a general class of higher-order in-time adaptive control algorithms which incorporate momentum into existing adaptation laws. We prove that our new momentum algorithms are stable and globally convergent for both linearly parameterized and nonlinearly parameterized systems. We connect these higher-order methods with the first advance by designing a number of natural gradient and mirror descent-like adaptive control algorithms with momentum, which also implicitly regularize the learned model.

Unlike standard problems in optimization and machine learning, explicit regularization terms cannot be naively added to adaptive control algorithms without impacting stability and performance. Our approach enables a provably stable and globally convergent implementation of regularization in adaptive control. We demonstrate the utility of these results through examples in the context of dynamics prediction, such as sparse estimation of a physical

system’s Hamiltonian or Lagrangian function, and estimating the weights of a continuous-time recurrent neural network model.

It is well-known in adaptive control that the true parameters are only recovered when the desired trajectory satisfies a strong condition known as *persistent excitation* (Narendra and Annaswamy, 2005; Slotine and Li, 1991). In general, an adaptation law need only find parameters that enable perfect tracking, and very little is known about what parameters are found when the estimator converges without persistent excitation. Our proof of implicit regularization provides an answer, and shows that standard Euclidean adaptation laws lead to parameters of minimum  $l_2$  norm.

For the second contribution, we utilize the Bregman Lagrangian (Wibisono et al., 2016; Betancourt et al., 2018; Wilson et al., 2016) in tandem with the velocity gradient methodology (Fradkov, 1980; Fradkov et al., 1999; Fradkov, 1986; Andrievskii et al., 1988) to define a general formalism that generates higher-order in-time (Morse, 1992) velocity gradient algorithms. Our key insight is that the velocity gradient formalism provides an optimization-like framework that encompasses many well-known adaptive control algorithms, and that the velocity gradient “loss function” can be placed directly in the Bregman Lagrangian.

## 1.2 SUMMARY OF RELATED WORK

Our work continues in a long-standing tradition that utilizes a continuous-time view to analyze optimization algorithms, and here we consider a non-exhaustive list. Diakonikolas and Jordan (2019) develop momentum algorithms from the perspective of Hamiltonian dynamics, while Maddison et al. (2018) use Hamiltonian dynamics to prove linear convergence of new optimization algorithms without strong convexity. Muehlebach and Jordan (2019; 2020) study momentum algorithms from the viewpoint of dynamical systems and control. Boffi and Slotine (2020) analyze distributed stochastic gradient descent algorithms via dynamical systems and nonlinear contraction theory. Su et al. (2016) provide an intuitive justification for Nesterov’s accelerated gradient method (Nesterov, 1983). Continuous-time differential equations were used as early as 1964 by Polyak to derive the classical momentum or “heavy ball” optimization method (Polyak, 1964). In all cases, continuous-time often affords simpler proofs, and it enables the application of physical intuition when reasoning about optimization algorithms. Given the gradient-based nature of many adaptive control algorithms, the continuous-time view of optimization provides a natural bridge from modern optimization to modern adaptive control.

Despite the simplicity of proofs in continuous-time, finding a discretization that provably retains the convergence rates of a given differential equation is challenging. In a significant advance, Wibisono et al. (2016) showed that many accelerated methods in optimization can be derived via a variational point of view from a single mathematical object known as the Bregman Lagrangian. The Bregman Lagrangian leads to second-order mass-spring-damper-like dynamics, and careful discretization provides discrete-time algorithms such as Nesterov’s celebrated accelerated gradient method (Nesterov, 1983). We similarly use the Bregman Lagrangian to generate our new adaptive control algorithms, which generalize and extend a recently developed algorithm due to Gaudio et al. (2019).

Progress has been made in nonlinearly parameterized adaptive control in a number specific cases. Annaswamy et al. (1998), Ai-Poh Loh et al. (1999), and Kojić and Annaswamy (2002) develop stable adaptive control laws for convex and concave parameterizations, though they may be overly conservative and require solving optimization problems at each timestep. Astolfi and Ortega (2003) and Liu et al. (2010) develop the Immersion and Invariance (I&I) approach, and prove global convergence if a certain monotone function can be constructed. Ortega et al. (2019) use a similar approach for system identification. Tyukin et al. (2007) consider dynamical systems satisfying a monotonicity assumption that is essentially identical to conditions required for learning generalized linear models in machine learning and statistics (Kakade et al., 2011; Goel and Klivans, 2017; Goel et al., 2018), and develop provably stable adaptive control algorithms for nonlinearly parameterized systems in this setting. Fradkov (1980), Andrievskii et al. (1988), Fradkov (1986), and Fradkov et al. (1999) develop the velocity gradient methodology, an optimization-like framework for adaptive control that allows for provably global convergence under a convexity assumption.

As mentioned in Section 1.1, this framework, in tandem with the Bregman Lagrangian, is central to our development of momentum algorithms.

Our work is strongly related to and inspired by a line of recent work that analyzes the implicit bias of optimization algorithms in machine learning. Soudry et al. (2018), Gunasekar et al. (2018b), and Gunasekar et al. (2018a) characterize implicit regularization of common gradient-based optimization algorithms such as gradient descent with and without momentum, as well as natural and mirror descent in the settings of regression and classification. Azizan et al. (2019), and Azizan and Hassibi (2019) arrive at similar results via a different derivation based on results from  $\mathcal{H}_\infty$  control. Similarly, Belkin et al. (2019) consider the importance of implicit regularization in the context of the successes of deep learning. Our results are the adaptive control analogues of those presented in these papers.

### 1.3 PAPER OUTLINE

The paper is organized as follows. In Section 2, we present some required mathematical background on direct adaptive control in the linearly and nonlinearly parameterized settings. In Section 3 we analyze the implicit bias of adaptive control algorithms, while in Section 4 we consider general observer and dynamics predictor design, Hamiltonian dynamics prediction, control of Lagrangian systems, and estimation of recurrent neural networks. In Section 5 we provide background for our development of momentum algorithms, including a review of the velocity gradient formalism (Section 5.1) and the Bregman Lagrangian (Section 5.2). In Section 6 we present adaptive control algorithms with momentum, and we extend them to the non-Euclidean setting in Section 7. We illustrate our results via simulation in Section 8, and we conclude with some closing remarks and future directions in Section 9.

## 2 DIRECT ADAPTIVE CONTROL

In this section, we provide an introduction to direct adaptive control for both linearly parameterized and nonlinearly parameterized systems, along with a description of some natural gradient-like adaptive laws that have appeared in the recent literature.

### 2.1 LINEARLY PARAMETERIZED DYNAMICS

For simplicity, we restrict ourselves to the class of  $n^{\text{th}}$ -order nonlinear systems

$$x^{(n)} + f(\mathbf{x}, \mathbf{a}, t) = u \quad (1)$$

where  $x^{(i)} \in \mathbb{R}$  denotes the  $i^{\text{th}}$  derivative of  $x$ ,  $\mathbf{x} = (x, x^{(1)}, \dots, x^{(n-1)})^\top \in \mathbb{R}^n$  is the system state,  $\mathbf{a} \in \mathbb{R}^p$  is a vector of unknown parameters,  $f : \mathbb{R}^n \times \mathbb{R}^p \times \mathbb{R}_+ \rightarrow \mathbb{R}$  is of known functional form but is unknown due to its dependence on  $\mathbf{a}$ , and  $u \in \mathbb{R}$  is the control input. We seek to design a feedback control law  $u = u(\mathbf{x}, \hat{\mathbf{a}})$  that depends on a set of adjustable parameters  $\hat{\mathbf{a}} \in \mathbb{R}^p$  and ensures that  $\mathbf{x}(t) \rightarrow \mathbf{x}_d(t)$  where  $\mathbf{x}_d(t) \in \mathbb{R}^n$  is a known desired trajectory. Along the way, we require that all system signals remain bounded. The estimated parameters  $\hat{\mathbf{a}}$  are updated according to a learning rule or adaptation law

$$\dot{\hat{\mathbf{a}}} = \mathbf{g}(\mathbf{a}, \hat{\mathbf{a}}, \mathbf{x}) \quad (2)$$

where  $\mathbf{g} : \mathbb{R}^p \times \mathbb{R}^p \times \mathbb{R}^n \rightarrow \mathbb{R}^p$  must be implementable solely in terms of known system signals despite its potential dependence on  $\mathbf{a}$ . Like reinforcement learning, adaptive control is fundamentally an online learning problem where the data-generating process is a nonlinear dynamical system coupled in feedback to the learning process, though adaptive control generally provides faster convergence. For  $n^{\text{th}}$  order systems as considered in (1), a common approach is to define the *sliding variable* (Slotine and Li, 1991)

$$s = \left( \frac{d}{dt} + \lambda \right)^{n-1} \tilde{x} = \tilde{x}^{(n-1)} - \tilde{x}_r^{(n-1)} \quad (3)$$

where  $\lambda > 0$  is a constant, and  $\tilde{x}(t) = x(t) - x_d(t)$ . We have defined  $\tilde{x}^{(i)}(t) = x^{(i)}(t) - x_d^{(i)}(t)$  and  $\tilde{x}_r^{(n-1)}$  as the remainder based on the definition of  $s$ . According to the definition (3),  $s$

obeys the differential equation

$$\dot{s} = u - f(\mathbf{x}, \mathbf{a}, t) - \tilde{x}_r^{(n)}. \quad (4)$$

Hence, from (4), we may choose

$$u = f(\mathbf{x}, \hat{\mathbf{a}}, t) + \tilde{x}_r^{(n)} - \eta s \quad (5)$$

to obtain the stable first-order linear filter

$$\dot{s} = -\eta s + f(\mathbf{x}, \hat{\mathbf{a}}, t) - f(\mathbf{x}, \mathbf{a}, t). \quad (6)$$

For future convenience, we define  $\tilde{f}(\mathbf{x}, \hat{\mathbf{a}}, \mathbf{a}, t) = f(\mathbf{x}, \hat{\mathbf{a}}, t) - f(\mathbf{x}, \mathbf{a}, t)$  and we will omit its arguments when clear from the context. From the definition of  $s$  in (3),  $s = 0$  defines the *dynamics*

$$\left( \frac{d}{dt} + \lambda \right)^{n-1} \tilde{x} = 0. \quad (7)$$

Equation (7) is a stable  $(n-1)^{\text{th}}$ -order filter which ensures that  $\tilde{x} \rightarrow 0$  exponentially. For systems of the form (1), it is thus sufficient to consider the two first-order dynamics (2) and (6). The adaptive control problem has thus been reduced to finding a learning algorithm that ensures  $s \rightarrow 0$ .

**Remark 2.1.** Systems in the matched uncertainty form

$$\dot{\mathbf{x}} = \mathbf{A}\mathbf{x} + \mathbf{b}(u - f(\mathbf{x}, \mathbf{a}, t)),$$

where the constant pair  $(\mathbf{A}, \mathbf{b})$  is controllable and the constant parameter vector  $\mathbf{a}$  in the nonlinear function  $f(\mathbf{x}, \mathbf{a}, t)$  is unknown, can always be put in the form (1) by using a state transformation to the second controllability canonical form – see Luenberger (1979), Chapter 8.8. After such a transformation, the new state variables  $\mathbf{z}$  satisfy  $\dot{z}_i = z_{i+1}$  for  $i < n$  and  $\dot{z}_n = -\sum_{i=1}^{n-1} a_i z_i + u - f(\mathbf{x}, \mathbf{a}, t)$ . Defining  $s$  as in (3) and choosing  $u$  accordingly leads to (6). Hence, all results in this paper extend immediately to such systems.  $\diamond$

**Remark 2.2.** The fundamental utility of defining the variable  $s$  is its conversion of the adaptive control problem for the  $n^{\text{th}}$ -order system (1) to an adaptive control problem for the first-order system (6). Our results may be simply extended to other error models (Narendra and Annaswamy, 2005; Ai-Poh Loh et al., 1999) of the form (6), or error models with similar input-output guarantees, as summarized by Lemma A.2.  $\diamond$

**Remark 2.3.** We will use  $\mathbf{f}$  to denote the equivalent first-order system to (1),  $\dot{\mathbf{x}} = \mathbf{f}(\mathbf{x}, \mathbf{a}, t) + \mathbf{u}$ , where  $\mathbf{f} = (x_2, x_3, \dots, f(\mathbf{x}, \mathbf{a}, t))$  and  $\mathbf{u} = (0, 0, \dots, u)$ .  $\diamond$

The classic setting for adaptive control assumes that the unknown nonlinear dynamics depends linearly on the set of unknown parameters, that is

$$f(\mathbf{x}, \mathbf{a}, t) = \mathbf{Y}(\mathbf{x}, t)\mathbf{a},$$

with  $\mathbf{Y} : \mathbb{R}^n \times \mathbb{R}_+ \rightarrow \mathbb{R}^{1 \times p}$  a known function. In this setting, a well-known algorithm is the adaptive controller of Slotine and Coetsee (1986), given by

$$\dot{\hat{\mathbf{a}}} = -\mathbf{P}\mathbf{Y}^T s, \quad (8)$$

and its extension to multi-input adaptive robot control (Slotine and Li, 1987), where  $\mathbf{P} = \mathbf{P}^T > 0 \in \mathbb{R}^{p \times p}$  is a constant positive definite matrix of learning rates. Consideration of the Lyapunov-like function  $V = \frac{1}{2}s^2 + \frac{1}{2}\hat{\mathbf{a}}^T \mathbf{P}^{-1} \hat{\mathbf{a}}$  shows stability of the feedback interconnection of (6) and (8) and convergence to the desired trajectory via an application of Barbalat's Lemma (Lemma A.1). We will refer to (8) as the Slotine and Li controller.

In this work, we make a mild additional assumption that simplifies some of the proofs.

**Assumption 2.1.** The dynamics  $\hat{f}(\mathbf{x}, \hat{\mathbf{a}}, t)$  is locally bounded in  $\hat{\mathbf{x}}$  and  $\hat{\mathbf{a}}$  uniformly in  $t$ . That is, if  $\|\mathbf{x}\| \leq \infty$  and  $\|\hat{\mathbf{a}}\| < \infty$ , then  $\forall t \geq 0$ ,  $|\hat{f}(\mathbf{x}, \hat{\mathbf{a}}, t)| < \infty$ .  $\diamond$

## 2.2 NONLINEARLY PARAMETERIZED DYNAMICS

While a difficult problem in general, significant progress has been made for the nonlinearly parameterized adaptive control problem under the assumption of *monotonicity*, and several notions of monotonicity have appeared in the literature (Tyukin et al., 2007; Tyukin, 2011; Astolfi and Ortega, 2003; Liu et al., 2010; Ortega et al., 2019). We consider one such notion as presented by Tyukin et al. (2007), which is captured in the following assumption.

**Assumption 2.2.** There exists a known time- and state-dependent function  $\alpha : \mathbb{R}^n \times \mathbb{R}_{\geq 0} \rightarrow \mathbb{R}^p$  such that

$$\hat{\mathbf{a}}^\top \alpha(\mathbf{x}, t) (f(\mathbf{x}, \hat{\mathbf{a}}, t) - f(\mathbf{x}, \mathbf{a}, t)) \geq 0, \quad (9)$$

$$|\alpha(\mathbf{x}, t)^\top \hat{\mathbf{a}}| \geq \frac{1}{D_1} |f(\mathbf{x}, \hat{\mathbf{a}}, t) - f(\mathbf{x}, \mathbf{a}, t)|. \quad (10)$$

where  $D_1 > 0$  is a positive scalar.  $\diamond$

This assumption is satisfied, for example, by all functions of the form

$$f(\mathbf{x}, \mathbf{a}, t) = \lambda(\mathbf{x}, t) f_m(\mathbf{x}, \phi(\mathbf{x}, t)^\top \mathbf{a}, t), \quad (11)$$

where  $\lambda : \mathbb{R}^n \times \mathbb{R}_{\geq 0} \rightarrow \mathbb{R}$ ,  $\phi : \mathbb{R}^n \times \mathbb{R}_{\geq 0} \rightarrow \mathbb{R}^p$ ,  $f_m : \mathbb{R}^n \times \mathbb{R} \times \mathbb{R}_{\geq 0} \rightarrow \mathbb{R}$ , and where  $f_m$  is monotonic and Lipschitz in  $\phi(\mathbf{x}, t)^\top \mathbf{a}$ . In this setting,  $\alpha(\mathbf{x}, t)$  may be taken as  $\alpha(\mathbf{x}, t) = (-1)^p D_1 \lambda(\mathbf{x}, t) \phi(\mathbf{x}, t)$  where  $p = 0$  if  $f_m$  is non-decreasing in  $\phi^\top \mathbf{a}$  and  $p = 1$  if  $f_m$  is non-increasing in  $\phi^\top \mathbf{a}$  (Tyukin et al., 2007; Tyukin, 2011).

Under Assumption 2.2, Tyukin et al. (2007) showed that the adaptation law

$$\dot{\hat{\mathbf{a}}} = -\tilde{f}(\mathbf{x}, \hat{\mathbf{a}}, \mathbf{a}, t) \mathbf{P} \alpha(\mathbf{x}, t) \quad (12)$$

with  $\mathbf{P} = \mathbf{P}^\top > 0$  a positive definite matrix of learning rates of appropriate dimensions ensures that  $\tilde{f} \in \mathcal{L}_2$  over the maximal interval of existence of  $\mathbf{x}$ . Under suitable conditions on the error model, this then ensures that  $\tilde{f} \in \mathcal{L}_2 \cap \mathcal{L}_\infty$ ,  $\mathbf{x}(t)$  and  $\hat{\mathbf{a}}(t)$  both remain bounded for all  $t$ , and that  $\mathbf{x} \rightarrow \mathbf{x}_d$ . The proof follows by consideration of the Lyapunov-like function  $V = \frac{1}{2} \hat{\mathbf{a}}^\top \mathbf{P}^{-1} \hat{\mathbf{a}}$ .

While  $\tilde{f}$  itself is unknown, and hence (12) is not directly implementable, it is contained in  $\dot{s}$ . Intuitively, unknown quantities contained in  $\dot{s}$  can be obtained in the adaptation dynamics through a proportional term in  $\dot{\hat{\mathbf{a}}}$  that contains  $s$ . This idea of gaining a “free” derivative is the basis of the reduced-order Luenberger observer for linear systems (Luenberger, 1979)<sup>1</sup>. Proportional-integral adaptive laws of this type have been known as algorithms in finite form (Fradkov et al., 1999; Tyukin, 2003) and appear in the well-known I&I framework (Astolfi and Ortega, 2003; Liu et al., 2010). Following this prescription, (12) may be implemented in a proportional-integral form,

$$\xi(\mathbf{x}, t) = -\mathbf{P} s(\mathbf{x}, t) \alpha(\mathbf{x}, t), \quad (13)$$

$$\rho(\mathbf{x}, t) = \mathbf{P} \int_{x_n(t_0)}^{x_n(t)} s(\mathbf{x}, t) \frac{\partial \alpha(\mathbf{x}, t)}{\partial x_n} dx_n, \quad (14)$$

$$\hat{\mathbf{a}} = \bar{\mathbf{a}} + \xi(\mathbf{x}, t) + \rho(\mathbf{x}, t), \quad (15)$$

$$\dot{\hat{\mathbf{a}}} = -\eta s \mathbf{P} \alpha + \mathbf{P} s \sum_{i=1}^{n-1} \frac{\partial \alpha}{\partial x_i} x_{i+1} - \sum_{i=1}^{n-1} \frac{\partial \rho}{\partial x_i} x_{i+1} - \left( \frac{\partial \rho}{\partial \mathbf{x}_d} \right)^\top \dot{\mathbf{x}}_d - \frac{\partial \xi}{\partial t} - \frac{\partial \rho}{\partial t}. \quad (16)$$

Algorithm (12) is similar to a gradient flow algorithm. If  $f(\mathbf{x}, \mathbf{a}, t)$  has the form (11) and is non-decreasing, gradient flow on the loss function  $L(\mathbf{x}, \hat{\mathbf{a}}, \mathbf{a}, t) = \frac{1}{2} \tilde{f}^2(\mathbf{x}, \hat{\mathbf{a}}, \mathbf{a}, t)$  with a gain matrix  $D_1 \mathbf{P}$  leads to

$$\dot{\hat{\mathbf{a}}} = -\tilde{f}(\mathbf{x}, \hat{\mathbf{a}}, \mathbf{a}, t) f'_m(\mathbf{x}, \phi^\top \hat{\mathbf{a}}, t) \mathbf{P} \alpha(\mathbf{x}, t)$$

where ' denotes differentiation with respect to the second argument.  $f'_m(\mathbf{x}, \phi^\top \hat{\mathbf{a}}, t)$  is of known sign due to the monotonicity assumption, but of unknown magnitude. It is sufficient

<sup>1</sup>Similar concepts can be extended to nonlinear observers; see Lohmiller and Slotine (1998), Section 4.1.

to remove this quantity from the adaptation law and instead to follow the *pseudogradient*  $\tilde{f}(\mathbf{x}, \hat{\mathbf{a}}, \mathbf{a}, t)\boldsymbol{\alpha}(\mathbf{x}, t)$  despite non-convexity of the square loss in this setting. Similarly, if  $f$  is non-increasing, we find

$$\dot{\hat{\mathbf{a}}} = \tilde{f}(\mathbf{x}, \hat{\mathbf{a}}, \mathbf{a}, t) f'_m(\mathbf{x}, \boldsymbol{\phi}^\top \hat{\mathbf{a}}, t) \mathbf{P} \boldsymbol{\alpha}(\mathbf{x}, t)$$

and it is sufficient to set  $f'_m$  to negative one.

### 2.3 THE BREGMAN DIVERGENCE AND NATURAL ADAPTATION LAWS

Lee et al. (2018) introduced an elegant modification of the Slotine and Li adaptive robot controller, later generalized by Wensing and Slotine (2018). It consists of replacing the usual parameter estimation error term  $\frac{1}{2}\tilde{\mathbf{a}}^\top \mathbf{P}^{-1} \tilde{\mathbf{a}}$  in the Lyapunov-like function  $V = \frac{1}{2}s^2 + \frac{1}{2}\tilde{\mathbf{a}}^\top \mathbf{P}^{-1} \tilde{\mathbf{a}}$  with the Bregman divergence (Bregman, 1967),

$$d_\psi(\mathbf{y} \parallel \mathbf{x}) = \psi(\mathbf{y}) - \psi(\mathbf{x}) - (\mathbf{y} - \mathbf{x})^\top \nabla \psi(\mathbf{x})$$

to obtain the new “non-Euclidean” Lyapunov-like function

$$V = \frac{1}{2}s^2 + d_\psi(\mathbf{a} \parallel \hat{\mathbf{a}}) \quad (17)$$

for an arbitrary strictly convex function  $\psi$ .

The Bregman divergence may be understood as the error made when approximating  $\psi(\mathbf{y})$  by a first-order Taylor expansion around  $\mathbf{x}$ . It is guaranteed to be non-negative for strictly convex functions by the first-order characterization of convexity. While it is not a norm in general, it defines a distance-like function for  $\psi$  strictly convex related to the *Hessian metric*  $\frac{1}{2}\|\mathbf{x}\|_{\nabla^2 \psi}^2 = \frac{1}{2}\mathbf{x}^\top \nabla^2 \psi(\mathbf{x}) \mathbf{x}$ . As two simple examples, for  $\psi(\mathbf{x}) = \frac{1}{2}\|\mathbf{x}\|^2$ ,  $d_\psi(\mathbf{x} \parallel \mathbf{y}) = \frac{1}{2}\|\mathbf{x} - \mathbf{y}\|^2$ . For  $\psi(\mathbf{x}) = \frac{1}{2}\mathbf{x}^\top \mathbf{Q}\mathbf{x}$  with  $\mathbf{Q} > 0$  a positive definite matrix,  $d_\psi(\mathbf{x} \parallel \mathbf{y}) = \frac{1}{2}(\mathbf{x} - \mathbf{y})^\top \mathbf{Q}(\mathbf{x} - \mathbf{y})$ . For general convex functions,  $d_\psi(\cdot \parallel \cdot)$  can always be written via Taylor’s formula with integral remainder for multivariate functions as

$$d_\psi(\mathbf{y} \parallel \mathbf{x}) = (\mathbf{y} - \mathbf{x})^\top \left( \int_0^1 \nabla^2 \psi(\mathbf{x} + s(\mathbf{y} - \mathbf{x})) (1 - s) ds \right) (\mathbf{y} - \mathbf{x}).$$

Indeed, a quick calculation shows that the derivative of the Bregman divergence is simply

$$\frac{d}{dt} d_\psi(\mathbf{a} \parallel \hat{\mathbf{a}}) = \hat{\mathbf{a}}^\top \nabla^2 \psi(\hat{\mathbf{a}}) \dot{\hat{\mathbf{a}}}, \quad (18)$$

which can be directly used to show stability of the adaptation law

$$\dot{\hat{\mathbf{a}}} = -[\nabla^2 \psi(\hat{\mathbf{a}})]^{-1} \mathbf{Y}^\top s.$$

This procedure replaces the gain matrix  $\mathbf{P}$  in the adaptation law by the  $\hat{\mathbf{a}}$ -dependent *inverse Hessian*  $[\nabla^2 \psi(\hat{\mathbf{a}})]^{-1}$  of the strictly convex function  $\psi$ . In essence, this amounts to the adaptive control equivalent of the *natural gradient* algorithm in the sense of Amari (1998), so that the resulting adaptation law respects the underlying Riemannian geometry captured by the Hessian metric  $\nabla^2 \psi(\hat{\mathbf{a}})$ . The standard adaptation law  $\dot{\hat{\mathbf{a}}} = -\mathbf{P} \mathbf{Y}^\top s$  uses the constant metric  $\mathbf{P}^{-1}$ , which in turn explains the appearance of  $\mathbf{P}$  in the natural gradient-like system.

The choice of  $\psi$  enables the design of adaptation algorithms that respect physical Riemannian constraints (Lee et al., 2019) obeyed by the true parameters, as in the estimation of mass properties in robotics (Wensing et al., 2018). Similarly, it allows one to introduce a priori bounds on parameter estimates without resorting to parameter projection techniques by choosing  $\psi$  to be a log-barrier function (Wensing and Slotine, 2018). In Section 3.1, we further prove that the choice of  $\psi$  implicitly regularizes the learned system model.

**Remark 2.4.** The relation (18) shows that Tyukin’s algorithm (12) can be generalized to have a parameter estimate-dependent gain matrix. Indeed, consideration of the Lyapunov-like function  $V = \frac{1}{\gamma} d_\psi(\mathbf{a} \parallel \hat{\mathbf{a}})$  shows that the algorithm

$$\dot{\hat{\mathbf{a}}} = -\gamma \tilde{f}(\mathbf{x}, \hat{\mathbf{a}}, \mathbf{a}, t) [\nabla^2 \psi(\hat{\mathbf{a}})]^{-1} \boldsymbol{\alpha}(\mathbf{x}, t),$$

with  $\psi$  strictly convex and  $\gamma > 0$ , ensures that  $\tilde{f} \in \mathcal{L}_2$  over the maximal interval of existence of  $\mathbf{x}(t)$  for nonlinearly parameterized systems categorized by Assumption 2.2. The proof is identical to that of Tyukin et al. (2007). The implementation of this algorithm in PI form will be described in Remark 3.2, and is based on a correspondence between mirror descent and natural gradient descent in continuous-time. This algorithm can be seen as the adaptive control equivalent of a mirror descent or natural gradient extension of the GLMTron of Kakade et al. (2011), and this correspondence will be considered in greater detail in Section 6.  $\diamond$

**Remark 2.5.** In the linearly parameterized setting, rather than the Lyapunov-like function  $V = \frac{1}{2}s^2 + d_\psi(\mathbf{a} \parallel \hat{\mathbf{a}})$ , the Lyapunov-like function  $V = \frac{1}{2}s^2 + d_\psi(\mathbf{P}\mathbf{a} \parallel \hat{\mathbf{P}}\hat{\mathbf{a}})$  may be used for any positive definite matrix  $\mathbf{P}$ . This shows stability of the adaptation law  $\dot{\mathbf{a}} = -\mathbf{P}^{-1}(\nabla^2\psi(\mathbf{P}\hat{\mathbf{a}}))^{-1}\mathbf{P}^{-1}\mathbf{Y}^\top s$ , where choice of the matrix  $\mathbf{P}$  offers an additional design flexibility.

**Remark 2.6.** In some practical applications, for example in adaptive robot control, the estimated parameters  $\hat{\mathbf{a}}$  may correspond to physical constants. In this case, the weighted parameter estimation error term  $\frac{1}{2}\hat{\mathbf{a}}^\top \mathbf{P}^{-1}\hat{\mathbf{a}}$  not only provides additional design flexibility through the elements of  $\mathbf{P}$  in the adaptation law, but is necessary for physical consistency of units. Indeed, the usual Lyapunov-like function  $V = \frac{1}{2}s^2 + \frac{1}{2}\tilde{\mathbf{a}}^\top \mathbf{P}^{-1}\tilde{\mathbf{a}}$  shows that  $\mathbf{P}^{-1}$  must be chosen so that the parameter estimation error term  $\frac{1}{2}\tilde{\mathbf{a}}^\top \mathbf{P}^{-1}\tilde{\mathbf{a}}$  has the same units as the tracking error term  $\frac{1}{2}s^2$ . Similar considerations apply when replacing this standard parameter estimation error term with the Bregman divergence  $d_\psi(\mathbf{a} \parallel \hat{\mathbf{a}})$ , which has the same units as  $\psi(\hat{\mathbf{a}})$ . In this case,  $\psi(\hat{\mathbf{a}})$  must be chosen to have the same units as the tracking error term, for example by introducing a diagonal matrix of constants to ensure consistent dimensions.

### 3 NATURAL GRADIENT ADAPTATION AND IMPLICIT REGULARIZATION

In this section, we show that the “natural” adaptation algorithms of the previous section implicitly regularize the learned system model.

#### 3.1 IMPLICIT REGULARIZATION AND ADAPTIVE CONTROL

With deep networks as the predominant example, modern machine learning often considers highly over-parameterized models that are capable of interpolating the training data (achieving zero error on the training set) while still generalizing well to unseen examples. The classical principles of statistical learning theory emphasize a trade-off between generalization performance and model capacity, and predict that in the highly over-parameterized regime, generalization performance should be poor due to a tendency of the model to fit noise in the training data. Nevertheless, empirical evidence indicates that deep networks and other modern machine learning models do not obey classical statistical learning wisdom (Belkin et al., 2019), and can even generalize with significant label noise (Zhang et al., 2016).

More surprisingly, the ability to simultaneously fit label noise in the training data yet generalize to new examples has been observed in over-parameterized linear models (Bartlett et al., 2019; Muthukumar et al., 2019). A possible explanation for the ability of highly over-parameterized models to generalize when optimized using simple first-order algorithms is their *implicit bias* – that is, the tendency of an algorithm to converge to a particular (e.g. minimum norm) solution when there are many that interpolate the training data (Soudry et al., 2018; Gunasekar et al., 2018b;a; Azizan et al., 2019; Azizan and Hassibi, 2019).

In adaptive control, the possibility of there being many possible parameter vectors  $\hat{\mathbf{a}}$  that lead to zero tracking error is not unique to the over-parameterized case. Unless the trajectory is *persistently exciting*<sup>2</sup> (Narendra and Annaswamy, 2005; Slotine and Li, 1991), it is well-known that  $\hat{\mathbf{a}}$  will not converge to the true parameters  $\mathbf{a}$  in general. Depending on the complexity of the trajectory, there may even be many solutions in the *under-parameterized* case where

<sup>2</sup>A typical characterization of persistent excitation in the linearly parameterized setting is that there exists some  $\delta > 0$  and some  $T > 0$  such that for all  $t$ ,  $\int_t^{t+T} \mathbf{Y}^\top(\mathbf{x}(\tau), \tau) \mathbf{Y}(\mathbf{x}(\tau), \tau) d\tau \geq \delta \mathbf{I}$ .

$\dim(\hat{\mathbf{a}}) < \dim(\mathbf{a})$ . To achieve perfect tracking, the adaptation algorithm need only fit the unknown dynamics  $f(\mathbf{x}(t), \mathbf{a}, t)$  along the trajectory rather than the whole state space, so that the *effective* number of parameters may be less than  $\dim(\mathbf{a})$ .

The wealth of possible solutions in the linearly parameterized case is captured by the time-dependent null space of  $\mathbf{Y}(\mathbf{x}(t), t)$ : when  $\mathbf{x} \rightarrow \mathbf{x}_d$ , we can conclude that  $\mathbf{Y}(\mathbf{x}_d(t), t)\hat{\mathbf{a}}(t) = 0$ , and hence that  $\hat{\mathbf{a}}(t) = \mathbf{a} + \hat{\mathbf{n}}(t)$  where  $\mathbf{Y}(\mathbf{x}_d(t), t)\hat{\mathbf{n}}(t) = 0$  for all  $t$ . This observation also highlights that any element of the null space  $\hat{\mathbf{n}}(t)$  may be added to the parameter estimates  $\hat{\mathbf{a}}$  without affecting the value of  $\hat{f}^3$ . In the over-parameterized case when  $\dim(\hat{\mathbf{a}}) > \dim(\mathbf{a})$ , the set of parameters that achieve zero tracking error is not unique regardless of the complexity of the desired trajectory. By deriving a continuous-time extension of a recent proof of the implicit bias of mirror descent algorithms (Azizan et al., 2019; Azizan and Hassibi, 2019), we now show that the natural adaptive laws of the previous section implicitly regularize  $\hat{\mathbf{a}}$ . This proof of implicit regularization provides an answer to the question, *with infinitely many parameter vectors that achieve zero tracking error, which does adaptation choose?*

Define the set

$$\mathcal{A} = \{\boldsymbol{\theta} | f(\mathbf{x}(t), \boldsymbol{\theta}, t) = f(\mathbf{x}(t), \mathbf{a}, t) \quad \forall t\} \quad (19)$$

i.e., (19) contains only parameters that interpolate the dynamics  $f(\mathbf{x}(t), \mathbf{a}, t)$  along the entire trajectory. We are now in a position to state the following proposition.

**Proposition 3.1.** *Consider the natural gradient-like adaptation law for a linearly parameterized dynamics*

$$\dot{\hat{\mathbf{a}}} = -[\nabla^2 \psi(\hat{\mathbf{a}})]^{-1} \mathbf{Y}^\top s, \quad (20)$$

where  $\psi(\cdot)$  is a strictly convex function. Assume that  $\hat{\mathbf{a}}(t) \rightarrow \hat{\mathbf{a}}_\infty \in \mathcal{A}$ . Then

$$\hat{\mathbf{a}}_\infty = \arg \min_{\boldsymbol{\theta} \in \mathcal{A}} d_\psi(\boldsymbol{\theta} \parallel \hat{\mathbf{a}}(0)).$$

In particular, if  $\hat{\mathbf{a}}(0) = \arg \min_{\boldsymbol{\theta} \in \mathbb{R}^p} \psi(\boldsymbol{\theta})$ , then

$$\hat{\mathbf{a}}_\infty = \arg \min_{\boldsymbol{\theta} \in \mathcal{A}} \psi(\boldsymbol{\theta}). \quad (21)$$

*Proof.* Let  $\boldsymbol{\theta}$  be any constant vector of parameters. The Bregman divergence  $d_\psi(\boldsymbol{\theta} \parallel \hat{\mathbf{a}}) = \psi(\boldsymbol{\theta}) - \psi(\hat{\mathbf{a}}) - \nabla \psi(\hat{\mathbf{a}})^\top (\boldsymbol{\theta} - \hat{\mathbf{a}})$  has time derivative

$$\frac{d}{dt} d_\psi(\boldsymbol{\theta} \parallel \hat{\mathbf{a}}) = -\left(\frac{d}{dt} \nabla \psi(\hat{\mathbf{a}})\right)^\top (\boldsymbol{\theta} - \hat{\mathbf{a}}).$$

From (20),  $\frac{d}{dt} \nabla \psi(\hat{\mathbf{a}}) = -\mathbf{Y}^\top s$ , so that

$$\frac{d}{dt} d_\psi(\boldsymbol{\theta} \parallel \hat{\mathbf{a}}) = s \mathbf{Y} (\boldsymbol{\theta} - \hat{\mathbf{a}}).$$

Integrating both sides of the above shows that

$$d_\psi(\boldsymbol{\theta} \parallel \hat{\mathbf{a}}(0)) = d_\psi(\boldsymbol{\theta} \parallel \hat{\mathbf{a}}(t)) + \int_0^t s(\tau) \mathbf{Y}(\mathbf{x}(\tau), \tau) (\hat{\mathbf{a}}(\tau) - \boldsymbol{\theta}) d\tau.$$

If we now take  $\boldsymbol{\theta} \in \mathcal{A}$ ,  $\mathbf{Y}(\mathbf{x}(\tau), \tau)\boldsymbol{\theta} = f(\mathbf{x}(\tau), \mathbf{a}, \tau)$  and the integral term is independent of  $\boldsymbol{\theta}$ . Assuming that  $\hat{\mathbf{a}} \rightarrow \hat{\mathbf{a}}_\infty \in \mathcal{A}$ , we can take the limit as  $t \rightarrow \infty$  and say that for any  $\boldsymbol{\theta} \in \mathcal{A}$ ,  $\hat{\mathbf{a}}_\infty \in \mathcal{A}$ ,

$$d_\psi(\boldsymbol{\theta} \parallel \hat{\mathbf{a}}(0)) = d_\psi(\boldsymbol{\theta} \parallel \hat{\mathbf{a}}_\infty) + \int_0^\infty s(\tau) (\mathbf{Y}(\mathbf{x}(\tau), \tau)\hat{\mathbf{a}}(\tau) - f(\mathbf{x}(\tau), \mathbf{a}, \tau)) d\tau.$$

Because the only dependence of the right-hand side on  $\boldsymbol{\theta}$  is in the first term, and because this relation holds for any  $\boldsymbol{\theta}$ , the  $\arg \min$  of the two Bregman divergences must be identical. The minimum of the right-hand side over  $\boldsymbol{\theta}$  is clearly obtained at  $\hat{\mathbf{a}}_\infty$ , while the minimum of the left-hand side is by definition obtained at  $\arg \min_{\boldsymbol{\theta} \in \mathcal{A}} d_\psi(\boldsymbol{\theta}, \hat{\mathbf{a}}(0))$ . From this, we conclude that

$$\hat{\mathbf{a}}_\infty = \arg \min_{\boldsymbol{\theta} \in \mathcal{A}} d_\psi(\boldsymbol{\theta} \parallel \hat{\mathbf{a}}(0)),$$

which completes the proof.  $\square$

<sup>3</sup>In principle,  $\hat{\mathbf{n}}(t)$  could be chosen to shape the parameters  $\hat{\mathbf{a}}(t)$  to satisfy some desired property.

(21) captures the implicit regularization imposed by the adaptation algorithm (20): out of all possible interpolating parameters, it chooses the  $\hat{\mathbf{a}}$  that achieves the minimum value of  $\psi$ .

**Remark 3.1.** The assumptions of Proposition 3.1 provide a setting where theoretical insight may be gained into the implicit regularization of adaptive control algorithms, but they are stronger than needed. In general, the parameters  $\hat{\mathbf{a}}(t)$  found by an adaptive controller need not converge to a constant despite the fact that  $\dot{\hat{\mathbf{a}}} \rightarrow 0$ <sup>4</sup>. Similarly, even in the case that the parameters converge, it is not strictly required that  $\mathbf{Y}(\mathbf{x}(t), t)\hat{\mathbf{a}}_\infty = f(\mathbf{x}(t), \mathbf{a}, t)$  along the entire trajectory, as this condition is satisfied asymptotically. Numerical simulations in Section 8 will demonstrate the implicit regularization of parameters  $\hat{\mathbf{a}}(t)$  found by adaptive control along the entire trajectory.  $\diamond$

We may make a similar claim in the nonlinearly parameterized setting captured by Assumption 2.2. To do so, we require an additional assumption.

**Assumption 3.1.** For any vector of parameters  $\boldsymbol{\theta}$  and the true parameters  $\mathbf{a}$ ,  $f(\mathbf{x}(t), \boldsymbol{\theta}, t) = f(\mathbf{x}(t), \mathbf{a}, t)$  implies that  $\boldsymbol{\alpha}(\mathbf{x}(t), t)^\top \boldsymbol{\theta} = \boldsymbol{\alpha}(\mathbf{x}(t), t)^\top \mathbf{a}$ .  $\diamond$

For the class of systems (11), a sufficient condition for Assumption 3.1 is that  $\lambda(\mathbf{x}(t), t) \neq 0$  and that the map  $\phi(\mathbf{x}, t)^\top \mathbf{a} \rightarrow f_m(\mathbf{x}(t), \phi(\mathbf{x}, t)^\top \mathbf{a})$  is invertible at every  $t$ . We may now state our implicit regularization result for nonlinearly parameterized systems.

**Proposition 3.2.** Consider the adaptation algorithm

$$\dot{\hat{\mathbf{a}}} = -[\nabla^2 \psi(\hat{\mathbf{a}})]^{-1} \tilde{f}(\mathbf{x}(t), \hat{\mathbf{a}}(t), \mathbf{a}, t) \boldsymbol{\alpha}(\mathbf{x}(t), t) \quad (22)$$

under Assumptions 2.2 & 3.1. Assume  $\hat{\mathbf{a}}(t) \rightarrow \hat{\mathbf{a}}_\infty \in \mathcal{A}$ . Then

$$\hat{\mathbf{a}}_\infty = \arg \min_{\boldsymbol{\theta} \in \mathcal{A}} d_\psi(\boldsymbol{\theta} \parallel \hat{\mathbf{a}}(0)).$$

*Proof.* The proof is much the same as Proposition 3.1. The Bregman divergence  $d_\psi(\boldsymbol{\theta} \parallel \hat{\mathbf{a}})$  for any fixed vector of parameters  $\boldsymbol{\theta}$  verifies

$$\frac{d}{dt} d_\psi(\boldsymbol{\theta} \parallel \hat{\mathbf{a}}) = \tilde{f}(\mathbf{x}(t), \hat{\mathbf{a}}(t), \mathbf{a}, t) \boldsymbol{\alpha}(\mathbf{x}(t), t)^\top (\boldsymbol{\theta} - \hat{\mathbf{a}}),$$

so that, integrating both sides,

$$d_\psi(\boldsymbol{\theta} \parallel \hat{\mathbf{a}}(0)) = d_\psi(\boldsymbol{\theta} \parallel \hat{\mathbf{a}}(t)) - \int_0^t \tilde{f}(\mathbf{x}(\tau), \hat{\mathbf{a}}(t), \mathbf{a}, \tau) \boldsymbol{\alpha}(\mathbf{x}(\tau), \tau)^\top (\boldsymbol{\theta} - \hat{\mathbf{a}}(\tau)) d\tau.$$

Now take  $\boldsymbol{\theta} \in \mathcal{A}$ . By the assumptions of the proposition,  $\boldsymbol{\alpha}(\mathbf{x}(\tau), \tau)^\top \boldsymbol{\theta} = \boldsymbol{\alpha}(\mathbf{x}(\tau), \tau)^\top \mathbf{a}$  is independent of  $\boldsymbol{\theta}$ . Hence, using that  $\hat{\mathbf{a}}(t) \rightarrow \hat{\mathbf{a}}_\infty \in \mathcal{A}$ , we can write

$$d_\psi(\boldsymbol{\theta} \parallel \hat{\mathbf{a}}(0)) = d_\psi(\boldsymbol{\theta} \parallel \hat{\mathbf{a}}_\infty) - \int_0^\infty \tilde{f}(\mathbf{x}(\tau), \hat{\mathbf{a}}(t), \mathbf{a}, \tau) \boldsymbol{\alpha}(\mathbf{x}(\tau), \tau)^\top (\mathbf{a} - \hat{\mathbf{a}}(\tau)) d\tau.$$

Optimizing both sides over  $\boldsymbol{\theta} \in \mathcal{A}$  as in Proposition 3.1 yields the result.  $\square$

**Remark 3.2.** Algorithm (22) must be implemented in PI form due to the appearance of  $\tilde{f}$ , but the use of the PI form (13)-(16) in  $\hat{\mathbf{a}}$  is complicated by the presence of the inverse Hessian of  $\psi$ . To implement (12), the Euclidean variant may be implemented through the usual PI form for an auxiliary variable  $\dot{\hat{\mathbf{v}}} = -\tilde{f}(\mathbf{x}(t), \hat{\mathbf{a}}(t), \mathbf{a}, t) \boldsymbol{\alpha}(\mathbf{x}(t), t)$ , and then the controller parameters may be computed by inverting the gradient of  $\psi$ ,  $\hat{\mathbf{a}}(t) = (\nabla \psi^{-1})(\hat{\mathbf{v}}(t))$ . This result follows by the equivalence of mirror descent and natural gradient descent in continuous-time. Concretely, the identity  $\frac{d}{dt} \nabla \psi(\hat{\mathbf{a}}) = \nabla^2 \psi(\hat{\mathbf{a}}) \dot{\hat{\mathbf{a}}}$  shows that  $\dot{\hat{\mathbf{a}}} = -(\nabla^2 \psi(\hat{\mathbf{a}}))^{-1} \tilde{f}(\mathbf{x}, \hat{\mathbf{a}}, \mathbf{a}, t) \boldsymbol{\alpha}(\mathbf{x}, t)$  is equivalent to  $\frac{d}{dt} \nabla \psi(\hat{\mathbf{a}}) = -\tilde{f}(\mathbf{x}, \hat{\mathbf{a}}, \mathbf{a}, t) \boldsymbol{\alpha}(\mathbf{x}, t)$ . The auxiliary variable  $\hat{\mathbf{v}}$  can then be identified with  $\nabla \psi(\hat{\mathbf{a}})$ .  $\diamond$

<sup>4</sup>Lyapunov function arguments based on a parameter estimation error term generally lead to the conclusion that the parameters remain bounded, and it is generally the case that  $\dot{\hat{\mathbf{a}}} \rightarrow 0$  as it is driven by an error term. Nevertheless,  $\hat{\mathbf{a}}$  may stay time-varying for all  $t$ . For instance, the function  $f(t) = \sin(\sqrt{t})$  remains bounded and time-varying for all  $t$ , but has  $f'(t) = \frac{1}{2\sqrt{t}} \cos(\sqrt{t}) \rightarrow 0$ . A sufficient condition (by Barbalat's Lemma [Lemma A.1]) for convergence to a constant  $\hat{\mathbf{a}}_\infty$  is that  $(\hat{\mathbf{a}} - \hat{\mathbf{a}}_\infty) \in \mathcal{L}_p$  for some  $p$ .

**Remark 3.3.** If the inverse gradient of  $\psi$  is unknown, but  $\psi$  is chosen to be strongly convex, the contracting (Lohmiller and Slotine, 1998) dynamics  $\dot{\mathbf{w}} = -\frac{1}{\tau}(\nabla\psi(\mathbf{w}) - \nabla\psi(\hat{\mathbf{v}}))$  with  $\tau > 0$  will converge to a ball around  $\hat{\mathbf{v}}$  with radius set by  $\|\frac{d}{dt}\nabla\psi(\hat{\mathbf{v}})\| \times \frac{\tau}{l}$  where  $l$  is the strong convexity parameter. By choosing  $\tau$  so that this contracting dynamics is fast on the timescale of adaptation,  $\mathbf{w}$  will thus represent a good approximation of the instantaneous  $\hat{\mathbf{v}}$ .  $\diamond$

**Remark 3.4.** Our results highlight – through the equivalence of their continuous-time limits – that both mirror descent-like and natural gradient-like adaptive laws impose implicit regularization. This observation extends recent results on the implicit regularization of mirror descent (Azizan et al., 2019; Azizan and Hassibi, 2019) to natural gradient descent, and furthermore applies to linearly parameterized and generalized linearly parameterized models in machine learning, not just in the context of adaptive control. This has previously been noted in Gunasekar et al. (2018a), where it was discussed that in discrete-time, natural gradient descent only approximately imposes implicit regularization due to discretization errors.

Propositions 3.1 & 3.2 demonstrate for the first time the implicit bias of adaptive control algorithms. In doing so, they identify an additional design choice that may be exploited for the application of interest. Proposition 3.1 implies that the Slotine and Li controller, when initialized with the parameters at  $\hat{\mathbf{a}}(0) = \mathbf{0}$ , finds the interpolating parameter vector of minimum  $l_2$  norm. Other norms, such as the  $l_1$ ,  $l_\infty$ ,  $l_p$  for arbitrary  $p$ , or group norms will find alternative parameter vectors that may have desirable properties such as sparsity<sup>5</sup>. The usual Euclidean geometry-based adaptive laws can be seen as a form of ridge regression, while imposing  $l_1$ ,  $l_2$  and  $l_\infty$  simultaneously, or  $l_p$  regularization through the choice of  $\psi$  can be seen as the adaptive control equivalents of LASSO (Tibshirani, 1996) or compressed sensing, elastic net, and bridge regression respectively. In the context of adaptive control, this notion of implicit regularization is particularly interesting, as typical regularization terms such as  $l_1$  and  $l_2$  penalties cannot in general be added to the adaptation law directly without affecting stability and performance of the algorithm.

**Remark 3.5.** Following Remark 2.6, if  $\psi(\cdot)$  is chosen as the  $l^{\text{th}}$  power of a  $p$  norm, in practical applications it is necessary to include a matrix  $\mathbf{\Gamma}$  to ensure that  $\psi(\hat{\mathbf{a}}) = \|\mathbf{\Gamma}\hat{\mathbf{a}}\|_p^l$  has the same units as the tracking error component of the Lyapunov function. For example, if  $l = 2$ , then  $\mathbf{\Gamma}$  may be chosen as  $\mathbf{\Gamma} = \mathbf{P}^{-1/2}$  for consistency of units where  $\mathbf{P}$  is a gain matrix tuned for the standard adaptive law  $\dot{\mathbf{a}} = -\mathbf{P}\mathbf{Y}^\top s$ . In addition,  $l = 2$  admits a simple inversion formula for  $\nabla\psi$  for any  $p$  as will be utilized in the simulations in Section 8, although the corresponding inverse Hessian  $(\nabla^2\psi(\cdot))^{-1}$  is non-diagonal for  $p \neq 2$ . For  $l = p$ , the inverse Hessian is diagonal, but  $\mathbf{\Gamma}$  must then be calibrated independently from  $\mathbf{P}$  tuned for the standard  $l_2$  law. Note that choosing  $\psi$  to be an  $l_1$  norm will impose sparsity on  $\mathbf{\Gamma}\hat{\mathbf{a}}$ , so that  $\mathbf{\Gamma}$  should be taken to be diagonal to ensure sparsity in  $\hat{\mathbf{a}}$  itself.

### 3.2 NON-EUCLIDEAN MEASURE OF THE TRACKING ERROR

The usual Lyapunov function incorporates a Euclidean tracking error term given by  $\frac{1}{2}s^2$ . In a similar vein to the derivation of the “natural” adaptive laws, for any strictly convex function  $\phi : \mathbb{R} \rightarrow \mathbb{R}$ , we may instead replace this tracking error term by the Bregman divergence  $d_\phi(0 \parallel s)$ . This quantity has time derivative

$$\frac{d}{dt}d_\phi(0 \parallel s) = -\eta s^2\phi''(s) + \phi''(s)\mathbf{Y}\hat{\mathbf{a}}$$

in the linearly parameterized case. Because  $\phi''(s) \geq 0$  for strictly convex  $\phi$ , it is simple to see that this modification to the usual Lyapunov function in combination with a non-Euclidean measure of the parameter estimation error leads to a family of stable adaptation laws parameterized by  $\phi$  and  $\psi$  of the form  $\dot{\mathbf{a}} = -[\nabla^2\psi(\hat{\mathbf{a}})]^{-1}\mathbf{Y}^\top\phi''(s)s$ . This shows, for example, that any odd power of  $s$  may be stably employed in the adaptation law by

<sup>5</sup>Because the  $l_1$  norm is not strictly convex, it may be replaced with a suitable approximation such as the  $l_{1+\epsilon}$  norm for  $\epsilon > 0$  and small (Azizan et al., 2019; Azizan and Hassibi, 2019).

taking  $\phi = s^p$  for some even power  $p$ . Surprisingly, more exotic adaptation laws such as  $\dot{\hat{\mathbf{a}}} = -[\nabla^2\psi(\hat{\mathbf{a}})]^{-1}\mathbf{Y}^\top e^{\lambda|s|}s$  for  $\lambda > 0$  may also be used.

In the single-input case, these laws could be more simply obtained by replacing the  $\frac{1}{2}s^2$  term in the Lyapunov-like function with a term of the form  $g(s)$  where  $g'(s)s \geq 0$  and  $g'(s)$  is known. In the multi-input case, these two approaches differ. Taking  $g$  to be a strongly convex function with minimum attained at  $s = 0$  and a known gradient, the Lyapunov-like function

$$V = g(\mathbf{s}) - \inf_{\mathbf{s}} g(\mathbf{s}) + d_\psi(\mathbf{a} \parallel \hat{\mathbf{a}})$$

shows that the adaptation law

$$\dot{\hat{\mathbf{a}}} = -[\nabla^2\psi(\hat{\mathbf{a}})]^{-1}\mathbf{Y}^\top \nabla g(\mathbf{s})$$

is globally convergent. On the other hand, the Lyapunov-like function

$$V = d_\phi(0 \parallel \mathbf{s}) + d_\psi(\mathbf{a} \parallel \hat{\mathbf{a}})$$

shows that the distinct adaptation law

$$\dot{\hat{\mathbf{a}}} = -[\nabla^2\psi(\hat{\mathbf{a}})]^{-1}\mathbf{Y}^\top [\nabla^2\phi(\mathbf{s})]\mathbf{s}$$

is also globally convergent.

## 4 ADAPTIVE DYNAMICS PREDICTION, CONTROL, AND OBSERVER DESIGN

In this section, we demonstrate how the new non-Euclidean adaptation laws of Section 3.1 may be used for regularized dynamics prediction, regularized adaptive control, and regularized observer design.

### 4.1 REGULARIZED ADAPTIVE DYNAMICS PREDICTION

Similar to direct adaptive control, online parameter estimation may also be used within an observer-like framework for dynamics prediction. This enables, for instance, the design of provably stable online learning rules for the weights of a recurrent neural network in the dynamics approximation context (Sussillo and Abbott, 2009; Alemi et al., 2018; Gilra and Gerstner, 2017). Consider a nonlinear system dynamics

$$\dot{\mathbf{x}} = \mathbf{f}(\mathbf{x}) + \mathbf{c}(t),$$

where  $\mathbf{x} \in \mathbb{R}^n$  is the system state,  $\mathbf{f} : \mathbb{R}^n \rightarrow \mathbb{R}^n$  is the system dynamics and  $\mathbf{c} : \mathbb{R}_+ \rightarrow \mathbb{R}^n$  is a system input. Define the observer-like system

$$\dot{\hat{\mathbf{x}}} = -k(\hat{\mathbf{x}} - \mathbf{x}) + \mathbf{Y}(\hat{\mathbf{x}})\hat{\mathbf{a}} + \mathbf{c}(t),$$

where  $\mathbf{Y} : \mathbb{R}^n \rightarrow \mathbb{R}^{n \times p}$ ,  $\hat{\mathbf{a}} \in \mathbb{R}^p$  and  $k > 0$  is a scalar gain. Assume that there exists a fixed parameter vector  $\mathbf{a}$  such that for all  $\mathbf{x} \in \mathbb{R}^n$ ,  $\mathbf{Y}(\mathbf{x})\mathbf{a} = \mathbf{f}(\mathbf{x})$ . By adding and subtracting  $\mathbf{f}(\hat{\mathbf{x}}) = \mathbf{Y}(\hat{\mathbf{x}})\mathbf{a}$ , the error  $\mathbf{e} = \hat{\mathbf{x}} - \mathbf{x}$  has dynamics

$$\dot{\mathbf{e}} = -k\mathbf{e} + \mathbf{Y}(\hat{\mathbf{x}})\tilde{\mathbf{a}} + \mathbf{f}(\hat{\mathbf{x}}) - \mathbf{f}(\mathbf{x}).$$

Consider the parameter estimator

$$\dot{\hat{\mathbf{a}}} = -\gamma [\nabla^2\psi(\hat{\mathbf{a}})]^{-1}\mathbf{Y}^\top(\hat{\mathbf{x}})\mathbf{\Gamma}\mathbf{e}, \quad (23)$$

where  $\gamma > 0$  is a constant learning rate,  $\psi$  is a strictly convex potential function, and  $\mathbf{\Gamma} \in \mathbb{R}^{n \times n} > 0$  is a constant symmetric positive definite matrix. Now consider the Lyapunov-like function

$$V = \frac{1}{2}\mathbf{e}^\top \mathbf{\Gamma} \mathbf{e} + \frac{1}{\gamma}d_\psi(\mathbf{a} \parallel \hat{\mathbf{a}}),$$

which has time derivative

$$\begin{aligned} \dot{V} &= \mathbf{e}^\top \mathbf{\Gamma} (-k\mathbf{e} + \mathbf{Y}(\hat{\mathbf{x}})\tilde{\mathbf{a}} + \mathbf{f}(\hat{\mathbf{x}}) - \mathbf{f}(\mathbf{x})) - \tilde{\mathbf{a}}^\top \mathbf{Y}^\top(\hat{\mathbf{x}})\mathbf{\Gamma}\mathbf{e}, \\ &= \mathbf{e}^\top \mathbf{\Gamma} (-k\mathbf{e} + \mathbf{f}(\hat{\mathbf{x}}) - \mathbf{f}(\mathbf{x})), \\ &= \mathbf{e}^\top \left( \int_0^1 \left( \mathbf{\Gamma} \frac{\partial \mathbf{f}}{\partial \mathbf{x}}(\mathbf{x} + s\mathbf{e}) - k\mathbf{\Gamma} \right) ds \right) \mathbf{e}. \end{aligned} \quad (24)$$

(24) shows that  $e \rightarrow 0$  as long as  $\mathbf{f}(\mathbf{x}) - k\mathbf{x}$  is contracting in the metric  $\mathbf{\Gamma}$  (Lohmiller and Slotine, 1998; Slotine, 2003), i.e., if

$$\left( \frac{\partial \mathbf{f}(\mathbf{x})}{\partial \mathbf{x}} \right)^T \mathbf{\Gamma} + \mathbf{\Gamma} \frac{\partial \mathbf{f}(\mathbf{x})}{\partial \mathbf{x}} \leq 2(k - \gamma) \mathbf{\Gamma}$$

uniformly over  $\mathbf{x}$  for some contraction rate  $\gamma > 0$ . It is simple to check that the metric  $\mathbf{\Gamma}$  may also be time-dependent,  $\mathbf{\Gamma} = \mathbf{\Gamma}(t)$ . More generally, rather than the proportional term  $-k\mathbf{e}$ , any term of the form  $\mathbf{g}(\dot{\mathbf{x}}) - \mathbf{g}(\mathbf{x})$  may be used in  $\dot{\mathbf{x}}$ , leading to the condition

$$\left( \frac{\partial \mathbf{f}(\mathbf{x})}{\partial \mathbf{x}} + \frac{\partial \mathbf{g}(\mathbf{x})}{\partial \mathbf{x}} \right)^T \mathbf{\Gamma} + \mathbf{\Gamma} \left( \frac{\partial \mathbf{f}(\mathbf{x})}{\partial \mathbf{x}} + \frac{\partial \mathbf{g}(\mathbf{x})}{\partial \mathbf{x}} \right) \leq -2\gamma' \mathbf{\Gamma}$$

uniformly over  $\mathbf{x}$  for some contraction rate  $\gamma' > 0$ . The implicit regularization results of Section 3.1 show that this framework provides a technique for provably regularizing learned predictive dynamics models without negatively impacting stability or convergence of the combined error and parameter estimation systems.

The above discussion demonstrates a separation theorem for adaptive dynamics prediction. If a dynamics predictor can be designed under the assumption that the true system dynamics is known – e.g., if bounds on  $\frac{\partial \mathbf{f}(\mathbf{x})}{\partial \dot{\mathbf{x}}}$  are available – then the same dynamics predictor can be made adaptive by incorporating the skew-symmetric law (23). Convergence properties then only depend on the nominal system with control feedback and are independent of the parameter estimator, as shown by the conditions for contraction.

**Remark 4.1.** In principle, these simple results could be made more general using the techniques developed in Lopez and Slotine (2019), or could be performed in a latent space computed via a nonlinear dimensionality reduction technique such as an autoencoder (Champion et al., 2019) or more generally a hierarchical expansion (Chen et al., 2018). This could also extend to adaptive control, for example in robot control applications where an adaptive controller could be designed in a latent space computed from raw pixels via a neural network.

## 4.2 REGULARIZED DYNAMICS PREDICTION FOR HAMILTONIAN SYSTEMS

If the underlying system is known to have a specific structure, this structure may be leveraged in a principled way to adaptively compute models for dynamics prediction (Sanner and Slotine, 1995). For example, large classes of physical systems are described via Hamiltonian dynamics,

$$\begin{aligned} \mathcal{H} &= \mathcal{H}(\mathbf{p}, \mathbf{q}), \\ \dot{\mathbf{p}} &= -\nabla_{\mathbf{q}} \mathcal{H}(\mathbf{p}, \mathbf{q}), \\ \dot{\mathbf{q}} &= \nabla_{\mathbf{p}} \mathcal{H}(\mathbf{p}, \mathbf{q}), \end{aligned}$$

where  $\mathcal{H}(\mathbf{p}, \mathbf{q})$  is the system Hamiltonian,  $\mathbf{p}$  is the generalized momentum, and  $\mathbf{q}$  is the generalized coordinate conjugate to  $\mathbf{p}$ . This structure was exploited in recent work by Chen et al. (2019) via direct estimation of the system Hamiltonian with a deep feedforward network in combination with symplectic integration of the resulting dynamics. In a similar spirit, rather than parameterizing the system dynamics as in Section 4.1, consider estimating the scalar Hamiltonian itself as a linear expansion in a set of known nonlinear basis functions  $\{Y_k\}$ ,

$$\hat{\mathcal{H}}(\hat{\mathbf{a}}, \mathbf{p}, \mathbf{q}) = \sum_k \hat{a}_k Y_k(\mathbf{p}, \mathbf{q}) = \mathbf{Y}(\mathbf{p}, \mathbf{q}) \hat{\mathbf{a}},$$

where  $\mathbf{Y}(\mathbf{p}, \mathbf{q}) \in \mathbb{R}^{1 \times p}$  is a row vector of basis functions. Assume that there exists some true parameter vector  $\mathbf{a}$  that exactly approximates the Hamiltonian globally, and consider the dynamics prediction model for  $k_p > 0$ ,  $k_q > 0$

$$\dot{\hat{\mathbf{p}}} = -(\nabla_{\mathbf{q}} \mathbf{Y}(\hat{\mathbf{p}}, \hat{\mathbf{q}})) \hat{\mathbf{a}} + k_p (\mathbf{p} - \hat{\mathbf{p}}), \quad (25)$$

$$\dot{\hat{\mathbf{q}}} = (\nabla_{\hat{\mathbf{p}}} \mathbf{Y}(\hat{\mathbf{p}}, \hat{\mathbf{q}})) \hat{\mathbf{a}} + k_q (\mathbf{q} - \hat{\mathbf{q}}). \quad (26)$$

The above predictor employs parameter sharing between both dynamics due to the direct estimation of the system Hamiltonian. The basis functions for the individual dynamics reflect

the symplectic structure, as they are given by partial derivatives of the basis functions for the Hamiltonian.

After subtracting the true dynamics  $\dot{\mathbf{p}}$  and  $\dot{\mathbf{q}}$  from above, consider the decomposition of the error dynamics

$$\begin{aligned}\dot{\tilde{\mathbf{p}}} &= -(\nabla_{\hat{\mathbf{q}}}\mathbf{Y}(\hat{\mathbf{p}}, \hat{\mathbf{q}}))\tilde{\mathbf{a}} - k_p\tilde{\mathbf{p}} - (\nabla_{\hat{\mathbf{q}}}\mathcal{H}(\hat{\mathbf{p}}, \hat{\mathbf{q}}) - \nabla_{\hat{\mathbf{q}}}\mathcal{H}(\mathbf{p}, \hat{\mathbf{q}})) - (\nabla_{\hat{\mathbf{q}}}\mathcal{H}(\mathbf{p}, \hat{\mathbf{q}}) - \nabla_{\mathbf{q}}\mathcal{H}(\mathbf{p}, \mathbf{q})), \\ \dot{\tilde{\mathbf{q}}} &= (\nabla_{\hat{\mathbf{p}}}\mathbf{Y}(\hat{\mathbf{p}}, \hat{\mathbf{q}}))\tilde{\mathbf{a}} - k_q\tilde{\mathbf{q}} + (\nabla_{\hat{\mathbf{p}}}\mathcal{H}(\hat{\mathbf{p}}, \hat{\mathbf{q}}) - \nabla_{\hat{\mathbf{p}}}\mathcal{H}(\hat{\mathbf{p}}, \mathbf{q})) + (\nabla_{\hat{\mathbf{p}}}\mathcal{H}(\hat{\mathbf{p}}, \mathbf{q}) - \nabla_{\mathbf{p}}\mathcal{H}(\mathbf{p}, \mathbf{q})),\end{aligned}$$

along with the adaptation law

$$\dot{\tilde{\mathbf{a}}} = \gamma [\nabla^2\psi(\hat{\mathbf{a}})]^{-1} \left( (\nabla_{\hat{\mathbf{q}}}\mathbf{Y}(\hat{\mathbf{p}}, \hat{\mathbf{q}}))^T \tilde{\mathbf{p}} - (\nabla_{\hat{\mathbf{p}}}\mathbf{Y}(\hat{\mathbf{p}}, \hat{\mathbf{q}}))^T \tilde{\mathbf{q}} \right),$$

with  $\gamma > 0$  a positive learning rate. The Lyapunov-like function

$$V = \frac{1}{2}\tilde{\mathbf{p}}^T\tilde{\mathbf{p}} + \frac{1}{2}\tilde{\mathbf{q}}^T\tilde{\mathbf{q}} + d_\psi(\mathbf{a} \parallel \hat{\mathbf{a}})$$

has time derivative

$$\begin{aligned}\dot{V} &= \tilde{\mathbf{p}}^T [ -(\nabla_{\hat{\mathbf{q}}}\mathbf{Y}(\hat{\mathbf{p}}, \hat{\mathbf{q}}))\tilde{\mathbf{a}} - k_p\tilde{\mathbf{p}} - (\nabla_{\hat{\mathbf{q}}}\mathcal{H}(\hat{\mathbf{p}}, \hat{\mathbf{q}}) - \nabla_{\hat{\mathbf{q}}}\mathcal{H}(\mathbf{p}, \hat{\mathbf{q}})) - (\nabla_{\hat{\mathbf{q}}}\mathcal{H}(\mathbf{p}, \hat{\mathbf{q}}) - \nabla_{\mathbf{q}}\mathcal{H}(\mathbf{p}, \mathbf{q})) ] \\ &\quad + \tilde{\mathbf{q}}^T [ (\nabla_{\hat{\mathbf{p}}}\mathbf{Y}(\hat{\mathbf{p}}, \hat{\mathbf{q}}))\tilde{\mathbf{a}} - k_q\tilde{\mathbf{q}} + (\nabla_{\hat{\mathbf{p}}}\mathcal{H}(\hat{\mathbf{p}}, \hat{\mathbf{q}}) - \nabla_{\hat{\mathbf{p}}}\mathcal{H}(\hat{\mathbf{p}}, \mathbf{q})) + (\nabla_{\hat{\mathbf{p}}}\mathcal{H}(\hat{\mathbf{p}}, \mathbf{q}) - \nabla_{\mathbf{p}}\mathcal{H}(\mathbf{p}, \mathbf{q})) ] \\ &\quad + \tilde{\mathbf{a}}^T \left( (\nabla_{\hat{\mathbf{q}}}\mathbf{Y}(\hat{\mathbf{p}}, \hat{\mathbf{q}}))^T \tilde{\mathbf{p}} - (\nabla_{\hat{\mathbf{p}}}\mathbf{Y}(\hat{\mathbf{p}}, \hat{\mathbf{q}}))^T \tilde{\mathbf{q}} \right) \\ &= \tilde{\mathbf{p}}^T [-k_p\tilde{\mathbf{p}} - (\nabla_{\hat{\mathbf{q}}}\mathcal{H}(\hat{\mathbf{p}}, \hat{\mathbf{q}}) - \nabla_{\hat{\mathbf{q}}}\mathcal{H}(\mathbf{p}, \hat{\mathbf{q}})) - (\nabla_{\hat{\mathbf{q}}}\mathcal{H}(\mathbf{p}, \hat{\mathbf{q}}) - \nabla_{\mathbf{q}}\mathcal{H}(\mathbf{p}, \mathbf{q}))] \\ &\quad + \tilde{\mathbf{q}}^T [-k_q\tilde{\mathbf{q}} + (\nabla_{\hat{\mathbf{p}}}\mathcal{H}(\hat{\mathbf{p}}, \hat{\mathbf{q}}) - \nabla_{\hat{\mathbf{p}}}\mathcal{H}(\hat{\mathbf{p}}, \mathbf{q})) + (\nabla_{\hat{\mathbf{p}}}\mathcal{H}(\hat{\mathbf{p}}, \mathbf{q}) - \nabla_{\mathbf{p}}\mathcal{H}(\mathbf{p}, \mathbf{q}))] \\ &= (\tilde{\mathbf{p}}^T \quad \tilde{\mathbf{q}}^T) \begin{pmatrix} -k_p\mathbf{I} - \int_0^1 \nabla_{\mathbf{p}+s\tilde{\mathbf{p}}}\nabla_{\hat{\mathbf{q}}}\mathcal{H}(\mathbf{p}+s\tilde{\mathbf{p}}, \hat{\mathbf{q}})ds & -\int_0^1 \nabla_{\mathbf{q}+s\tilde{\mathbf{q}}}\nabla_{\hat{\mathbf{p}}}\mathcal{H}(\hat{\mathbf{p}}, \mathbf{q}+s\tilde{\mathbf{q}})ds \\ \int_0^1 \nabla_{\mathbf{p}+s\tilde{\mathbf{p}}}^2\mathcal{H}(\mathbf{p}+s\tilde{\mathbf{p}}, \mathbf{q})ds & -k_q\mathbf{I} + \int_0^1 \nabla_{\mathbf{q}+s\tilde{\mathbf{q}}}\nabla_{\hat{\mathbf{p}}}\mathcal{H}(\hat{\mathbf{p}}, \mathbf{q}+s\tilde{\mathbf{q}})ds \end{pmatrix} \begin{pmatrix} \tilde{\mathbf{p}} \\ \tilde{\mathbf{q}} \end{pmatrix}\end{aligned}$$

A sufficient condition for convergence of  $\tilde{\mathbf{p}} \rightarrow 0$  and  $\tilde{\mathbf{q}} \rightarrow 0$  is uniform negative definiteness of the Jacobian matrix

$$\mathbf{J} = \begin{pmatrix} -k_p\mathbf{I} - \nabla_{\mathbf{p}}\nabla_{\mathbf{q}}\mathcal{H}(\mathbf{p}, \mathbf{q}) & -\nabla_{\mathbf{q}}^2\mathcal{H}(\mathbf{q}, \mathbf{p}) \\ \nabla_{\mathbf{p}}^2\mathcal{H}(\mathbf{p}, \mathbf{q}) & -k_q\mathbf{I} + \nabla_{\mathbf{q}}\nabla_{\mathbf{p}}\mathcal{H}(\mathbf{p}, \mathbf{q}) \end{pmatrix},$$

in  $\mathbf{p}$  and  $\mathbf{q}$ , i.e., contraction of the nominal  $\dot{\mathbf{p}}$  and  $\dot{\mathbf{q}}$  system in the Euclidean metric. Sufficient conditions for this are

$$\begin{aligned}k_p &> -\frac{1}{2}\lambda_{\min}(\nabla_{\mathbf{p}}\nabla_{\mathbf{q}}\mathcal{H}(\mathbf{p}, \mathbf{q}) + \nabla_{\mathbf{q}}\nabla_{\mathbf{p}}\mathcal{H}(\mathbf{p}, \mathbf{q})), \\ k_q &> \frac{1}{2}\lambda_{\max}(\nabla_{\mathbf{p}}\nabla_{\mathbf{q}}\mathcal{H}(\mathbf{p}, \mathbf{q}) + \nabla_{\mathbf{q}}\nabla_{\mathbf{p}}\mathcal{H}(\mathbf{p}, \mathbf{q})), \\ \lambda_p\lambda_q &> \frac{1}{4}\lambda_{\max}^2 [\nabla_{\mathbf{p}}^2\mathcal{H}(\mathbf{p}, \mathbf{q}) - \nabla_{\mathbf{q}}^2\mathcal{H}(\mathbf{p}, \mathbf{q})],\end{aligned}$$

where  $\lambda_p$  and  $\lambda_q$  are the contraction rates of the  $\dot{\mathbf{p}}$  and  $\dot{\mathbf{q}}$  systems respectively, given by the difference of the left- and right-hand sides of the first two inequalities above. More general conditions can be obtained by utilizing a non-identity metric, i.e., replacing the  $\frac{1}{2}\tilde{\mathbf{p}}^T\tilde{\mathbf{p}}$  and  $\frac{1}{2}\tilde{\mathbf{q}}^T\tilde{\mathbf{q}}$  terms in  $V$  by the Mahalanobis distances  $\frac{1}{2}\tilde{\mathbf{p}}^T\mathbf{\Gamma}_p\tilde{\mathbf{p}}$  and  $\frac{1}{2}\tilde{\mathbf{q}}^T\mathbf{\Gamma}_q\tilde{\mathbf{q}}$  where  $\mathbf{\Gamma}_p$  and  $\mathbf{\Gamma}_q$  are symmetric positive definite matrices. The adaptation law will need to be modified accordingly.

Rather than a general Hamiltonian  $\mathcal{H} = \mathcal{H}(\mathbf{p}, \mathbf{q})$ , it is common to have a separable Hamiltonian structure,

$$\mathcal{H}(\mathbf{p}, \mathbf{q}) = T(\mathbf{p}) + U(\mathbf{q}).$$

Above,  $T(\cdot)$  is the kinetic energy and  $U(\cdot)$  is the potential energy. Following an identical proof, the Jacobian matrix then reduces to

$$\mathbf{J} = \begin{pmatrix} -k_p\mathbf{I} & -\nabla_{\mathbf{q}}^2U(\hat{\mathbf{q}}) \\ \nabla_{\mathbf{p}}^2T(\hat{\mathbf{p}}) & -k_q\mathbf{I} \end{pmatrix},$$

so that the conditions for contraction in the Euclidean metric are simplified to

$$k_q k_p > \frac{1}{4} \lambda_{\max}^2 (\nabla_{\hat{\mathbf{p}}}^2 T(\hat{\mathbf{p}}) - \nabla_{\hat{\mathbf{q}}}^2 U(\hat{\mathbf{q}})). \quad (27)$$

The results of Section 3.1 show that the choice of  $\psi$  may be used to regularize the estimate of the Hamiltonian, and in turn, the dynamics. This may be used, for instance, for parsimonious Hamiltonian estimation through the combination of a rich set of physically motivated scalar basis functions and a sparse representation obtained via  $l_1$  regularization, similar to Champion et al. (2019). Further results that exploit the structure of separable Hamiltonians through independent estimation of the kinetic and potential energies are presented in Appendix B.

#### 4.3 REGULARIZED ADAPTIVE CONTROL FOR LAGRANGIAN SYSTEMS

A similar methodology can be applied to parameterize a scalar Lagrangian rather than Hamiltonian, leading to a second order differential equation with inertia matrix, centripetal and Coriolis forces, and potential energy parameterized by a shared set of weights. As we now show, generalizing the derivation of the Slotine and Li robot controller (Slotine and Li, 1987) to this setting allows for stable adaptive control of Lagrangian systems by direct estimation of the Lagrangian itself. Consider the Lagrangian

$$\mathcal{L} = \frac{1}{2} \dot{\mathbf{q}}^T \mathbf{H}(\mathbf{q}) \dot{\mathbf{q}} - U(\mathbf{q}),$$

with  $\mathbf{H}(\mathbf{q})$  an unknown inertia matrix and  $U(\mathbf{q})$  an unknown potential. Assume that the inertia matrix and scalar potential are given exactly by an expansion in physically motivated basis functions. That is, for a set of positive definite matrices  $\mathbf{M}^l > 0$  and scalar functions  $\phi^l$ ,

$$\begin{aligned} \mathbf{H}(\mathbf{q}) &= \sum_l a_l^{(K)} \mathbf{M}^l(\mathbf{q}), \\ U(\mathbf{q}) &= \sum_l a_l^{(P)} \phi^l(\mathbf{q}), \end{aligned}$$

where superscript  $(K)$  and  $(P)$  denote kinetic and potential, respectively, and the vectors  $\mathbf{a}^{(K)}$  and  $\mathbf{a}^{(P)}$  are unknown. The Euler-Lagrange equations of motion  $\frac{d}{dt} \frac{\partial \mathcal{L}}{\partial \dot{\mathbf{q}}} - \frac{\partial \mathcal{L}}{\partial \mathbf{q}} = \mathbf{u}$  with  $\mathbf{u}$  a control input then give the dynamics

$$\sum_{lj} a_l^{(K)} M_{ij}^l(\mathbf{q}) \ddot{q}_j + \sum_{lkj} a_l^{(K)} \dot{q}_k \dot{q}_j \left[ \frac{\partial M_{ij}^l(\mathbf{q})}{\partial q_k} - \frac{1}{2} \frac{\partial M_{kj}^l(\mathbf{q})}{\partial q_i} \right] + \sum_l a_l^{(P)} \frac{\partial \phi^l(\mathbf{q})}{\partial q_i} = u_i.$$

Above, the second term

$$\sum_{lkj} a_l^{(K)} \dot{q}_k \dot{q}_j \left[ \frac{\partial M_{ij}^l(\mathbf{q})}{\partial q_k} - \frac{1}{2} \frac{\partial M_{kj}^l(\mathbf{q})}{\partial q_i} \right]$$

uniquely defines the centripetal and Coriolis forces (traditionally written as  $\mathbf{C}(\mathbf{q}, \dot{\mathbf{q}})\dot{\mathbf{q}}$  with  $\mathbf{C}$  the Coriolis matrix), but does not uniquely define the Coriolis matrix (Slotine and Li, 1991). Choosing

$$C_{ij}(\mathbf{q}, \dot{\mathbf{q}}) = \sum_{kl} a_l^{(K)} \frac{1}{2} \left[ \frac{\partial M_{ij}^l(\mathbf{q})}{\partial q_k} - \left( \frac{\partial M_{kj}^l(\mathbf{q})}{\partial q_i} - \frac{\partial M_{ki}^l(\mathbf{q})}{\partial q_j} \right) \right] \dot{q}_k$$

preserves the Coriolis force  $\mathbf{C}(\mathbf{q}, \dot{\mathbf{q}})\dot{\mathbf{q}}$  and ensures that  $\dot{\mathbf{H}}(\mathbf{q}) - 2\mathbf{C}(\mathbf{q}, \dot{\mathbf{q}})$  is a skew-symmetric matrix. In matrix notation, the dynamics are then given by

$$\mathbf{H}(\mathbf{q}) \ddot{\mathbf{q}} + \mathbf{C}(\mathbf{q}, \dot{\mathbf{q}}) \dot{\mathbf{q}} + \mathbf{g}(\mathbf{q}) = \mathbf{u}$$

with the potential force  $\mathbf{g}(\mathbf{q}) = \sum_l a_l^{(P)} \nabla_{\mathbf{q}} \phi^l(\mathbf{q})$ . Defining  $\mathbf{s}$  and  $\dot{\mathbf{q}}_r$  as  $\mathbf{s} = \left( \frac{d}{dt} + \lambda \right) \tilde{\mathbf{q}} = \dot{\mathbf{q}} - \dot{\mathbf{q}}_r$ , these dynamics can be equivalently rewritten

$$\mathbf{H}(\mathbf{q}) \ddot{\mathbf{s}} + \mathbf{C}(\mathbf{q}, \dot{\mathbf{q}}) \mathbf{s} = \mathbf{u} - (\mathbf{H}(\mathbf{q}) \ddot{\mathbf{q}}_r + \mathbf{C}(\mathbf{q}, \dot{\mathbf{q}}) \dot{\mathbf{q}}_r + \mathbf{g}(\mathbf{q})). \quad (28)$$

Observe that because the Lagrangian was linearly parameterized, the resulting dynamics are also linearly parameterized. Defining the known basis functions

$$Y_{il}^{(P)} = \frac{\partial \phi^l(\mathbf{q})}{\partial q_i},$$

$$Y_{il}^{(K)} = \sum_{kj} \frac{1}{2} \left[ \frac{\partial M_{ij}^l(\mathbf{q})}{\partial q_k} - \left( \frac{\partial M_{kj}^l(\mathbf{q})}{\partial q_i} - \frac{\partial M_{ki}^l(\mathbf{q})}{\partial q_j} \right) \right] \dot{q}_k \dot{q}_{r,j} + \sum_j M_{ij}^l \ddot{q}_{r,j},$$

we can write (28) as

$$\mathbf{H}(\mathbf{q})\dot{\mathbf{s}} + \mathbf{C}(\mathbf{q}, \dot{\mathbf{q}})\mathbf{s} = \mathbf{u} - \mathbf{Y}^{(P)}\mathbf{a}^{(P)} - \mathbf{Y}^{(K)}\mathbf{a}^{(K)}.$$

For  $\mathbf{K} > 0$  a positive definite matrix and for parameter estimates  $\hat{\mathbf{a}}^{(P)}$  and  $\hat{\mathbf{a}}^{(K)}$ , taking  $\mathbf{u} = -\mathbf{K}\mathbf{s} + \mathbf{Y}^{(P)}\hat{\mathbf{a}}^{(P)} + \mathbf{Y}^{(K)}\hat{\mathbf{a}}^{(K)}$  leads to

$$\mathbf{H}(\mathbf{q})\dot{\mathbf{s}} + \mathbf{C}(\mathbf{q}, \dot{\mathbf{q}})\mathbf{s} = -\mathbf{K}\mathbf{s} + \mathbf{Y}^{(P)}\hat{\mathbf{a}}^{(P)} + \mathbf{Y}^{(K)}\hat{\mathbf{a}}^{(K)}.$$

The proof in Slotine and Li (1987) can now be directly extended. For  $\psi^{(K)}, \psi^{(P)}$  strictly convex functions and  $\gamma_K > 0, \gamma_P > 0$  positive gains, the Lyapunov-like function

$$V = \frac{1}{2}\mathbf{s}^T \mathbf{H}(\mathbf{q})\mathbf{s} + \frac{1}{\gamma_K} d_{\psi^{(K)}} \left( \mathbf{a}^{(K)} \parallel \hat{\mathbf{a}}^{(K)} \right) + \frac{1}{\gamma_P} d_{\psi^{(P)}} \left( \mathbf{a}^{(P)} \parallel \hat{\mathbf{a}}^{(P)} \right),$$

shows stability of the adaptation laws

$$\dot{\hat{\mathbf{a}}}^{(K)} = -\gamma_K \left( \nabla^2 \psi^{(K)} \left( \hat{\mathbf{a}}^{(K)} \right) \right)^{-1} \left[ \mathbf{Y}^{(K)} \right]^T \mathbf{s},$$

$$\dot{\hat{\mathbf{a}}}^{(P)} = -\gamma_P \left( \nabla^2 \psi^{(P)} \left( \hat{\mathbf{a}}^{(P)} \right) \right)^{-1} \left[ \mathbf{Y}^{(P)} \right]^T \mathbf{s},$$

after an application of Barbalat's Lemma (Lemma A.1) and using skew-symmetry of  $\dot{\mathbf{H}} - 2\mathbf{C}$  to eliminate  $\frac{1}{2}\mathbf{s}^T \dot{\mathbf{H}}\mathbf{s}$ . In physical applications, dimensions or relative scaling of the components of  $\hat{\mathbf{a}}^{(K)}$  and  $\hat{\mathbf{a}}^{(P)}$  can be handled as described in Remarks 2.6 and 3.5.

As in Section 4.2, by using an  $l_1$  approximation for  $\psi$ , this approach may find sparse, interpretable models of the kinetic and potential energies. Estimating the potential energy directly may in some cases lead to simpler parameterizations than estimating the resulting forces.

If more structure in the inertia matrix is known, for example that it depends only on a few unknown parameters, it may still be approximated using the usual Slotine and Li controller. The external forces can then be estimated by directly estimating the corresponding potential that generates them.

#### 4.4 REGULARIZED ADAPTIVE OBSERVER DESIGN

In many physical and engineering systems, only a low-dimensional output of the system  $\mathbf{y}(\mathbf{x}) \in \mathbb{R}^m$  is available for measurement. Assuming that  $\mathbf{y}(\mathbf{x}) = \mathbf{C}\mathbf{x}$  is a linear readout for some known matrix  $\mathbf{C} \in \mathbb{R}^{m \times n}$ , we now show that the tools of the previous two subsections can be used to design regularized adaptive observers for the full system state. Assume that the true system dynamics satisfies

$$\dot{\mathbf{x}} = \mathbf{f}(\mathbf{x}) + \mathbf{c}(t) = \mathbf{Y}(\mathbf{y}(\mathbf{x}))\mathbf{a} + \mathbf{c}(t),$$

with  $\mathbf{a} \in \mathbb{R}^p$  a vector of unknown parameters, and where the known regressor matrix  $\mathbf{Y} \in \mathbb{R}^{n \times p}$  only depends on the system output  $\mathbf{y}(\mathbf{x})$ . Consider the adaptive observer

$$\dot{\hat{\mathbf{x}}} = \mathbf{Y}(\hat{\mathbf{y}})\hat{\mathbf{a}} + \mathbf{c}(t) + \mathbf{g}(\hat{\mathbf{y}}) - \mathbf{g}(\mathbf{y}),$$

$$\dot{\hat{\mathbf{a}}} = -\gamma \left( \nabla^2 \psi(\hat{\mathbf{a}}) \right)^{-1} \mathbf{Y}^T(\hat{\mathbf{y}}) \mathbf{C}^T \mathbf{\Gamma} \tilde{\mathbf{y}},$$

with  $\gamma > 0$  a positive learning rate,  $\hat{\mathbf{y}} = \mathbf{y}(\hat{\mathbf{x}})$ ,  $\psi$  a strictly convex potential function, and  $\mathbf{\Gamma}$  a positive definite matrix. The Lyapunov-like function

$$V = \frac{1}{2} \tilde{\mathbf{y}}^T \mathbf{\Gamma} \tilde{\mathbf{y}} + \frac{1}{\gamma} d_\psi(\mathbf{a} \parallel \hat{\mathbf{a}}),$$

has time derivative

$$\begin{aligned}\dot{V} &= \tilde{\mathbf{y}}^T \mathbf{\Gamma} \mathbf{C} (\mathbf{Y}(\hat{\mathbf{y}}) \tilde{\mathbf{a}} + [\mathbf{Y}(\hat{\mathbf{y}}) - \mathbf{Y}(\mathbf{y})] \mathbf{a} + \mathbf{g}(\hat{\mathbf{y}}) - \mathbf{g}(\mathbf{y})) - \tilde{\mathbf{y}}^T \mathbf{\Gamma} \mathbf{C} \mathbf{Y}(\hat{\mathbf{y}}) \tilde{\mathbf{a}}, \\ &= \tilde{\mathbf{y}}^T \mathbf{\Gamma} \mathbf{C} ([\mathbf{Y}(\hat{\mathbf{y}}) - \mathbf{Y}(\mathbf{y})] \mathbf{a} + \mathbf{g}(\hat{\mathbf{y}}) - \mathbf{g}(\mathbf{y})), \\ &= \tilde{\mathbf{y}}^T \left( \mathbf{\Gamma} \mathbf{C} \int_0^1 \left( \frac{\partial \mathbf{Y}(\mathbf{y} + s\tilde{\mathbf{y}})}{\partial \mathbf{y}} \mathbf{a} + \frac{\partial \mathbf{g}(\mathbf{y} + s\tilde{\mathbf{y}})}{\partial \mathbf{y}} \right) ds \right) \tilde{\mathbf{y}},\end{aligned}$$

which shows that a sufficient condition for convergence of  $\tilde{\mathbf{y}} \rightarrow 0$  is

$$\mathbf{\Gamma} \mathbf{C} \left( \frac{\partial \mathbf{Y}(\mathbf{y}) \mathbf{a}}{\partial \mathbf{y}} + \frac{\partial \mathbf{g}(\mathbf{y})}{\partial \mathbf{y}} \right) + \left( \frac{\partial \mathbf{Y}(\mathbf{y}) \mathbf{a}}{\partial \mathbf{y}} + \frac{\partial \mathbf{g}(\mathbf{y})}{\partial \mathbf{y}} \right)^T \mathbf{C}^T \mathbf{\Gamma} \leq -\lambda \mathbf{\Gamma}$$

uniformly in  $\mathbf{y}$  for some contraction rate  $\lambda > 0$ . A natural choice of  $\mathbf{g}(\mathbf{y})$  to satisfy this condition with  $\mathbf{\Gamma} = \mathbf{I}$  is  $\mathbf{g}(\mathbf{y}) = -k \mathbf{C}^T \mathbf{y}$  for some  $k > 0$  if  $\mathbf{C} \mathbf{C}^T$  is full rank. The requirement is equivalent to contraction of the unknown output dynamics

$$\dot{\mathbf{y}} = \mathbf{C} \mathbf{Y}(\mathbf{y}) \mathbf{a} + \mathbf{C} \mathbf{g}(\mathbf{y}) + \mathbf{C} \mathbf{c}(t)$$

in the metric  $\mathbf{\Gamma}$ . Under suitable observability assumptions on the system, convergence of  $\hat{\mathbf{y}}$  to  $\mathbf{y}$  ensures that  $\hat{\mathbf{x}}$  converges to  $\mathbf{x}$ , and hence that the full system state can be observed (Luenberger, 1979).

As in Section 4.1, this discussion demonstrates a separation theorem for adaptive observer design. If an observer can be designed for the true system with unknown parameters, then the same observer can be made adaptive by incorporating the adaptation law presented in this section. Convergence properties then depend only on the true system with feedback, and are independent of the parameter estimator. The results of Section 3.1 show that the choice of  $\psi$  can be used to regularize the observer model while maintaining provable reconstruction of the full system state.

#### 4.5 REGULARIZED DYNAMICS PREDICTION FOR RECURRENT NEURAL NETWORKS

Consider a recurrent neural network model

$$\tau \dot{\mathbf{x}} = -\mathbf{x} + \boldsymbol{\sigma}(\mathbf{\Theta} \mathbf{x}) \quad (29)$$

with  $\mathbf{x} \in \mathbb{R}^n$  a vector of neuron firing rates,  $\mathbf{\Theta} \in \mathbb{R}^{n \times n}$  the synaptic weights,  $\boldsymbol{\sigma}(\mathbf{\Theta} \mathbf{x})$  the post-synaptic potentials, and  $\tau > 0$  a relaxation timescale. Let  $\boldsymbol{\sigma}(\cdot)$  be an elementwise Lipschitz and monotonic activation function, i.e.,

$$\begin{aligned}\boldsymbol{\sigma}(\mathbf{x})_i &= \sigma_i(x_i), \\ |\sigma_i(x) - \sigma_i(y)| &\leq L_i |x - y|, \\ (x - y)(\sigma_i(x) - \sigma_i(y)) &\geq 0.\end{aligned}$$

These requirements are satisfied by common activation functions such as the ReLU, softplus, tanh, and sigmoid. For  $\psi$  a strictly convex function on  $n \times n$  matrices or vectors in  $\mathbb{R}^{n^2}$  and  $\gamma > 0$  a positive gain, consider the regularized adaptive dynamics predictor for (29),

$$\tau \dot{\hat{\mathbf{x}}} = -\hat{\mathbf{x}} + \boldsymbol{\sigma}(\hat{\mathbf{\Theta}} \mathbf{x}) + k(\mathbf{x} - \hat{\mathbf{x}}), \quad (30)$$

$$\dot{\hat{\mathbf{\Theta}}} = -\gamma \left( \nabla^2 \psi(\hat{\mathbf{\Theta}}) \right)^{-1} \left( \boldsymbol{\sigma}(\hat{\mathbf{\Theta}} \mathbf{x}) - \boldsymbol{\sigma}(\mathbf{\Theta} \mathbf{x}) \right) \mathbf{x}^T. \quad (31)$$

In (30), the true vector of firing rates  $\mathbf{x}$  is used underneath the application of  $\boldsymbol{\sigma}(\cdot)$  in the  $\hat{\mathbf{x}}$  dynamics. The update law (31) can be seen as the vector-valued generalization of the algorithm considered in Remark 2.4. The Lyapunov-like function

$$V = \frac{1}{\gamma} d_\psi(\mathbf{\Theta} \parallel \hat{\mathbf{\Theta}}),$$

has time derivative

$$\begin{aligned}
\dot{V} &= - \sum_{ij} \tilde{\Theta}_{ij} \left( \boldsymbol{\sigma}(\hat{\Theta}\mathbf{x}) - \boldsymbol{\sigma}(\Theta\mathbf{x}) \right)_i x_j, \\
&= - \sum_{ij} \tilde{\Theta}_{ij} \left( \sigma_i \left( \sum_k \hat{\Theta}_{ik} x_k \right) - \sigma_i \left( \sum_k \Theta_{ik} x_k \right) \right) x_j, \\
&= - \sum_i \left( \sum_k \tilde{\Theta}_{ik} x_k \right) \left( \sigma_i \left( \sum_k \hat{\Theta}_{ik} x_k \right) - \sigma_i \left( \sum_k \Theta_{ik} x_k \right) \right), \\
&\leq - \sum_i \frac{1}{L_i} \left( \sigma_i \left( \sum_k \hat{\Theta}_{ik} x_k \right) - \sigma_i \left( \sum_k \Theta_{ik} x_k \right) \right)^2, \\
&\leq - \frac{1}{\max_k L_k} \left\| \boldsymbol{\sigma}(\hat{\Theta}\mathbf{x}) - \boldsymbol{\sigma}(\Theta\mathbf{x}) \right\|_2^2 \leq 0.
\end{aligned}$$

Integrating the above inequality shows that  $[\boldsymbol{\sigma}(\hat{\Theta}\mathbf{x}) - \boldsymbol{\sigma}(\Theta\mathbf{x})]$  is an  $\mathcal{L}_2$  signal and hence that each component  $[\sigma_i(\hat{\Theta}\mathbf{x}) - \sigma_i(\Theta\mathbf{x})]$  is also an  $\mathcal{L}_2$  signal. The error dynamics

$$\dot{\mathbf{e}} = -(k+1)\mathbf{e} + \boldsymbol{\sigma}(\hat{\Theta}\mathbf{x}) - \boldsymbol{\sigma}(\Theta\mathbf{x}),$$

shows that each component  $e_i$  is a low-pass filter of each component of the function approximation error  $[\sigma_i(\hat{\Theta}\mathbf{x}) - \sigma_i(\Theta\mathbf{x})]$ . Applying Lemma A.2 shows that  $\mathbf{e} \rightarrow 0$ . This approach could be used, for example, for identifying regularized low-dimensional models in computational neuroscience. Our results are similar to those of Foster et al. (2020), but handle a mirror descent or natural gradient extension valid in the continuous-time deterministic setting.

The adaptation law (31) cannot be implemented directly through a PI form. However, it can be well-approximated, for example by the PI construction

$$\begin{aligned}
\dot{\bar{\mathbf{x}}} &= \lambda(\mathbf{x} - \bar{\mathbf{x}}), \\
\nabla \psi(\hat{\Theta}) &= \gamma(\Theta - \mathbf{e}\bar{\mathbf{x}}^\top), \\
\dot{\bar{\Theta}} &= -(k+1)\mathbf{e}\bar{\mathbf{x}}^\top + \lambda\mathbf{e}(\mathbf{x} - \bar{\mathbf{x}})^\top,
\end{aligned}$$

for  $\lambda > 0$  a positive gain ensuring  $\bar{\mathbf{x}} \approx \mathbf{x}$ .

## 5 VELOCITY GRADIENT ALGORITHMS AND THE BREGMAN LAGRANGIAN

In this section, we provide background material on the velocity gradient formalism (Fradkov, 1980; Fradkov et al., 1999; Andrievskii et al., 1988; Fradkov, 1986) and the Bregman Lagrangian (Wibisono et al., 2016; Betancourt et al., 2018; Wilson et al., 2016).

### 5.1 VELOCITY GRADIENT ALGORITHMS

We now provide a brief introduction to a class of adaptive control methods known as velocity gradient algorithms (Fradkov et al., 1999; Fradkov, 1980; Andrievskii et al., 1988; Fradkov, 1986). In their most basic form, they are specified by a “local” goal functional  $Q(\mathbf{x}, t) : \mathbb{R}^n \times \mathbb{R}_+ \rightarrow \mathbb{R}$  we would like to drive to zero. The adaptation law is defined as

$$\dot{\hat{\mathbf{a}}} = -\mathbf{P} \nabla_{\hat{\mathbf{a}}} \dot{Q}(\mathbf{x}, \hat{\mathbf{a}}, t). \quad (32)$$

where  $\mathbf{P} = \mathbf{P}^\top > 0$  is a positive definite matrix of learning rates of appropriate dimension, and  $\dot{Q}(\mathbf{x}, \hat{\mathbf{a}}, t) = (\nabla_{\mathbf{x}} Q(\mathbf{x}, t))^\top \dot{\mathbf{x}} + \frac{\partial Q(\mathbf{x}, t)}{\partial t}$ . Intuitively, while the goal functional  $Q(\mathbf{x}, t)$  may only depend on the control parameters  $\hat{\mathbf{a}}$  indirectly through  $\mathbf{x}$ , its time derivative will depend

explicitly on  $\hat{\mathbf{a}}$  through  $\dot{\mathbf{x}}$ <sup>6</sup>. The adaptation law (32) ensures that  $\hat{\mathbf{a}}$  moves in a direction that instantaneously decreases  $\dot{Q}(\mathbf{x}, \hat{\mathbf{a}}, t)$ . Under the conditions specified by Assumptions 5.1-5.3, this causes  $\dot{Q}(\mathbf{x}, \hat{\mathbf{a}}, t)$  to be negative for long enough to accomplish the control goal (Fradkov et al., 1999).  $Q(\mathbf{x}, t)$  is required to satisfy three main assumptions to ensure that this is the case.

**Assumption 5.1.**  $Q(\mathbf{x}, t)$  is non-negative and radially unbounded, so that  $Q(\mathbf{x}, t) \geq 0$  for all  $\mathbf{x}, t$  and  $Q(\mathbf{x}, t) \rightarrow \infty$  when  $\|\mathbf{x}\| \rightarrow \infty$ .  $Q(\mathbf{x}, t)$  is uniformly continuous in  $t$  whenever  $\mathbf{x}$  is bounded. ◇

**Assumption 5.2.** There exists an ideal set of control parameters  $\mathbf{a}$  such that the origin of the system (1) is globally asymptotically stable when the control is evaluated at  $\mathbf{a}$ . Furthermore,  $Q(\mathbf{x}, t)$  is a Lyapunov function for the system when the control is evaluated at  $\mathbf{a}$ . That is, there exists a strictly increasing function  $\rho$  such that  $\rho(0) = 0$  with  $\dot{Q}(\mathbf{x}, \mathbf{a}, t) \leq -\rho(Q)$ . ◇

**Assumption 5.3.** The time derivative of  $Q$  is convex in the control parameters  $\hat{\mathbf{a}}$ , i.e.,

$$\dot{Q}(\mathbf{x}, \mathbf{a}_1, t) \geq \dot{Q}(\mathbf{x}, \mathbf{a}_2, t) + (\mathbf{a}_1 - \mathbf{a}_2)^\top \nabla_{\mathbf{a}_2} \dot{Q}(\mathbf{x}, \mathbf{a}_2, t), \quad (33)$$

is satisfied for all  $\mathbf{a}_1$  and  $\mathbf{a}_2$ . ◇

The properties of (32) are summarized in the following proposition (Fradkov et al., 1999).

**Proposition 5.1.** *Consider the local velocity gradient algorithm (32) under Assumptions 5.1-5.3. Then all solutions  $(\mathbf{x}(t), \hat{\mathbf{a}}(t))$  of (1) and (32) remain bounded, and*

$$\lim_{t \rightarrow \infty} Q(\mathbf{x}(t), t) = 0$$

for all  $\mathbf{x}(0) \in \mathbb{R}^n$ .

The proof follows by consideration of the Lyapunov-like function  $V = Q + \frac{1}{2}\hat{\mathbf{a}}^\top \mathbf{P}^{-1} \hat{\mathbf{a}}$ .

**Remark 5.1.** If  $Q(\mathbf{x}, t)$  is chosen so that  $\dot{Q}(\mathbf{x}, \hat{\mathbf{a}}, t)$  depends on  $\hat{\mathbf{a}}$  only through  $\hat{f}(\mathbf{x}, \hat{\mathbf{a}}, t)$  and  $f(\mathbf{x}, \mathbf{a}, t)$  is linearly parameterized, then Assumption 5.3 will immediately be satisfied by convexity of affine functions. Indeed, consider defining the goal functional  $Q(\mathbf{x}, t) = \frac{1}{2}s(\mathbf{x}, t)^2$  for system (1) where  $s$  depends on  $t$  through  $x_d(t)$ . It is clear that this proposed goal functional satisfies Assumptions 5.1 and 5.2 for bounded  $x_d(t)$ . Then  $\dot{Q}(\mathbf{x}, \hat{\mathbf{a}}, t) = -\eta s(\mathbf{x}, t)^2 + s\hat{f}(\mathbf{x}, \hat{\mathbf{a}}, \mathbf{a}, t)$ , and (32) exactly recovers the Slotine and Li controller (8). ◇

**Remark 5.2.** An alternative perspective on velocity gradient algorithms can be found by using the expression  $\dot{Q}(\mathbf{x}, \hat{\mathbf{a}}, t) = (\nabla_{\mathbf{x}} Q(\mathbf{x}, t))^\top \dot{\mathbf{x}} + \frac{\partial Q(\mathbf{x}, t)}{\partial t}$ . Assume that  $\dot{\mathbf{x}} = \mathbf{u} - \mathbf{Y}(\mathbf{x}, t)\mathbf{a}$ , and set  $\mathbf{u} = \mathbf{Y}(\mathbf{x}, t)\hat{\mathbf{a}} + \mathbf{u}_d$  where  $\mathbf{u}_d$  ensures that  $\mathbf{x}(t) \rightarrow \mathbf{x}_d(t)$  for  $\hat{\mathbf{a}} = \mathbf{a}$ . Then  $\nabla_{\hat{\mathbf{a}}} \dot{Q}(\mathbf{x}, \hat{\mathbf{a}}, t) = \mathbf{Y}^\top \nabla_{\mathbf{x}} Q(\mathbf{x}, t)$ . This shows that the adaptation law  $\dot{\hat{\mathbf{a}}} = -\mathbf{P} \nabla_{\hat{\mathbf{a}}} \dot{Q}(\mathbf{x}, \hat{\mathbf{a}}, t) = -\mathbf{P} \mathbf{Y}(\mathbf{x}, t)^\top \nabla_{\mathbf{x}} Q(\mathbf{x}, t)$  transforms the gradient of  $Q(\mathbf{x}, t)$  with respect to  $\mathbf{x}$  by pre-multiplication by the regressor  $\mathbf{Y}(\mathbf{x}, t)^\top$ . This interpretation applies to the observers and dynamics predictors designed in Section 4, as well as the adaptation law for contracting systems developed in (Lopez and Slotine, 2019). Conversely, this perspective shows that if a Lyapunov function  $V(\mathbf{x}, t)$  is known for a nominal system  $\dot{\mathbf{x}} = \mathbf{f}(\mathbf{x}, t)$ , then the control input  $\mathbf{u} = \mathbf{Y}(\mathbf{x}, t)\hat{\mathbf{a}}$  with adaptation law  $\dot{\hat{\mathbf{a}}} = -\mathbf{P} \mathbf{Y}^\top \nabla_{\mathbf{x}} V(\mathbf{x}, t)$  will return the perturbed system  $\dot{\mathbf{x}} = \mathbf{f}(\mathbf{x}, t) + \mathbf{u} - \mathbf{Y}(\mathbf{x}, t)\mathbf{a}$  back to its nominal behavior.

Rather than a local functional, one may instead specify an integral goal functional of the form  $Q(\mathbf{x}, \hat{\mathbf{a}}, t) = \int_0^t R(\mathbf{x}(t'), \hat{\mathbf{a}}(t'), t') dt'$ . In this case, (32) takes the form

$$\dot{\hat{\mathbf{a}}} = -\mathbf{P} \nabla_{\hat{\mathbf{a}}} R(\mathbf{x}, \hat{\mathbf{a}}, t). \quad (34)$$

Equation (34) is a gradient flow algorithm on the loss function  $R(\mathbf{x}, \hat{\mathbf{a}}, t)$ . We now replace Assumptions 5.1 and 5.2 by a slightly modified setting.

**Assumption 5.4.**  $R$  is a non-negative function and  $R(\mathbf{x}(t), \hat{\mathbf{a}}(t), t)$  is uniformly continuous in  $t$  for bounded  $\mathbf{x}$  and  $\hat{\mathbf{a}}$ . Furthermore,  $\nabla_{\hat{\mathbf{a}}} R(\mathbf{x}, \hat{\mathbf{a}}, t)$  is locally bounded in  $\mathbf{x}$  and  $\hat{\mathbf{a}}$  uniformly in  $t$ . ◇

<sup>6</sup>It will also depend on  $\mathbf{a}$ , but we suppress this dependence for notational simplicity.

**Assumption 5.5.** There exists an ideal set of controller parameters  $\mathbf{a}$  and a scalar function  $\mu$  such that  $\int_0^\infty \mu(t')dt' < \infty$ ,  $\lim_{t \rightarrow \infty} \mu(t) = 0$ , and  $R(\mathbf{x}(t), \mathbf{a}, t) \leq \mu(t)$  for all  $t$ .  $\diamond$

The properties of algorithm (34) are summarized in the following proposition (Fradkov et al., 1999).

**Proposition 5.2.** *Consider the integral velocity gradient algorithm (34) where the goal functional  $Q$  satisfies Assumptions 5.3-5.5. Then  $Q(t) \leq \alpha$  where*

$$\alpha = \frac{1}{2} \tilde{\mathbf{a}}(0)^\top \mathbf{P}^{-1} \tilde{\mathbf{a}}(0) + \int_0^\infty \mu(t')dt',$$

and  $\int R(\mathbf{x}(t'), \hat{\mathbf{a}}(t'), t')dt' < \infty$  over the maximal interval of existence of  $\mathbf{x}$ . Furthermore,  $R(\mathbf{x}, \hat{\mathbf{a}}, t) \rightarrow 0$  for any bounded solution  $\mathbf{x}(t)$ .

The proof follows by consideration of the Lyapunov-like function  $V = \int_0^t R(\mathbf{x}(t'), \hat{\mathbf{a}}(t'), t')dt' + \frac{1}{2} \tilde{\mathbf{a}}^\top \mathbf{P}^{-1} \tilde{\mathbf{a}} + \int_t^\infty \mu(t')dt'$ .

Integral functionals allow the specification of a control goal that depends on all past data.  $R(\mathbf{x}, \hat{\mathbf{a}}, t)$  is chosen so that it does not necessarily depend on the structure of the dynamics, but depends explicitly on  $\hat{\mathbf{a}}$ . Local functionals, on the other hand, result in adaptation laws that do have an explicit dependence on the dynamics through the appearance of the term  $\left(\frac{\partial Q}{\partial \mathbf{x}}\right)^\top \dot{\mathbf{x}}$  in  $\dot{Q}(\mathbf{x}, \hat{\mathbf{a}}, t)$ .

Integral functionals can be particularly useful if  $R(\mathbf{x}, \hat{\mathbf{a}}, t) \rightarrow 0$  implies the desired control goal. In this work, we will focus on the choice  $R(\mathbf{x}, \hat{\mathbf{a}}, t) = \frac{1}{2} \tilde{f}(\mathbf{x}, \hat{\mathbf{a}}, \mathbf{a}, t)^2$ , which will require a PI form as described in Section 2 in the context of Tyukin's algorithm<sup>7</sup>. In particular, note that for this choice of  $R$  the result of Proposition 5.2 implies that  $\tilde{f} \in \mathcal{L}_2$  over the maximal interval of existence of  $\mathbf{x}$ . For some error models, this is enough to ensure that  $\mathbf{x} \in \mathcal{L}_\infty$ , and hence that  $\tilde{f}(\mathbf{x}, \hat{\mathbf{a}}, \mathbf{a}, t) \rightarrow 0$  and  $\mathbf{x} \rightarrow \mathbf{x}_d$ <sup>8</sup>.

Goal functionals can also be written as a sum of local and integral functionals with similar guarantees, and these approaches will lead to composite algorithms in the subsequent sections. The interested reader is referred to Fradkov et al. (1999), Chapter 3 for more details.

**Remark 5.3.** Following the developments of Section 3, we can immediately prove analogous results for natural gradient or mirror descent-like analogues of velocity gradient algorithms. For local functionals, the adaptation law

$$\dot{\hat{\mathbf{a}}} = -\gamma (\nabla^2 \psi(\hat{\mathbf{a}}))^{-1} \nabla_{\hat{\mathbf{a}}} \dot{Q}(\mathbf{x}, \hat{\mathbf{a}}, t)$$

with  $\gamma > 0$  a positive learning rate and  $\psi$  a strictly convex function will lead to the same conclusions as Proposition 5.1 under the same conditions. The proof follows by consideration of the Lyapunov-like function

$$V = Q(\mathbf{x}, t) + d_\psi(\mathbf{a} \parallel \hat{\mathbf{a}}).$$

Similarly, the Lyapunov-like function

$$V = \int_0^t R(\mathbf{x}(t'), \hat{\mathbf{a}}(t'), t')dt' + d_\psi(\mathbf{a} \parallel \hat{\mathbf{a}}) + \int_t^\infty \mu(t')dt'$$

shows that the same conclusions as in Proposition 5.2 hold under the same conditions for the integral natural velocity gradient algorithm

$$\dot{\hat{\mathbf{a}}} = -\gamma (\nabla^2 \psi(\hat{\mathbf{a}}))^{-1} \nabla_{\hat{\mathbf{a}}} R(\mathbf{x}, \hat{\mathbf{a}}, t).$$

In both cases, the choice of  $\psi$  offers a principled way to regularize velocity gradient algorithms.  $\diamond$

<sup>7</sup>Indeed, Tyukin's algorithm can be seen as an integral velocity gradient algorithm with the pseudogradient modification described in Section 2.

<sup>8</sup>See, for example, Lemma A.2, which shows that our error model (4) has this property.

## 5.2 THE BREGMAN LAGRANGIAN AND ACCELERATED OPTIMIZATION ALGORITHMS

In Wibisono et al. (2016), the *Bregman Lagrangian* was shown to generate a suite of accelerated optimization algorithms in continuous-time by appealing to the Euler Lagrange equations through the principle of least action. In its original form, the Bregman Lagrangian is given by

$$\mathcal{L}(\mathbf{x}, \dot{\mathbf{x}}, t) = e^{\bar{\alpha} + \bar{\gamma}} \left( d_\psi(\mathbf{x} + e^{-\bar{\alpha}} \dot{\mathbf{x}} \parallel \mathbf{x}) - e^{\bar{\beta}} f(\mathbf{x}) \right). \quad (35)$$

In (35),  $f(\mathbf{x})$  is the loss function to be optimized, and  $\psi(\mathbf{x})$  is a strictly convex function. We will take  $\psi(\cdot) = \frac{1}{2} \|\cdot\|_2^2$  in Section 6, and will consider extensions to arbitrary  $\psi$  in Section 7. Allowing for arbitrary  $\psi$  extends the algorithms presented in Section 6 to the natural gradient-like setting of Section 2.3.

The quantities  $\bar{\alpha}(t) : \mathbb{R}_+ \rightarrow \mathbb{R}$ ,  $\bar{\beta}(t) : \mathbb{R}_+ \rightarrow \mathbb{R}$ , and  $\bar{\gamma}(t) : \mathbb{R}_+ \rightarrow \mathbb{R}$  in (35) are arbitrary time-dependent functions that will ultimately set the damping and learning rates in the second-order Euler Lagrange dynamics. To generate accelerated optimization algorithms, Wibisono, Wilson, and Jordan required two *ideal scaling conditions*:  $\dot{\bar{\beta}} \leq e^{\bar{\alpha}}$  and  $\dot{\bar{\gamma}} = e^{\bar{\alpha}}$ . These conditions originate from the Euler Lagrange equations, where the second is used to eliminate an unwanted term, and a Lyapunov argument, where the first is used to ensure decrease of a chosen Lyapunov function.

Gaudio et al. (2019) recently utilized the Bregman Lagrangian to derive a momentum-like adaptive control algorithm. To do so, they defined  $\bar{\alpha} = \log(\beta\mathcal{N})$ ,  $\bar{\beta} = \log\left(\frac{\gamma}{\beta\mathcal{N}}\right)$ , and  $\bar{\gamma} = \int e^{\bar{\alpha}} dt$ <sup>9</sup>. Here,  $\gamma \geq 0$  and  $\beta \geq 0$  are non-negative scalar hyperparameters and  $\mathcal{N} = \mathcal{N}(t)$  is a context-dependent signal chosen based on the system. With these definitions, choosing the Euclidean norm  $\psi(\cdot) = \frac{1}{2} \|\cdot\|^2$ , and modifying the Bregman Lagrangian presented in Gaudio et al. (2019) to the adaptive control framework defined in Section 2, (35) becomes

$$\mathcal{L}(\hat{\mathbf{a}}, \dot{\hat{\mathbf{a}}}, t) = e^{\int_0^t \beta\mathcal{N}(s) ds} \frac{1}{\beta\mathcal{N}} \left( \frac{1}{2} \dot{\hat{\mathbf{a}}}^\top \dot{\hat{\mathbf{a}}} - \gamma\beta\mathcal{N} \frac{d}{dt} \left[ \frac{1}{2} s^2 \right] \right). \quad (36)$$

Comparing (35) and (36), it is clear that the loss function  $f(\mathbf{x})$  in (35) has been replaced by  $\frac{1}{2} s^2$  in (36). Following Remark 5.1, this is precisely the  $\dot{Q}$  velocity gradient functional that gives rise to the Slotine and Li controller. For (36), the Euler-Lagrange equations lead to the adaptation law

$$\ddot{\hat{\mathbf{a}}} + \dot{\hat{\mathbf{a}}} \left( \beta\mathcal{N} - \frac{\dot{\mathcal{N}}}{\mathcal{N}} \right) = -\gamma\beta\mathcal{N} \mathbf{Y}^\top s. \quad (37)$$

(37) may be understood as a modification of the Slotine and Li adaptive controller to incorporate momentum and time-dependent damping. (37) may also be re-written as two first-order systems

$$\dot{\hat{\mathbf{v}}} = -\gamma \mathbf{Y}^\top s, \quad (38)$$

$$\dot{\hat{\mathbf{a}}} = \beta\mathcal{N} (\hat{\mathbf{v}} - \hat{\mathbf{a}}), \quad (39)$$

which are useful for proving stability. The properties of (37) are summarized in the following proposition.

**Proposition 5.3.** *Consider the higher-order adaptation algorithm (37) with  $\mathcal{N} = 1 + \mu \|\mathbf{Y}\|^2$  and  $\mu > \frac{\gamma}{\eta\beta}$ . Then, all trajectories  $(\mathbf{x}, \hat{\mathbf{v}}, \hat{\mathbf{a}})$  remain bounded,  $s \in \mathcal{L}_\infty \cap \mathcal{L}_2$ ,  $(\hat{\mathbf{a}} - \hat{\mathbf{v}}) \in \mathcal{L}_2$ ,  $s \rightarrow 0$  and  $\mathbf{x} \rightarrow \mathbf{x}_d$ .*

The proof follows by consideration of the Lyapunov-like function  $V = \frac{1}{2} \left( s^2 + \frac{1}{\gamma} \|\hat{\mathbf{v}}\|^2 + \frac{1}{\gamma} \|\hat{\mathbf{v}} - \hat{\mathbf{a}}\|^2 \right)$ .

<sup>9</sup>Note that these conditions validate the second ideal scaling condition but not the first. As mentioned above, the first ideal scaling condition is required only by the choice of Lyapunov function in the original work, which was used to derive convergence rates for optimization algorithms (Wibisono et al., 2016). In this sense, it is not strictly required for adaptive control.

**Remark 5.4.** The transformation to a system of two first-order equations may seem somewhat *ad-hoc*, but it follows immediately by consideration of the non-Euclidean Bregman Lagrangian (35). Indeed, it is easy to check that  $\hat{\mathbf{v}} = \hat{\mathbf{a}} + \frac{\dot{\hat{\mathbf{a}}}}{\beta\mathcal{N}}$ , which is precisely the adaptive control equivalent of  $\mathbf{x} + e^{-\bar{\alpha}}\dot{\mathbf{x}}$  in the first argument of  $d_\psi(\cdot \parallel \cdot)$  in (35). The transformation is also readily apparent by use of the *Bregman Hamiltonian*

$$\mathcal{H}(\hat{\mathbf{a}}, \mathbf{p}) = \frac{1}{2}\beta\mathcal{N}e^{-\bar{\gamma}}\|\mathbf{p}\|^2 + \gamma e^{\bar{\gamma}} \left[ \frac{d}{dt} \frac{1}{2}s^2 \right], \quad (40)$$

which, via Hamilton's equations, leads to

$$\begin{aligned} \dot{\mathbf{p}} &= -\frac{\partial \mathcal{H}}{\partial \hat{\mathbf{a}}} = -\gamma e^{\bar{\gamma}} \mathbf{Y}^\top s, \\ \dot{\hat{\mathbf{a}}} &= \frac{\partial \mathcal{H}}{\partial \mathbf{p}} = \beta\mathcal{N}e^{-\bar{\gamma}}\mathbf{p}. \end{aligned}$$

Defining  $\hat{\mathbf{v}} = e^{-\bar{\gamma}}\mathbf{p} + \hat{\mathbf{a}}$  immediately leads to (38) & (39). This line of reasoning was recently investigated further by Gaudio et al. (2021). As is typical in classical mechanics, the Bregman Hamiltonian may be obtained from a Legendre transform of the Bregman Lagrangian. The Hamiltonian dynamics may be useful for discrete-time algorithm development through application of symplectic discretization techniques (Betancourt et al., 2018; França et al., 2019; Shi et al., 2019).  $\diamond$

**Remark 5.5.** It is well known, for example from a passivity interpretation of the Lyapunov-like analysis (see, e.g., (Slotine and Li, 1991)), that the pure integrator in the standard Slotine and Li adaptation law (8) can be replaced by any linear positive real transfer function containing a pure integrator. The higher-order algorithms presented in this work are distinct from this approach, as most clearly seen by the state-dependent damping term in (37).  $\diamond$

**Remark 5.6.** In Wibisono et al. (2016), the suggested Lyapunov function in the Euclidean setting is  $V = \|\mathbf{x} + e^{-\bar{\alpha}}\dot{\mathbf{x}} - \mathbf{x}_*\|^2 + e^{\bar{\beta}}f(\mathbf{x})$  where  $\mathbf{x}_*$  is the global optimum and  $f(\mathbf{x})$  is the loss function. Noting that  $\hat{\mathbf{v}}$  is the equivalent of  $\mathbf{x} + e^{-\bar{\alpha}}\dot{\mathbf{x}}$  in the adaptive control context (see Remark 5.4), we see that the Lyapunov-like function used to prove stability of the adaptive law (37) is similar to that used to prove convergence in the optimization context. The loss function term  $f(\mathbf{x})$  is replaced by  $\frac{1}{2}s^2$ , and it is necessary to add the additional term  $\frac{1}{\gamma}\|\hat{\mathbf{v}} - \hat{\mathbf{a}}\|^2$ .

## 6 ADAPTATION LAWS WITH MOMENTUM

In this section, we develop several new adaptation laws for both linearly and nonlinearly parameterized systems. We begin by noting that the Bregman Lagrangian generates velocity gradient algorithms with momentum. We prove some general conditions under which these momentum algorithms will achieve tracking. By analogy with integral velocity gradient functionals, we then derive a proportional-integral scheme to implement a first-order composite adaptation law (Slotine and Li, 1991) driven directly by the function approximation error rather than its filtered version. We subsequently fuse the generating functional for the composite law with the Bregman Lagrangian to construct a composite algorithm with momentum.

We then employ a connection between recent developments in isotonic regression – the GLMTron of Kakade et al. (2011), along with extensions due to Goel and Klivans (2017) and Goel et al. (2018) – and Tyukin's algorithm (12) to derive momentum algorithms for nonlinearly parameterized systems. These momentum algorithms can be seen as the adaptive control equivalent of the GLMTron with momentum.

We follow this development by discussing a new form of high-order algorithm inspired by the Elastic Averaging Stochastic Gradient Descent (EASGD) algorithm (Zhang et al., 2014; Boffi and Slotine, 2020). We subsequently demonstrate the capability of using time-varying learning rates with our presented algorithms (Slotine and Li, 1991).

## 6.1 VELOCITY GRADIENT ALGORITHMS WITH MOMENTUM

As noted in Section 5.2, the Bregman Lagrangian (36) that generates the higher-order algorithm (37) contains the local velocity gradient functional  $Q(\mathbf{x}, t) = \frac{1}{2}s(\mathbf{x}, t)^2$  that gives rise to the Slotine and Li controller (8). Based on this observation, we define local and integral higher-order velocity gradient algorithms via the Euclidean Bregman Lagrangian. We begin with the local functional

$$\mathcal{L}(\hat{\mathbf{a}}, \dot{\hat{\mathbf{a}}}, t) = e^{\int_0^t \beta \mathcal{N}(t) dt} \frac{1}{\beta \mathcal{N}(t)} \left( \frac{1}{2} \dot{\hat{\mathbf{a}}}^\top \dot{\hat{\mathbf{a}}} - \gamma \beta \mathcal{N}(t) \frac{d}{dt} Q(\mathbf{x}, t) \right),$$

which generates the higher-order law

$$\ddot{\hat{\mathbf{a}}} + \dot{\hat{\mathbf{a}}} \left( \beta \mathcal{N} - \frac{\dot{\mathcal{N}}}{\mathcal{N}} \right) = -\gamma \beta \mathcal{N} \nabla_{\hat{\mathbf{a}}} \dot{Q}(\mathbf{x}, \hat{\mathbf{a}}, t). \quad (41)$$

Algorithm (41) can be re-written as two first-order systems

$$\dot{\hat{\mathbf{v}}} = -\gamma \nabla_{\hat{\mathbf{a}}} \dot{Q}(\mathbf{x}, \hat{\mathbf{a}}, t), \quad (42)$$

$$\dot{\hat{\mathbf{a}}} = \beta \mathcal{N}(\hat{\mathbf{v}} - \hat{\mathbf{a}}). \quad (43)$$

To achieve the control goal, we require the following technical assumption in addition to Assumptions 5.1 & 5.3. This assumption replaces Assumption 5.2 for first-order velocity gradient algorithms.

**Assumption 6.1.** There exists a time-dependent signal  $\mathcal{N}(t)$  and non-negative scalar values  $\beta \geq 0, \mu \geq 0$  such that the time-derivative of the goal functional evaluated at the true parameters,  $\dot{Q}(\mathbf{x}, \mathbf{a}, t)$ , satisfies the following inequality

$$\dot{Q}(\mathbf{x}, \mathbf{a}, t) - \frac{\beta \mu}{\gamma} N(t) \|\hat{\mathbf{a}} - \hat{\mathbf{v}}\|^2 + 2(\hat{\mathbf{a}} - \hat{\mathbf{v}})^\top \nabla_{\hat{\mathbf{a}}} \dot{Q}(\mathbf{x}, \hat{\mathbf{a}}, t) \leq -\rho(Q). \quad (44)$$

In (44),  $\rho(\cdot)$  is positive definite, continuous in  $Q$ , and satisfies  $\rho(0) = 0$ .  $\diamond$

Assumption 6.1 is a formal statement that we may “complete the square” on the left-hand side of (44). For example, for  $\nabla_{\hat{\mathbf{a}}} \dot{Q}(\mathbf{x}, \hat{\mathbf{a}}, t) = \mathbf{Y}^\top s$  and for  $\dot{Q}(\mathbf{x}, \mathbf{a}, t) = -\eta s^2$ , we may choose  $N = \|\mathbf{Y}^\top\|^2$ .

With Assumption 6.1 in hand, we can state the following proposition.

**Proposition 6.1.** Consider the algorithm (41) or its equivalent form (42) & (43), and assume  $Q$  satisfies Assumptions 5.1, 5.3, and 6.1. Then, all solutions  $(\mathbf{x}(t), \hat{\mathbf{v}}(t), \hat{\mathbf{a}}(t))$  remain bounded,  $(\hat{\mathbf{a}} - \hat{\mathbf{v}}) \in \mathcal{L}_2$ , and  $\lim_{t \rightarrow \infty} Q = 0$ .

*Proof.* Consider the Lyapunov-like function

$$V = Q(\mathbf{x}, t) + \frac{1}{2\gamma} \tilde{\mathbf{v}}^\top \tilde{\mathbf{v}} + \frac{1}{2\gamma} (\hat{\mathbf{a}} - \hat{\mathbf{v}})^\top (\hat{\mathbf{a}} - \hat{\mathbf{v}}). \quad (45)$$

Equation (45) implies that, with  $\mathcal{N}(t) = 1 + \mu N(t)$ ,

$$\begin{aligned} \dot{V} &= \dot{Q}(\mathbf{x}, \hat{\mathbf{a}}, t) - \hat{\mathbf{a}}^\top \nabla_{\hat{\mathbf{a}}} \dot{Q}(\mathbf{x}, \hat{\mathbf{a}}, t) - \frac{\beta}{\gamma} \|\hat{\mathbf{a}} - \hat{\mathbf{v}}\|^2 - \frac{\beta \mu}{\gamma} N(t) \|\hat{\mathbf{a}} - \hat{\mathbf{v}}\|^2 + 2(\hat{\mathbf{a}} - \hat{\mathbf{v}})^\top \nabla_{\hat{\mathbf{a}}} \dot{Q}(\mathbf{x}, \hat{\mathbf{a}}, t), \\ &\leq \dot{Q}(\mathbf{x}, \mathbf{a}, t) - \frac{\beta}{\gamma} \|\hat{\mathbf{a}} - \hat{\mathbf{v}}\|^2 - \frac{\beta \mu}{\gamma} N(t) \|\hat{\mathbf{a}} - \hat{\mathbf{v}}\|^2 + 2(\hat{\mathbf{a}} - \hat{\mathbf{v}})^\top \nabla_{\hat{\mathbf{a}}} \dot{Q}(\mathbf{x}, \hat{\mathbf{a}}, t), \\ &\leq -\rho(Q) - \frac{\beta}{\gamma} \|\hat{\mathbf{a}} - \hat{\mathbf{v}}\|^2. \end{aligned} \quad (46)$$

By radial unboundedness of  $Q(\mathbf{x}, t)$  in  $\mathbf{x}$ , (45) & (46) show that  $\mathbf{x}$  remains bounded. Similarly, radial unboundedness of  $V$  in  $\tilde{\mathbf{v}}$  and  $\hat{\mathbf{a}} - \hat{\mathbf{v}}$  show that  $\hat{\mathbf{v}}$  and  $\hat{\mathbf{a}}$  remain bounded. Integrating (46) shows that  $\frac{\beta}{\gamma} \int_0^\infty \|\hat{\mathbf{a}} - \hat{\mathbf{v}}\|^2 dt \leq V(0) - V(\infty) < \infty$ , so that  $(\hat{\mathbf{a}} - \hat{\mathbf{v}}) \in \mathcal{L}_2$ . An identical argument shows that  $\int_0^\infty \rho(Q) dt < \infty$ . Now, because  $\mathbf{x}$  and  $\hat{\mathbf{a}}$  are bounded,

and because  $\tilde{f}(\mathbf{x}, \hat{\mathbf{a}}, \mathbf{a}, t)$  is locally bounded in  $\mathbf{x}$  and  $\hat{\mathbf{a}}$  uniformly in  $t$  by assumption, writing  $\mathbf{x}(t) - \mathbf{x}(s) = \int_s^t (\mathbf{f}(\mathbf{x}(t'), \mathbf{a}, t') + \mathbf{u}(\hat{\mathbf{a}}(t'), t')) dt'$  shows that  $\mathbf{x}(t)$  is uniformly continuous in  $t$ . Because  $Q(\mathbf{x}, t)$  is uniformly continuous in  $t$  when  $\mathbf{x}$  is bounded, because  $Q$  is bounded, and because  $\rho$  is continuous in  $Q$ , we conclude  $\rho$  is uniformly continuous in  $t$  and  $\lim_{t \rightarrow \infty} \rho(t) = \lim_{t \rightarrow \infty} \rho(Q(\mathbf{x}(t), t)) = 0$  by Barbalat's Lemma (Lemma A.1). This shows that  $\lim_{t \rightarrow \infty} Q(\mathbf{x}(t), t) = 0$ .  $\square$

By taking  $Q = \frac{1}{2}s^2$  in Proposition 6.1, we immediately recover Proposition 5.3.

We now consider the integral functional

$$\mathcal{L}(\hat{\mathbf{a}}, \dot{\hat{\mathbf{a}}}, t) = e^{\int_0^t \beta \mathcal{N}(t') dt} \frac{1}{\beta \mathcal{N}(t)} \left( \frac{1}{2} \dot{\hat{\mathbf{a}}}^\top \dot{\hat{\mathbf{a}}} - \gamma \beta \mathcal{N}(t) \frac{d}{dt} \int_0^t R(\mathbf{x}(t'), \hat{\mathbf{a}}(t'), t') dt' \right),$$

which generates the higher-order law

$$\ddot{\hat{\mathbf{a}}} + \dot{\hat{\mathbf{a}}} \left( \beta \mathcal{N} - \frac{\dot{\mathcal{N}}}{\mathcal{N}} \right) = -\gamma \beta \mathcal{N} \nabla_{\hat{\mathbf{a}}} R(\mathbf{x}, \hat{\mathbf{a}}, t). \quad (47)$$

We again re-write (47) as two first-order systems

$$\dot{\hat{\mathbf{v}}} = -\gamma \nabla_{\hat{\mathbf{a}}} R(\mathbf{x}, \hat{\mathbf{a}}, t), \quad (48)$$

$$\dot{\hat{\mathbf{a}}} = \beta \mathcal{N}(\hat{\mathbf{v}} - \hat{\mathbf{a}}), \quad (49)$$

and now require a modified version of Assumption 6.1.

**Assumption 6.2.**  $R(\mathbf{x}, \hat{\mathbf{a}}, t) \geq 0$  for all  $\mathbf{x}, \hat{\mathbf{a}}$ , and  $t$ , and is uniformly continuous in  $t$  for bounded  $\mathbf{x}$  and  $\hat{\mathbf{a}}$ .  $\nabla_{\hat{\mathbf{a}}} R(\mathbf{x}, \hat{\mathbf{a}}, t)$  is locally bounded in  $\mathbf{x}$  and  $\hat{\mathbf{a}}$  uniformly in  $t$ . Furthermore, there exists a time-dependent signal  $N(t)$  and non-negative scalar values  $\beta \geq 0, \mu \geq 0$  such that

$$R(\mathbf{x}, \mathbf{a}, t) - R(\mathbf{x}, \hat{\mathbf{a}}, t) - \frac{\beta \mu}{\gamma} N(t) \|\hat{\mathbf{a}} - \hat{\mathbf{v}}\|^2 + 2(\hat{\mathbf{a}} - \hat{\mathbf{v}})^\top \nabla_{\hat{\mathbf{a}}} R(\mathbf{x}, \hat{\mathbf{a}}, t) \leq -k R(\mathbf{x}, \hat{\mathbf{a}}, t)$$

for some constant  $k > 0$ .  $\diamond$

Similar to Assumption 6.1, Assumption 6.2 is a formal requirement that we may “complete the square”. Consider the case when  $R(\mathbf{x}, \hat{\mathbf{a}}, t) = \frac{1}{2}\tilde{f}(\mathbf{x}, \hat{\mathbf{a}}, \mathbf{a}, t)^2$ . Then  $R(\mathbf{x}, \mathbf{a}, t) = 0$ ,  $\nabla_{\hat{\mathbf{a}}} R(\mathbf{x}, \hat{\mathbf{a}}, t) = \tilde{f}(\mathbf{x}, \hat{\mathbf{a}}, \mathbf{a}, t) \nabla_{\hat{\mathbf{a}}} \tilde{f}(\mathbf{x}, \hat{\mathbf{a}}, t)$ , and we may choose  $N(t) = \|\nabla_{\hat{\mathbf{a}}} \tilde{f}(\mathbf{x}, \hat{\mathbf{a}}, t)\|^2$ .

With Assumption 6.2, we can state the following proposition.

**Proposition 6.2.** Consider algorithm (47) along with Assumptions 5.3 & 6.2. Let  $T_x$  denote the maximal interval of existence of  $\mathbf{x}(t)$ . Then,  $\hat{\mathbf{v}}$  and  $\hat{\mathbf{a}}$  remain bounded for  $t \in [0, T_x]$ ,  $(\hat{\mathbf{a}} - \hat{\mathbf{v}}) \in \mathcal{L}_2$  over this interval, and  $\int_0^{T_x} R(\mathbf{x}(t'), \hat{\mathbf{a}}(t'), t') dt' < \infty$ . Furthermore, for any bounded solution  $\mathbf{x}$ , these conclusions hold for all  $t$  and  $R(\mathbf{x}(t), \hat{\mathbf{a}}(t), t) \rightarrow 0$ .

*Proof.* Consider the Lyapunov-like function

$$V = \frac{1}{2\gamma} \tilde{\mathbf{v}}^\top \tilde{\mathbf{v}} + \frac{1}{2\gamma} (\hat{\mathbf{a}} - \hat{\mathbf{v}})^\top (\hat{\mathbf{a}} - \hat{\mathbf{v}}). \quad (50)$$

Equation (50) implies that, with  $\mathcal{N}(t) = 1 + \mu N(t)$ ,

$$\begin{aligned} \dot{V} &= -\hat{\mathbf{a}}^\top \nabla_{\hat{\mathbf{a}}} R(\mathbf{x}, \hat{\mathbf{a}}, t) - \frac{\beta}{\gamma} \|\hat{\mathbf{a}} - \hat{\mathbf{v}}\|^2 - \frac{\beta \mu}{\gamma} N(t) \|\hat{\mathbf{a}} - \hat{\mathbf{v}}\|^2 + 2(\hat{\mathbf{a}} - \hat{\mathbf{v}})^\top \nabla_{\hat{\mathbf{a}}} R(\mathbf{x}, \hat{\mathbf{a}}, t), \\ &\leq R(\mathbf{x}, \mathbf{a}, t) - R(\mathbf{x}, \hat{\mathbf{a}}, t) - \frac{\beta}{\gamma} \|\hat{\mathbf{a}} - \hat{\mathbf{v}}\|^2 - \frac{\beta \mu}{\gamma} N(t) \|\hat{\mathbf{a}} - \hat{\mathbf{v}}\|^2 + 2(\hat{\mathbf{a}} - \hat{\mathbf{v}})^\top \nabla_{\hat{\mathbf{a}}} R(\mathbf{x}, \hat{\mathbf{a}}, t), \\ &\leq -k R(\mathbf{x}, \hat{\mathbf{a}}, t) - \frac{\beta}{\gamma} \|\hat{\mathbf{a}} - \hat{\mathbf{v}}\|^2. \end{aligned} \quad (51)$$

(50) & (51) show boundedness of  $\hat{\mathbf{v}}$  and  $\hat{\mathbf{a}}$  over  $[0, T_x]$ . Furthermore, integrating (51) shows that  $\int_0^{T_x} \|\hat{\mathbf{a}} - \hat{\mathbf{v}}\|^2 dt' < \infty$  and  $\int_0^{T_x} R(\mathbf{x}(t'), \hat{\mathbf{a}}(t'), t') dt' < \infty$ . For any bounded solution  $\mathbf{x}$ ,

these integrals may be extended to infinity, and we conclude that  $(\hat{\mathbf{a}} - \hat{\mathbf{v}}) \in \mathcal{L}_2$ ,  $\hat{\mathbf{a}} \in \mathcal{L}_\infty$ , and  $\hat{\mathbf{v}} \in \mathcal{L}_\infty$ . Writing  $\mathbf{x}(t) - \mathbf{x}(s)$  in integral form as in the proof of Proposition 6.1 shows that  $\mathbf{x}(t)$  is uniformly continuous in  $t$ , and in light of the local boundedness assumption on  $\nabla_{\hat{\mathbf{a}}} R$ , the same procedure can be applied to  $\hat{\mathbf{v}}$  and  $\hat{\mathbf{a}}$ . Because  $R(\mathbf{x}(t), \hat{\mathbf{a}}(t), t)$  is uniformly continuous in  $t$  for bounded  $\mathbf{x}$  and  $\hat{\mathbf{a}}$ , and because  $\mathbf{x}(t)$  and  $\hat{\mathbf{a}}(t)$  are both uniformly continuous in  $t$ , we conclude that  $R(\mathbf{x}(t), \hat{\mathbf{a}}(t), t)$  is uniformly continuous in  $t$  and  $R \rightarrow 0$  by Barbalat's Lemma (Lemma A.1).  $\square$

As mentioned in Section 5.1, we will be particularly interested in Proposition 6.2 when  $R = \frac{1}{2} \tilde{f}^2$ , which will generate composite adaptation algorithms and algorithms applicable to nonlinearly parameterized systems. Proposition 6.2 then shows that  $\tilde{f} \in \mathcal{L}_2$  over the interval of existence of  $\mathbf{x}(t)$ . As shown by Lemma A.2, with our error model this is enough to show that  $\mathbf{x}(t)$  always remains bounded and hence  $\tilde{f} \rightarrow 0$ .

**Remark 6.1.** Classically, Lyapunov-like functions used in adaptive control consist of a sum of tracking and parameter estimation error terms, with  $\hat{\mathbf{a}}$  chosen to cancel a term of unknown sign. Several Lyapunov functions in this work consist only of parameter estimation error terms, such as (50). From a mathematical point of view, all that matters is that  $\dot{V}$  is negative semi-definite and contains signals related to the tracking error. Integrating  $\dot{V}$  allows the application of tools from functional analysis to ensure that the control goal is accomplished. The lack of tracking error term in  $V$  is the origin of the additional complication that  $\mathbf{x}(t)$  must be shown to be bounded even after it is known that  $\dot{V} \leq 0$ .  $\diamond$

## 6.2 FIRST- AND SECOND-ORDER COMPOSITE ADAPTATION LAWS

Here we consider the linearly parameterized setting  $f(\mathbf{x}, \mathbf{a}, t) = \mathbf{Y}(\mathbf{x}, t)\mathbf{a}$ , and derive new first- and second-order composite adaptation laws. Composite adaptation laws are driven by two sources of error: the tracking error itself, as summarized by  $s$  in the Slotine and Li controller, and a prediction error. The prediction error term is generally obtained from an algebraic relation constructed by filtering the dynamics (Slotine and Li, 1991). We present a composite algorithm that does not require any explicit filtering of the dynamics, but is instead driven simultaneously by  $s$  and  $\tilde{f}$ .

A starting point for our first proposed algorithm is to consider a hybrid local and integral velocity gradient functional

$$Q(\mathbf{x}, t) = \frac{\gamma}{2} s(\mathbf{x}, t)^2 + \frac{\kappa}{2} \int_0^t \tilde{f}^2(\mathbf{x}(t'), \hat{\mathbf{a}}(t'), \mathbf{a}, t') dt', \quad (52)$$

where  $\kappa > 0$  and  $\gamma > 0$  are positive learning rates weighting the contributions of each term. As discussed in Section 5.1, the first term leads to the Slotine and Li controller. The second can be clearly seen to satisfy Assumptions 5.4 and 5.5 with  $\mu(t) = 0$ . It also satisfies Assumption 5.3, as  $\tilde{f}^2$  is a quadratic function of  $\hat{\mathbf{a}}$  for linear  $\tilde{f}$ . Following the velocity gradient formalism, the resulting adaptation law is given by

$$\dot{\hat{\mathbf{a}}} = -\mathbf{P}\mathbf{Y}^\top (\gamma s + \kappa \mathbf{Y}\tilde{\mathbf{a}}), \quad (53)$$

which is a composite adaptation law simultaneously driven by  $s$  and the instantaneous function approximation error  $\mathbf{Y}\tilde{\mathbf{a}} = \tilde{f}$ . Equation (53) depends on the function approximation error  $\tilde{f}$ , which is not measured and hence cannot be used directly in an adaptation law. Nevertheless, it can be obtained through a proportional-integral form for  $\hat{\mathbf{a}}$  in an identical

manner to Section 2.2. To do so, we define

$$\xi(\mathbf{x}, t) = -\kappa \mathbf{P} s(\mathbf{x}, t) \mathbf{Y}(\mathbf{x}, t)^\top, \quad (54)$$

$$\rho(\mathbf{x}, t) = \kappa \mathbf{P} \int_{x_n(t_0)}^{x_n(t)} s(\mathbf{x}, t) \frac{\partial \mathbf{Y}(\mathbf{x}, t)^\top}{\partial x_n} dx_n, \quad (55)$$

$$\hat{\mathbf{a}} = \bar{\mathbf{a}} + \xi(\mathbf{x}, t) + \rho(\mathbf{x}, t), \quad (56)$$

$$\begin{aligned} \dot{\hat{\mathbf{a}}} = & -(\kappa\eta + \gamma) s \mathbf{P} \mathbf{Y}^\top + \kappa s \sum_{i=1}^{n-1} \mathbf{P} \frac{\partial \mathbf{Y}}{\partial x_i} \dot{x}_i - \sum_{i=1}^{n-1} \left( \frac{\partial \rho}{\partial x_i} \right)^\top \dot{x}_i, \\ & - \left( \frac{\partial \rho}{\partial \mathbf{x}_d} \right)^\top \dot{\mathbf{x}}_d - \frac{\partial \xi}{\partial t} - \frac{\partial \rho}{\partial t}. \end{aligned} \quad (57)$$

Computing  $\dot{\hat{\mathbf{a}}}$  demonstrates that (53) is obtained through only the known signals contained in (54)-(57) despite its dependence on  $\mathbf{Y}\hat{\mathbf{a}}$ . A few remarks concerning the algorithm (53)-(57) are in order.

**Remark 6.2.** The  $\mathbf{Y}\hat{\mathbf{a}}$  term may also be obtained by following the I&I formalism (Astolfi and Ortega, 2003; Liu et al., 2010). To our knowledge, this discussion is the first that demonstrates the possibility of using a PI law in combination with a standard Lyapunov-stability motivated adaptation law to obtain a composite law.  $\diamond$

**Remark 6.3.** More error signals may be used for additional terms in the adaptation law. For example, a prediction error obtained by filtering the dynamics may also be employed, leading to a three-term composite algorithm.  $\diamond$

**Remark 6.4.** Much like the standard composite law obtained by filtering the dynamics, rearranging (53) shows that  $\dot{\hat{\mathbf{a}}} + \mathbf{P} \mathbf{Y}^\top \mathbf{Y} \hat{\mathbf{a}} = -\mathbf{P} \mathbf{Y}^\top s$ , so that the additional term can be seen to add a damping term that smooths adaptation (Slotine and Li, 1991).  $\diamond$

**Remark 6.5.** As mentioned in Section 2.1, for clarity of presentation we have restricted our discussion to the  $n^{\text{th}}$ -order system (1). In general, the PI form (56) leads to *undesired* unknown terms contained in  $\left( \frac{\partial \xi(\mathbf{x}, \mathbf{x}_d)}{\partial \mathbf{x}} \right)^\top \dot{\mathbf{x}}$  in addition to the *desired* unknown term. In this case, the desired unknown term is  $-\kappa \mathbf{P} \mathbf{Y}^\top \mathbf{Y} \hat{\mathbf{a}}$  while the undesired unknown term is  $-\kappa \mathbf{P} \frac{\partial \mathbf{Y}}{\partial x_n} \dot{x}_n s$ . Indeed, the purpose of introducing the additional proportional term  $\rho(\mathbf{x}, \mathbf{x}_d)$  in (54) is to cancel this undesired unknown term. In general, cancellation of the undesired terms can be obtained by choosing  $\rho$  to solve a PDE, and solutions to this PDE will only exist if the undesired term is the gradient of an auxiliary function.  $\rho$  is then chosen to be exactly this auxiliary function. In some cases, the PDE can be avoided, such as through dynamic scaling techniques (Karagiannis et al., 2009) or the similar embedding technique of Tyukin (2011).  $\diamond$

The properties of the adaptive law (53) may be summarized with the following proposition.

**Proposition 6.3.** Consider the adaptation algorithm (53) with a linearly parameterized unknown,  $f(\mathbf{x}, \mathbf{a}, t) = \mathbf{Y}(\mathbf{x}, t) \mathbf{a}$ . Then all trajectories  $(\mathbf{x}, \hat{\mathbf{a}})$  remain bounded,  $s \in L_2 \cap L_\infty$ ,  $\tilde{f} \in L_2$ ,  $s \rightarrow 0$ , and  $\mathbf{x} \rightarrow \mathbf{x}_d$ .

The proof is given in Appendix A.1.

Following the velocity gradient with momentum approach of Section 6.1, we now obtain a higher-order composite algorithm, and give a PI implementation. We again consider a hybrid local and integral velocity gradient functional, so that (35) takes the form

$$\mathcal{L}(\hat{\mathbf{a}}, \dot{\hat{\mathbf{a}}}, t) = e^{\int_0^t \beta \mathcal{N}(t') dt} \frac{1}{\beta \mathcal{N}(t)} \left( \frac{1}{2} \dot{\hat{\mathbf{a}}}^\top \dot{\hat{\mathbf{a}}} - \beta \mathcal{N}(t) \frac{d}{dt} \left[ \frac{\gamma}{2} s^2 + \frac{\kappa}{2} \int_0^t \tilde{f}^2(\mathbf{x}(t'), \hat{\mathbf{a}}(t'), \mathbf{a}, t') dt' \right] \right) \quad (58)$$

where  $\gamma > 0$  and  $\kappa > 0$  are positive constants weighting the two error terms. The Euler-Lagrange equations then lead to the higher-order composite system

$$\ddot{\hat{\mathbf{a}}} + \left( \beta \mathcal{N} - \frac{\dot{\mathcal{N}}}{\mathcal{N}} \right) \dot{\hat{\mathbf{a}}} = -\beta \mathcal{N} \mathbf{Y}^\top (\gamma s + \kappa \mathbf{Y} \hat{\mathbf{a}}). \quad (59)$$

As in Section 5.2, (59) may be implemented as two first-order systems

$$\dot{\hat{\mathbf{v}}} = -\mathbf{Y}^T (\gamma s + \kappa \mathbf{Y} \tilde{\mathbf{a}}), \quad (60)$$

$$\dot{\tilde{\mathbf{a}}} = \beta \mathcal{N} (\hat{\mathbf{v}} - \tilde{\mathbf{a}}). \quad (61)$$

In an implementation, (60) is obtained through the PI form  $\hat{\mathbf{v}} = \bar{\mathbf{v}} + \boldsymbol{\xi}(\mathbf{x}, t) + \boldsymbol{\rho}(\mathbf{x}, t)$  with  $\boldsymbol{\xi}$ ,  $\boldsymbol{\rho}$ , and  $\dot{\bar{\mathbf{v}}}$  given by (54), (55), and (57) respectively with  $\mathbf{P} = \mathbf{I}$ . The properties of the higher-order composite adaptation law (59) are stated in the following proposition.

**Proposition 6.4.** *Consider the higher-order composite adaptation algorithm (59) for a linearly parameterized unknown,  $f(\mathbf{x}, \mathbf{a}, t) = \mathbf{Y}(\mathbf{x}, t)\mathbf{a}$ . Set  $\mathcal{N} = 1 + \mu \|\mathbf{Y}\|^2$  and  $\mu > \frac{\gamma}{\beta} \left( \frac{1}{\eta} + \frac{\kappa}{\gamma} \right)$ . Then all trajectories  $(\mathbf{x}, \hat{\mathbf{v}}, \tilde{\mathbf{a}})$  remain bounded,  $\|\hat{\mathbf{v}} - \tilde{\mathbf{a}}\| \in L_2$ ,  $s \in L_\infty \cap L_2$ ,  $\tilde{f} \in L_\infty \cap L_2$ ,  $s \rightarrow 0$ , and  $\mathbf{x} \rightarrow \mathbf{x}_d$ .*

The proof is given in Appendix A.2.

**Remark 6.6.** By following the proof, the signal  $\mathcal{N}$  may be chosen alternatively to be matrix-valued as  $\mathbf{N} = \mathbf{I} + \mu \mathbf{Y}^T \mathbf{Y}$ .  $\diamond$

**Remark 6.7.** The  $\mathbf{Y} \tilde{\mathbf{a}}$  term may be used in isolation, by considering the Lyapunov function  $V = \frac{1}{2} \|\tilde{\mathbf{v}}\|^2 + \frac{1}{2} \|\tilde{\mathbf{a}} - \hat{\mathbf{v}}\|^2$ .  $\diamond$

**Remark 6.8.** A gain matrix  $\mathbf{P} = \mathbf{P}^T > 0$  of appropriate dimension may be placed in front of  $\mathbf{Y}^T$  in  $\dot{\hat{\mathbf{v}}}$ . The quadratic parameter estimation error terms in the Lyapunov function should then be replaced by the weighted terms  $\frac{1}{2} \tilde{\mathbf{v}}^T \mathbf{P}^{-1} \tilde{\mathbf{v}} + \frac{1}{2} (\tilde{\mathbf{a}} - \hat{\mathbf{v}})^T \mathbf{P}^{-1} (\tilde{\mathbf{a}} - \hat{\mathbf{v}})$ , and bounds on  $\mu$  will be given in terms of  $\|\mathbf{P}\|$ .  $\diamond$

### 6.3 A MOMENTUM ALGORITHM FOR NONLINEARLY PARAMETERIZED ADAPTIVE CONTROL

We now use the development in Section 6.2 to present a new momentum algorithm applicable when the unknown parameters appear nonlinearly in the dynamics. We begin with an analogy to statistics.

Generalized linear model (GLM) regression is an extension of linear regression where the data is assumed to be generated by a function of the form  $f(\mathbf{x}) = u(\mathbf{w}^T \mathbf{x})$  for a known ‘link function’  $u$  and unknown parameters  $\mathbf{w}$ . The first computationally and statistically efficient algorithm for this problem – the GLM-Tron of Kakade et al. (2011) – assumes that  $u$  is Lipschitz and monotonic, much like Assumption 2.2.

The GLM-Tron algorithm was recently extended to the setting of kernel methods, and was subsequently used to provably learn two hidden layer neural networks by Goel and Klivans (2017); this extension is known as the Alphatron. In the kernel GLM setting handled by the Alphatron, the function to be approximated is assumed to be of the form  $f(\mathbf{x}) = u(\sum_{i=1}^m w_i \mathcal{K}(\mathbf{x}, \mathbf{x}_i))$  where  $\mathcal{K}$  is the kernel function for a Reproducing Kernel Hilbert Space (RKHS)  $\mathcal{H}$ .  $\mathcal{K}$  is thus given by the RKHS inner product of a feature map  $\phi$ ,  $\mathcal{K}(\mathbf{x}, \mathbf{y}) = \langle \phi(\mathbf{x}), \phi(\mathbf{y}) \rangle_{\mathcal{H}}$ .

The Alphatron initializes all weights to zero, and given a batch of labeled training data  $(\mathbf{x}_i, f(\mathbf{x}_i))_{i=1}^m$ , updates them with a learning rate  $\lambda > 0$  according to the iteration

$$\hat{w}_i^{t+1} = \hat{w}_i^t - \frac{\lambda}{m} \left( \hat{f}(\hat{\mathbf{w}}^t, \mathbf{x}_i) - f(\mathbf{x}_i) \right). \quad (62)$$

We now demonstrate an equivalence between Tyukin’s adaptation law (12) and the Alphatron weight update (62) in the following proposition.

**Proposition 6.5.** *The adaptation law (12) is an application of the Alphatron algorithm (62) to adaptive control.*

The proof is given in Appendix A.3.

Proposition 6.5 shows a convergence of techniques in nonlinearly parameterized adaptive control and nonconvex learning. This correspondence suggests the momentum-like variant of

(12)

$$\ddot{\hat{\mathbf{a}}} + \left( \beta \mathcal{N} - \frac{\dot{\mathcal{N}}}{\mathcal{N}} \right) \dot{\hat{\mathbf{a}}} = -\gamma \beta \mathcal{N} \tilde{f}(\mathbf{x}, \hat{\mathbf{a}}, \mathbf{a}, t) \boldsymbol{\alpha}(\mathbf{x}, t), \quad (63)$$

which, as before, admits an equivalent representation in terms of two first-order systems,

$$\dot{\hat{\mathbf{v}}} = -\gamma \tilde{f}(\mathbf{x}, \hat{\mathbf{a}}, \mathbf{a}, t) \boldsymbol{\alpha}(\mathbf{x}, t), \quad (64)$$

$$\dot{\hat{\mathbf{a}}} = \beta \mathcal{N} (\hat{\mathbf{v}} - \hat{\mathbf{a}}). \quad (65)$$

Equation (63) may be implemented through (64) & (65) via the PI form (13)-(16) applied to the  $\hat{\mathbf{v}}$  variable.

Equation (63) may be obtained via the Bregman Lagrangian (58) for velocity gradient laws with momentum by choosing only the integral term. It is then necessary to modify the resulting Euler-Lagrange equations by setting  $f'_m$  to  $\pm 1$  based on monotonicity of  $\tilde{f}$  as described in Section 2.2. The following proposition summarizes the properties of (64) and (65).

**Proposition 6.6.** *Consider the algorithm (63) or its equivalent form (64) & (65) under Assumption 2.2 with  $\mathcal{N} = 1 + \mu \|\boldsymbol{\alpha}(\mathbf{x}, t)\|^2$  and  $\mu > \frac{\gamma D_1}{\beta}$ . Then, all trajectories  $(\mathbf{x}, \hat{\mathbf{a}}, \hat{\mathbf{v}})$  remain bounded,  $\tilde{f} \in L_2$ ,  $(\hat{\mathbf{a}} - \hat{\mathbf{v}}) \in \mathcal{L}_2$ ,  $s \in \mathcal{L}_2 \cap \mathcal{L}_\infty$ ,  $s \rightarrow 0$  and  $\mathbf{x} \rightarrow \mathbf{x}_d$ .*

The proof is given in Appendix A.4.

**Remark 6.9.** As noted in Remark 6.6, by following the proof of Proposition 6.6, one may also take  $\mathcal{N}$  to be matrix-valued as  $\mathbf{N} = 1 + \mu \boldsymbol{\alpha}(\mathbf{x}, t) \boldsymbol{\alpha}(\mathbf{x}, t)^\top$ .  $\diamond$

**Remark 6.10.** As in Remark 6.8, a gain matrix  $\mathbf{P} = \mathbf{P}^\top > 0$  of appropriate dimension may be placed in front of  $\boldsymbol{\alpha}(\mathbf{x}, t)$  in  $\dot{\hat{\mathbf{v}}}$ .  $\diamond$

Predominantly inspired by deep learning, there has recently been strong interest in nonconvex models that are nevertheless amenable to gradient-based or gradient-inspired optimization. The development in this section suggests that machine learning models that can be provably optimized using gradient techniques represent a promising class of nonlinear parameterizations for adaptive control development.

#### 6.4 THE ELASTIC MODIFICATION

We now consider a modification to the previously discussed adaptive control laws inspired by the Elastic Averaging SGD (EASGD) algorithm (Zhang et al., 2014; Boffi and Slotine, 2020). EASGD is an algorithm intended for distributed training of deep neural networks across  $p$  graphics processing units (GPUs). Each GPU is used to train a local copy of the deep network model, and each local copy maintains its own set of parameters  $\hat{\mathbf{a}}^{(i)}$ . These parameters are updated according to the iteration

$$\hat{\mathbf{a}}_{t+1}^{(i)} = \hat{\mathbf{a}}_t^{(i)} - \lambda \mathbf{g}_t^{(i)} + \lambda k \left( \bar{\mathbf{a}}_t - \hat{\mathbf{a}}_t^{(i)} \right), \quad (66)$$

$$\bar{\mathbf{a}}_{t+1} = \bar{\mathbf{a}}_t + \lambda k \left( \frac{1}{p} \sum_{i=1}^p \hat{\mathbf{a}}^{(i)} - \bar{\mathbf{a}}_t \right), \quad (67)$$

where  $\lambda$  is the learning rate,  $\mathbf{g}_t^{(i)}$  is the stochastic gradient approximation computed by the  $i^{\text{th}}$  agent at timestep  $t$ ,  $k$  is the coupling strength, and  $\bar{\mathbf{a}}$  is the *center* variable. Equation (67) takes the form of a low-pass filter of the instantaneous average of the set of local parameters.

It was observed by Boffi and Slotine (2020) that in the non-distributed ( $p = 1$ ) case, (66) & (67) do not reduce to standard stochastic gradient descent, and that application of EASGD in this setting has different generalization properties than standard SGD when used to train deep neural networks. In a similar spirit, by construction of suitable Lyapunov functions, we now show that adding a center-like variable to the adaptive laws considered in previous sections maintains their stability. This immediately gives rise to a new class of higher-order adaptive control algorithms. Interestingly, these algorithms do not seem to admit an equivalent representation in terms of a single second-, third-, or fourth-order system for  $\hat{\mathbf{a}}$ , but must be written as a system of first-order equations.

**Remark 6.11.** The algorithms considered in this subsection immediately extend to the case of cloud-based adaptation for networked robotic systems (Wensing and Slotine, 2018), where the center variable is allowed to have its own dynamics as in (67) rather than simply representing the instantaneous spatial average of the distributed parameters.  $\diamond$

We first apply the elastic modification to the Slotine & Li adaptive controller (8) for linearly parameterized unknown dynamics  $\tilde{f} = \mathbf{Y}\tilde{\mathbf{a}}$ . These results extend trivially to the non-filtered composite algorithm of Section 6.2. To this end, we define the adaptation law

$$\dot{\hat{\mathbf{a}}} = -\mathbf{P}\mathbf{Y}^\top s + k(\bar{\mathbf{a}} - \hat{\mathbf{a}}), \quad (68)$$

$$\dot{\bar{\mathbf{a}}} = k(\hat{\mathbf{a}} - \bar{\mathbf{a}}), \quad (69)$$

whose basic stability properties are summarized in the following proposition.

**Proposition 6.7.** *Consider the adaptation law (68) & (69). Then all trajectories  $(\mathbf{x}, \hat{\mathbf{a}}, \bar{\mathbf{a}})$  remain bounded,  $s \in \mathcal{L}_2 \cap \mathcal{L}_\infty$ ,  $(\hat{\mathbf{a}} - \bar{\mathbf{a}}) \in \mathcal{L}_2$ ,  $s \rightarrow 0$  and  $\mathbf{x} \rightarrow \mathbf{x}_d$ .*

The proof is given in Appendix A.5

We now apply the elastic modification to the algorithm (12) for nonlinearly parameterized unknown dynamics satisfying Assumption 2.2. As in (68) & (69), we define

$$\dot{\hat{\mathbf{a}}} = -\tilde{f}\mathbf{P}\alpha + k(\bar{\mathbf{a}} - \hat{\mathbf{a}}), \quad (70)$$

$$\dot{\bar{\mathbf{a}}} = k(\hat{\mathbf{a}} - \bar{\mathbf{a}}). \quad (71)$$

**Proposition 6.8.** *Consider the adaptation law (70) & (71). Then all trajectories  $(\mathbf{x}, \hat{\mathbf{a}}, \bar{\mathbf{a}})$  remain bounded,  $\tilde{f} \in \mathcal{L}_2 \cap \mathcal{L}_\infty$ ,  $(\hat{\mathbf{a}} - \bar{\mathbf{a}}) \in \mathcal{L}_2$ ,  $s \in \mathcal{L}_\infty \cap \mathcal{L}_2$ ,  $s \rightarrow 0$  and  $\mathbf{x} \rightarrow \mathbf{x}_d$ .*

The proof is given in Appendix A.6.

We now consider the higher-order algorithms presented in Sections 6.2 and 6.3. In the higher-order setting, there are three clear possibilities for the elastic modification: coupling to a quorum variable for the  $\hat{\mathbf{a}}$  variable, coupling to a center variable for the  $\hat{\mathbf{v}}$  variable, or coupling to center variables in both  $\hat{\mathbf{a}}$  and  $\hat{\mathbf{v}}$ . We prove stability for all three possibilities only in the nonlinearly parameterized setting described by Assumption 2.2. The results extend naturally to the higher-order composite algorithm for linearly parameterized systems presented in Section 6.2. We begin with the first possibility,

$$\dot{\hat{\mathbf{v}}} = -\gamma\tilde{f}\alpha, \quad (72)$$

$$\dot{\hat{\mathbf{a}}} = \beta\mathcal{N}(\hat{\mathbf{v}} - \hat{\mathbf{a}}) + k\beta\mathcal{N}(\bar{\mathbf{a}} - \hat{\mathbf{a}}), \quad (73)$$

$$\dot{\bar{\mathbf{a}}} = k\beta\mathcal{N}(\hat{\mathbf{a}} - \bar{\mathbf{a}}). \quad (74)$$

The basic stability properties of the algorithm (72)-(74) are summarized in the following proposition.

**Proposition 6.9.** *Consider the algorithm (72)-(74) under Assumption 2.2. Set  $\frac{1}{3} \leq k < 1$ ,  $\mathcal{N} = 1 + \mu\|\alpha(\mathbf{x}, t)\|^2$ , and  $\mu > \frac{2D_1\gamma}{\beta(1-k)}$ . Then all trajectories  $(\mathbf{x}, \hat{\mathbf{a}}, \hat{\mathbf{v}}, \bar{\mathbf{a}})$  remain bounded,  $\tilde{f} \in \mathcal{L}_2 \cap \mathcal{L}_\infty$ ,  $s \in \mathcal{L}_2 \cap \mathcal{L}_\infty$ ,  $(\hat{\mathbf{a}} - \hat{\mathbf{v}}) \in \mathcal{L}_2$ ,  $(\hat{\mathbf{a}} - \bar{\mathbf{a}}) \in \mathcal{L}_2$ ,  $s \rightarrow 0$  and  $\mathbf{x} \rightarrow \mathbf{x}_d$ .*

The proof is given in Appendix A.7. We now consider the second possibility of adding a center variable in the  $\hat{\mathbf{v}}$  variable,

$$\dot{\hat{\mathbf{v}}} = -\gamma\tilde{f}\alpha + \rho(\bar{\mathbf{v}} - \hat{\mathbf{v}}), \quad (75)$$

$$\dot{\bar{\mathbf{v}}} = \rho(\hat{\mathbf{v}} - \bar{\mathbf{v}}), \quad (76)$$

$$\dot{\hat{\mathbf{a}}} = \beta\mathcal{N}(\hat{\mathbf{v}} - \hat{\mathbf{a}}). \quad (77)$$

The basic stability properties of (75)-(77) are summarized in the following proposition.

**Proposition 6.10.** *Consider the algorithm (75)-(77) under Assumption 2.2. Set  $\rho < 2\beta$ ,  $\mathcal{N} = 1 + \mu\|\alpha(\mathbf{x}, t)\|^2$ , and  $\mu > \frac{\gamma D_1}{\beta}$ . Then all trajectories  $(\mathbf{x}, \hat{\mathbf{a}}, \hat{\mathbf{v}}, \bar{\mathbf{v}})$  remain bounded,  $\tilde{f} \in \mathcal{L}_2 \cap \mathcal{L}_\infty$ ,  $s \in \mathcal{L}_2 \cap \mathcal{L}_\infty$ ,  $(\hat{\mathbf{v}} - \bar{\mathbf{v}}) \in \mathcal{L}_2$ ,  $(\hat{\mathbf{v}} - \hat{\mathbf{a}}) \in \mathcal{L}_2$ ,  $s \rightarrow 0$  and  $\mathbf{x} \rightarrow \mathbf{x}_d$ .*

The proof is given in Appendix A.8. Finally, we consider adding coupling to center variables in both  $\hat{\mathbf{a}}$  and  $\hat{\mathbf{v}}$ ,

$$\dot{\hat{\mathbf{v}}} = -\gamma \tilde{f} \boldsymbol{\alpha} + \rho (\bar{\mathbf{v}} - \hat{\mathbf{v}}), \quad (78)$$

$$\dot{\bar{\mathbf{v}}} = \rho (\hat{\mathbf{v}} - \bar{\mathbf{v}}), \quad (79)$$

$$\dot{\hat{\mathbf{a}}} = \beta \mathcal{N} (\hat{\mathbf{v}} - \hat{\mathbf{a}}) + k \beta \mathcal{N} (\bar{\mathbf{a}} - \hat{\mathbf{a}}), \quad (80)$$

$$\dot{\bar{\mathbf{a}}} = k \beta \mathcal{N} (\hat{\mathbf{a}} - \bar{\mathbf{a}}). \quad (81)$$

The basic stability properties of (78)-(81) are summarized in the following proposition.

**Proposition 6.11.** *Consider the algorithm (78)-(81) under Assumption 2.2. Set  $\rho < \beta(1 - k)$ ,  $\frac{1}{3} \leq k < 1$ ,  $\mathcal{N} = 1 + \mu \|\boldsymbol{\alpha}(\mathbf{x}, t)\|^2$  and  $\mu > \frac{2\gamma D_1}{\beta(1-k)}$ . Then, all trajectories  $(\mathbf{x}, \hat{\mathbf{v}}, \bar{\mathbf{v}}, \hat{\mathbf{a}}, \bar{\mathbf{a}})$  remain bounded,  $\tilde{f} \in \mathcal{L}_2 \cap \mathcal{L}_\infty$ ,  $s \in \mathcal{L}_2 \cap \mathcal{L}_\infty$ ,  $(\hat{\mathbf{v}} - \bar{\mathbf{v}}) \in \mathcal{L}_2$ ,  $(\hat{\mathbf{a}} - \bar{\mathbf{a}}) \in \mathcal{L}_2$ ,  $(\hat{\mathbf{v}} - \hat{\mathbf{a}}) \in \mathcal{L}_2$ ,  $s \rightarrow 0$  and  $\mathbf{x} \rightarrow \mathbf{x}_d$ .*

The proof is given in Appendix A.9.

We have thus shown that all Euclidean adaptive control algorithms presented in this paper<sup>10</sup>, as well as the classic algorithm of Slotine and Li, can be modified to include feedback coupling to a low-pass filtered version of the adaptation variables. It is well known that iterate averaging for stochastic optimization algorithms such as stochastic gradient descent can improve convergence rates via variance reduction (Polyak and Juditsky, 1992). The elastic modification is similar in spirit, but employs feedback rather than series coupling. This suggests that adding the elastic term may improve robustness of adaptation algorithms, and we leave a theoretical investigation of this conjecture for future work.

## 6.5 EXPONENTIAL FORGETTING LEAST SQUARES AND BOUNDED GAIN FORGETTING

We now demonstrate how to apply the techniques of exponential forgetting and bounded gain forgetting least squares (Slotine and Li, 1991) to the adaptation algorithms we have developed. These techniques are useful for estimation of time-varying parameters, as they rapidly discard previous information used for parameter estimation. Exponential forgetting least squares is described by a time-dependent learning rate matrix  $\mathbf{P}(t)$ , which, in the linearly parameterized case  $\tilde{f} = \mathbf{Y}\tilde{\mathbf{a}}$  takes the form

$$\dot{\mathbf{P}} = \begin{cases} \lambda \mathbf{P} - \mathbf{P} \mathbf{Y}^\top \mathbf{Y} \mathbf{P} & \text{if } \|\mathbf{P}\| \leq P_0 \\ 0 & \text{else} \end{cases} \quad (82)$$

where  $\lambda > 0$  is a constant forgetting factor,  $P_0$  is a maximum bound on the norm, and  $\|\mathbf{P}\|$  is a matrix norm such as the operator norm. Equation (82) implies for the inverse matrix

$$\frac{d}{dt} \mathbf{P}^{-1} = \begin{cases} -\lambda \mathbf{P}^{-1} + \mathbf{Y}^\top \mathbf{Y} \mathbf{P}^{-1} & \text{if } \|\mathbf{P}\| \leq P_0 \\ 0 & \text{else} \end{cases} \quad (83)$$

In the nonlinearly parameterized case described by Assumption 2.2, we will replace  $\mathbf{Y}^\top$  in (82) & (83) by  $\boldsymbol{\alpha}(\mathbf{x}, t)$ . In the bounded gain forgetting technique,  $\lambda$  is a time-dependent function

$$\lambda(t) = \lambda_0 \left( 1 - \frac{\|\mathbf{P}\|}{P_0} \right), \quad (84)$$

where  $\lambda_0 > 0$  sets the forgetting factor when the norm of  $\mathbf{P}$  is small. It can be shown that this choice of  $\lambda(t)$  ensures that  $\|\mathbf{P}\| \leq P_0$ , and thus we may drop the case statement in (82) & (83) (Slotine and Li, 1991). The choice of  $\lambda(t)$  in bounded gain forgetting and the case statement used in (82) & (83) are both employed to prevent unboundedness of the learning rate matrix.

We focus on algorithms without the elastic modification of Section 6.4; extension to the elastic modification is simple. We also focus on the bounded gain forgetting technique: proofs

<sup>10</sup>Similar results apply for the natural algorithms with additional technical details by replacing quadratic terms in the Lyapunov functions with Bregman divergences

for the exponential forgetting least squares technique are identical, with the addition of an appropriate case statement in the time derivative of the Lyapunov function. For simplicity, we include only the time-dependent gain  $\mathbf{P}(t)$  and set the scalar gains  $\kappa = \gamma = 1$  where applicable.

We begin with the first-order non-filtered composite (53) with  $\mathbf{P}$  given by (82). In this case, the composite algorithm may be implemented via the PI form (54)-(57) where now  $\mathbf{P} = \mathbf{P}(t)$ .

**Proposition 6.12.** *Consider the adaptation algorithm (53) with  $\mathbf{P}(t)$  given by (82),  $\lambda(t)$  given by (84), and  $\kappa = \gamma = 1$ . Then all trajectories  $(\mathbf{x}, \hat{\mathbf{a}})$  remain bounded,  $\tilde{f} \in \mathcal{L}_2 \cap \mathcal{L}_\infty$ ,  $s \in \mathcal{L}_2 \cap \mathcal{L}_\infty$ ,  $s \rightarrow 0$  and  $\mathbf{x} \rightarrow \mathbf{x}_d$ .*

The proof is given in Appendix A.10

We can state a similar result for the higher-order non-filtered composite with time-dependent  $\mathbf{P}(t)$  given by (82),

$$\ddot{\hat{\mathbf{a}}} + \left( \beta \mathcal{N} - \frac{\dot{\mathcal{N}}}{\mathcal{N}} - \dot{\mathbf{P}} \mathbf{P}^{-1} \right) \dot{\hat{\mathbf{a}}} = -\beta \mathcal{N} \mathbf{P}(t) \mathbf{Y}^T (s + \tilde{f}), \quad (85)$$

which admits a representation as two first-order equations,

$$\dot{\hat{\mathbf{v}}} = -\mathbf{P}(t) \mathbf{Y}^T (s + \tilde{f}), \quad (86)$$

$$\dot{\hat{\mathbf{a}}} = \beta \mathcal{N} \mathbf{P}(t) (\hat{\mathbf{v}} - \hat{\mathbf{a}}). \quad (87)$$

Equation (86) can be implemented via the PI form  $\dot{\hat{\mathbf{v}}} = \bar{\mathbf{v}} + \boldsymbol{\xi}(\mathbf{x}, t) + \boldsymbol{\rho}(\mathbf{x}, t)$  where  $\boldsymbol{\xi}$ ,  $\boldsymbol{\rho}$ , and  $\bar{\mathbf{v}}$  are given by (54), (55), and (57) respectively with  $\gamma = \kappa = 1$ .

**Proposition 6.13.** *Consider the adaptation algorithm (85) with  $\mathbf{P}(t)$  given by (82),  $\lambda(t)$  given by (84),  $\mathcal{N}(t) = 1 + \mu \|\mathbf{Y}\|^2$  and  $\mu > \frac{3\eta+2}{2\eta\beta}$ . Then all trajectories  $(\mathbf{x}, \hat{\mathbf{v}}, \hat{\mathbf{a}})$  remain bounded,  $\tilde{f} \in \mathcal{L}_2 \cap \mathcal{L}_\infty$ ,  $s \in \mathcal{L}_2 \cap \mathcal{L}_\infty$ ,  $s \rightarrow 0$  and  $\mathbf{x} \rightarrow \mathbf{x}_d$ .*

The proof is given in Appendix A.11.

**Remark 6.12.** Because  $\mathbf{P}(t)$  is uniformly bounded in  $t$ , it is not necessary to include  $\mathbf{P}(t)$  in (87); by a slight modification of the proof, it is easy to show that the modified higher-order law

$$\ddot{\hat{\mathbf{a}}} + \left( \beta \mathcal{N} - \frac{\dot{\mathcal{N}}}{\mathcal{N}} \right) \dot{\hat{\mathbf{a}}} = -\beta \mathcal{N} \mathbf{P}(t) \mathbf{Y}^T (s + \tilde{f}),$$

is also a stable adaptive law with a suitable choice of gains.  $\diamond$

We now consider Tyukin's first-order algorithm for nonlinearly parameterized systems (12) with  $\mathbf{P} = \mathbf{P}(t)$  given by (82). To do so, we require an additional assumption

**Assumption 6.3.** For the same function  $\boldsymbol{\alpha}(\mathbf{x}, t)$  as in Assumption 2.2, there exists a constant  $D_2$  such that

$$|\tilde{f}(\mathbf{x}, \hat{\mathbf{a}}, \mathbf{a}, t)| \geq D_2 |\boldsymbol{\alpha}(\mathbf{x}, t)^T \hat{\mathbf{a}}|. \quad (88)$$

Together with Assumption 2.2, Assumption 6.3 states that  $\tilde{f}$  lies between two linear functions. Given that the update (82) is derived based on recursive *linear* least squares considerations, it is unsurprising that such an assumption is required in the nonlinearly parameterized setting. We are now in a position to state the following proposition.

**Proposition 6.14.** *Consider the adaptation algorithm (12) with  $\mathbf{P}(t)$  given by (82) and  $\lambda(t)$  given by (84) for  $\tilde{f}$  satisfying Assumptions 2.2 and 6.3. Further assume that  $D_1 < 2D_2^2$  or that  $D_2 > \frac{1}{2}$ . Then, all trajectories  $(\mathbf{x}, \hat{\mathbf{a}})$  remain bounded,  $\tilde{f} \in \mathcal{L}_2$ ,  $s \in \mathcal{L}_2 \cap \mathcal{L}_\infty$ ,  $s \rightarrow 0$  and  $\mathbf{x} \rightarrow \mathbf{x}_d$ .*

The proof is given in Appendix A.12.

Last, we consider the momentum algorithm for nonlinearly parameterized systems

$$\ddot{\hat{\mathbf{a}}} + \left( \beta \mathcal{N} - \frac{\dot{\mathcal{N}}}{\mathcal{N}} - \dot{\mathbf{P}} \mathbf{P}^{-1} \right) \dot{\hat{\mathbf{a}}} = -\beta \mathcal{N} \tilde{f} \mathbf{P}(t) \boldsymbol{\alpha}(\mathbf{x}, t), \quad (89)$$

which admits a representation as two first-order equations,

$$\dot{\mathbf{v}} = -\tilde{f}\mathbf{P}(t)\boldsymbol{\alpha}(\mathbf{x}, t), \quad (90)$$

$$\dot{\mathbf{a}} = \beta\mathcal{N}\mathbf{P}(t)(\hat{\mathbf{v}} - \hat{\mathbf{a}}). \quad (91)$$

**Proposition 6.15.** *Consider the adaptation algorithm (89) with  $\mathbf{P}(t)$  given by (82),  $\lambda(t)$  given by (84),  $\mathcal{N} = 1 + \mu\|\boldsymbol{\alpha}\|^2$ , and  $\mu > \frac{4D_2-2+(2D_1+1)^2}{\beta(4D_2-1)}$ . Suppose  $\tilde{f}$  satisfies Assumptions 2.2 and 6.3. Further assume that  $D_2 > \frac{1}{2}$ . Then, all trajectories  $(\mathbf{x}, \hat{\mathbf{v}}, \hat{\mathbf{a}})$  remain bounded,  $\tilde{f} \in \mathcal{L}_2$ ,  $s \in \mathcal{L}_2 \cap \mathcal{L}_\infty$ ,  $s \rightarrow 0$  and  $\mathbf{x} \rightarrow \mathbf{x}_d$ .*

The proof is given in Appendix A.13.

**Remark 6.13.** As in Remark 6.12, because  $\mathbf{P}(t)$  is uniformly bounded in  $t$ , it is not necessary to include  $\mathbf{P}(t)$  in (91). It is simple to show by modification of the proof that

$$\ddot{\mathbf{a}} + \left( \beta\mathcal{N} - \frac{\dot{\mathcal{N}}}{\mathcal{N}} \right) \dot{\mathbf{a}} = -\beta\mathcal{N}\tilde{f}\mathbf{P}(t)\boldsymbol{\alpha}(\mathbf{x}, t)$$

is also a stable adaptive law with a suitable choice of gains.

## 7 NATURAL MOMENTUM ALGORITHMS

The Bregman Lagrangian allows for the introduction of non-Euclidean metrics. In Section 5.2, we took the potential function  $\psi$  to be the Euclidean norm,  $\psi(\mathbf{x}) = \frac{1}{2}\|\mathbf{x}\|^2$ . We now show that taking  $\psi$  to be an arbitrary strictly convex function leads to a more general class of algorithms that can be seen as the higher-order variants of those discussed in Sections 2.3 and 3. With the same definitions of  $\bar{\alpha}$ ,  $\bar{\gamma}$ , and  $\bar{\beta}$  as in Section 5.2, but now taking the general Bregman divergence  $d_\psi(\cdot \parallel \cdot)$ , the Bregman Lagrangian (36) takes the form

$$\mathcal{L} = e^{\int_0^t \beta\mathcal{N}(s)dt} \left( \beta\mathcal{N}d_\psi\left(\hat{\mathbf{a}} + \frac{\dot{\mathbf{a}}}{\beta\mathcal{N}} \parallel \hat{\mathbf{a}}\right) - \gamma \frac{d}{dt} \left[ \frac{1}{2}s^2 \right] \right). \quad (92)$$

The Euler-Lagrange equations for (92) lead to the natural adaptation law with momentum

$$\ddot{\mathbf{a}} + \left( \beta\mathcal{N} - \frac{\dot{\mathcal{N}}}{\mathcal{N}} \right) \dot{\mathbf{a}} + \gamma\beta\mathcal{N} \left( \nabla^2\psi\left(\hat{\mathbf{a}} + \frac{\dot{\mathbf{a}}}{\beta\mathcal{N}}\right) \right)^{-1} \mathbf{Y}^\top s = 0. \quad (93)$$

Above, the Euclidean adaptive law has been modified so that  $\mathbf{Y}^\top s$  is now pre-multiplied by the inverse Hessian of  $\psi$  evaluated at  $\hat{\mathbf{a}} + \frac{\dot{\mathbf{a}}}{\beta\mathcal{N}}$ . As discussed in Section 5.2, this quantity is precisely  $\hat{\mathbf{v}}$ . The resulting adaptation law can thus be written in the equivalent form

$$\dot{\mathbf{v}} = -\gamma (\nabla^2\psi(\hat{\mathbf{v}}))^{-1} \mathbf{Y}^\top s, \quad (94)$$

$$\dot{\mathbf{a}} = \beta\mathcal{N}(\hat{\mathbf{v}} - \hat{\mathbf{a}}). \quad (95)$$

Equations (94) & (95) demonstrate that using the Bregman divergence in the Bregman Lagrangian leads to momentum variants of the natural algorithms of Section 2.3. Taking the  $\beta \rightarrow \infty$  limit immediately recovers the first-order laws discussed in Section 2.3. The stability of the above laws for strongly convex  $\psi$  is stated in the following proposition.

**Proposition 7.1.** *Consider the higher-order “natural” adaptation law (93). Assume that  $\psi$  is  $l$ -strongly convex so that  $\nabla^2\psi(\cdot) \geq l \mathbf{I}$  globally. Take  $\mathcal{N} = 1 + \mu\|\mathbf{Y}\|^2$  and  $\mu > \frac{\gamma(1+l^{-1})^2}{4\beta\eta}$ . Then all trajectories  $(\mathbf{x}, \hat{\mathbf{v}}, \hat{\mathbf{a}})$  remain bounded,  $s \in \mathcal{L}_2 \cap \mathcal{L}_\infty$ ,  $s \rightarrow 0$  and  $\mathbf{x} \rightarrow \mathbf{x}_d$ .*

The proof is given in Appendix A.14. A second, related variant is given by

$$\dot{\mathbf{v}} = -\gamma (\nabla^2\psi(\hat{\mathbf{v}}))^{-1} \mathbf{Y}^\top s, \quad (96)$$

$$\dot{\mathbf{a}} = \beta\mathcal{N} (\nabla^2\psi(\hat{\mathbf{a}}))^{-1} (\nabla\psi(\hat{\mathbf{v}}) - \nabla\psi(\hat{\mathbf{a}})). \quad (97)$$

Algorithm (96) & (97) is equivalent to algorithm (37) entirely in the mirrored domain. Indeed, it may be re-written

$$\begin{aligned}\frac{d}{dt}\nabla\psi(\hat{\mathbf{v}}) &= -\gamma\mathbf{Y}^\top s, \\ \frac{d}{dt}\nabla\psi(\hat{\mathbf{a}}) &= \beta\mathcal{N}(\nabla\psi(\hat{\mathbf{v}}) - \nabla\psi(\hat{\mathbf{a}})),\end{aligned}$$

which shows that  $\nabla\psi(\hat{\mathbf{a}})$  obtains the same values over time as  $\hat{\mathbf{a}}$  computed via algorithm (37). The stability of this adaptive law (shown in Proposition 7.2) implies that the parameters obtained by the momentum algorithm (37) may be transformed via the inverse of the gradient of an  $l$ -strongly convex and  $L$ -smooth function, and the resulting transformed parameters will still ensure stability and tracking for the closed-loop system.

A modification of (97) that is driven by  $\hat{\mathbf{v}}$  rather than  $\nabla\psi(\hat{\mathbf{v}})$  is given by

$$\dot{\hat{\mathbf{v}}} = -\gamma(\nabla^2\psi(\hat{\mathbf{v}}))^{-1}\mathbf{Y}^\top s, \quad (98)$$

$$\dot{\hat{\mathbf{a}}} = \beta\mathcal{N}(\nabla^2\psi(\hat{\mathbf{a}}))^{-1}(\hat{\mathbf{v}} - \hat{\mathbf{a}}). \quad (99)$$

The properties of these two possible adaptation laws are given in the following proposition.

**Proposition 7.2.** *Consider the adaptation algorithm (96) & (97) or the adaptation algorithm (98) & (99). Assume that  $\psi$  is  $l$ -strongly convex and  $L$ -smooth, so that  $l\mathbf{I} \leq \nabla^2\psi(\cdot) \leq L\mathbf{I}$ . Take  $\mathcal{N} = 1 + \mu\|\mathbf{Y}\|^2$  and choose  $\mu > \frac{\gamma(l+\gamma L)^2}{4\beta\eta l^3}$  in the former case and  $\mu > \frac{\gamma(l+\gamma L)^2}{4\beta\eta l^2}$  in the latter. Then all trajectories  $(\mathbf{x}, \hat{\mathbf{v}}, \hat{\mathbf{a}})$  remain bounded,  $s \in \mathcal{L}_2 \cap \mathcal{L}_\infty$ ,  $s \rightarrow 0$  and  $\mathbf{x} \rightarrow \mathbf{x}_d$ .*

The proof is presented in Appendix A.15.

**Remark 7.1.** For efficient implementation of the proposed natural momentum algorithms, as well as for their first-order equivalents,  $\psi$  should be chosen so that  $[\nabla^2\psi(\cdot)]^{-1}$  is efficiently computable and ideally sparse. Alternatively, if the inverse function of the gradient  $(\nabla\psi^{-1})(\cdot)$  is efficiently computable,  $\nabla\psi(\hat{\mathbf{a}})$  or  $\nabla\psi(\hat{\mathbf{v}})$  may be updated directly and subsequently inverted to arrive at the parameter values. Discretization of these algorithms is a subtle issue, and discretization of the  $\dot{\hat{\mathbf{a}}}$  and  $\dot{\hat{\mathbf{v}}}$  dynamics directly results in a natural gradient-like update (Amari, 1998), while discretization of the  $\frac{d}{dt}\nabla\psi(\hat{\mathbf{a}})$  and  $\frac{d}{dt}\nabla\psi(\hat{\mathbf{v}})$  dynamics leads to a mirror descent-like update (Beck and Teboulle, 2003; Nemirovski and Yudin, 1983); these discrete-time algorithms have the same continuous-time limit (Krichene et al., 2015).  $\diamond$

The above natural adaptation laws with momentum may be generalized to composite algorithms, as well as to algorithms for nonlinearly parameterized adaptive control, by replacing Euclidean norms by Bregman divergences where appropriate in the proofs of the corresponding Euclidean algorithms (see, e.g., the proofs of Propositions 7.1 & 7.2). Rather than derive this for each algorithm, we now show how the general results on velocity gradient algorithms with momentum (Propositions 6.1 & 6.2) can be extended to the non-Euclidean setting. We start with the case of a local functional, which requires the modification of Assumption 6.1 to an equivalent non-Euclidean version.

**Assumption 7.1.** There exists a time-dependent signal  $N(t)$  and non-negative scalar values  $\beta \geq 0, \mu \geq 0$  such that the time-derivative of the goal functional evaluated at the true parameters,  $\dot{Q}(\mathbf{x}, \mathbf{a}, t)$ , satisfies the following inequality

$$\dot{Q}(\mathbf{x}, \mathbf{a}, t) - \frac{\beta\mu}{\gamma}N(t)\|\hat{\mathbf{a}} - \hat{\mathbf{v}}\|^2 + (\hat{\mathbf{a}} - \hat{\mathbf{v}})^\top \left(\mathbf{I} + [\nabla^2\psi(\hat{\mathbf{v}})]^{-1}\right) \nabla_{\hat{\mathbf{a}}}\dot{Q}(\mathbf{x}, \hat{\mathbf{a}}, t) \leq -\rho(Q). \quad (100)$$

In (100),  $\rho(\cdot)$  is positive definite, continuous in  $Q$ , and satisfies  $\rho(0) = 0$ .  $\diamond$

With Assumption 7.1 in hand, we can state the following non-Euclidean equivalent of Proposition 6.1. We focus on the variant (93), as the other possibilities are similar.

**Proposition 7.3.** *Consider the algorithm*

$$\ddot{\hat{\mathbf{a}}} + \left(\beta\mathcal{N} - \frac{\dot{\mathcal{N}}}{\mathcal{N}}\right)\dot{\hat{\mathbf{a}}} + \gamma\beta\mathcal{N}\left[\nabla^2\psi\left(\hat{\mathbf{a}} + \frac{\dot{\hat{\mathbf{a}}}{\beta\mathcal{N}}}\right)\right]^{-1}\nabla_{\hat{\mathbf{a}}}\dot{Q}(\mathbf{x}, \hat{\mathbf{a}}, t) = 0$$

or its equivalent first order form

$$\begin{aligned}\dot{\hat{\mathbf{v}}} &= -\gamma [\nabla^2 \psi(\hat{\mathbf{v}})]^{-1} \nabla_{\hat{\mathbf{a}}} \dot{Q}(\mathbf{x}, \hat{\mathbf{a}}, t), \\ \dot{\hat{\mathbf{a}}} &= \beta \mathcal{N}(\hat{\mathbf{v}} - \hat{\mathbf{a}}),\end{aligned}$$

and assume  $Q$  satisfies Assumptions 5.1, 5.3, and 7.1. Then all solutions  $(\mathbf{x}(t), \hat{\mathbf{v}}(t), \hat{\mathbf{a}}(t))$  remain bounded,  $(\hat{\mathbf{a}} - \hat{\mathbf{v}}) \in \mathcal{L}_2$ , and  $\lim_{t \rightarrow \infty} Q = 0$ .

*Proof.* Consider the Lyapunov-like function

$$V = Q(\mathbf{x}, t) + \frac{1}{\gamma} d_\psi(\mathbf{a} \parallel \hat{\mathbf{v}}) + \frac{1}{2\gamma} (\hat{\mathbf{a}} - \hat{\mathbf{v}})^\top (\hat{\mathbf{a}} - \hat{\mathbf{v}}). \quad (101)$$

Equation (101) implies that, with  $\mathcal{N}(t) = 1 + \mu N(t)$ ,

$$\begin{aligned}\dot{V} &= \dot{Q}(\mathbf{x}, \hat{\mathbf{a}}, t) - \hat{\mathbf{a}}^\top \nabla_{\hat{\mathbf{a}}} \dot{Q}(\mathbf{x}, \hat{\mathbf{a}}, t) - \frac{\beta}{\gamma} \|\hat{\mathbf{a}} - \hat{\mathbf{v}}\|^2 - \frac{\beta\mu}{\gamma} N(t) \|\hat{\mathbf{a}} - \hat{\mathbf{v}}\|^2 + (\hat{\mathbf{a}} - \hat{\mathbf{v}})^\top \left( \mathbf{I} + [\nabla^2 \psi(\hat{\mathbf{v}})]^{-1} \right) \nabla_{\hat{\mathbf{a}}} \dot{Q}(\mathbf{x}, \hat{\mathbf{a}}, t), \\ &\leq \dot{Q}(\mathbf{x}, \mathbf{a}, t) - \frac{\beta}{\gamma} \|\hat{\mathbf{a}} - \hat{\mathbf{v}}\|^2 - \frac{\beta\mu}{\gamma} N(t) \|\hat{\mathbf{a}} - \hat{\mathbf{v}}\|^2 + (\hat{\mathbf{a}} - \hat{\mathbf{v}})^\top \left( \mathbf{I} + [\nabla^2 \psi(\hat{\mathbf{v}})]^{-1} \right) \nabla_{\hat{\mathbf{a}}} \dot{Q}(\mathbf{x}, \hat{\mathbf{a}}, t), \\ &\leq -\rho(Q) - \frac{\beta}{\gamma} \|\hat{\mathbf{a}} - \hat{\mathbf{v}}\|^2.\end{aligned} \quad (102)$$

The first line to the second follows by convexity of  $\dot{Q}(\mathbf{x}, \hat{\mathbf{a}}, t)$  in its second argument, while the second line to the third follows by Assumption 7.1. The remainder of the proof is identical to Proposition 6.1.  $\square$

For the integral variant, we require a non-Euclidean version of Assumption 6.2.

**Assumption 7.2.**  $R(\mathbf{x}, \hat{\mathbf{a}}, t) \geq 0$  for all  $\mathbf{x}, \hat{\mathbf{a}}$ , and  $t$ , and is uniformly continuous in  $t$  for bounded  $\mathbf{x}$  and  $\hat{\mathbf{a}}$ .  $\nabla_{\hat{\mathbf{a}}} R(\mathbf{x}, \hat{\mathbf{a}}, t)$  is locally bounded in  $\mathbf{x}$  and  $\hat{\mathbf{a}}$  uniformly in  $t$ . Furthermore, there exists a time-dependent signal  $N(t)$  and non-negative scalar values  $\beta \geq 0, \mu \geq 0$  such that

$$R(\mathbf{x}, \mathbf{a}, t) - R(\mathbf{x}, \hat{\mathbf{a}}, t) - \frac{\beta\mu}{\gamma} N(t) \|\hat{\mathbf{a}} - \hat{\mathbf{v}}\|^2 + (\hat{\mathbf{a}} - \hat{\mathbf{v}})^\top \left( \mathbf{I} + [\nabla^2 \psi(\hat{\mathbf{v}})]^{-1} \right) \nabla_{\hat{\mathbf{a}}} R(\mathbf{x}, \hat{\mathbf{a}}, t) \leq -k R(\mathbf{x}, \hat{\mathbf{a}}, t)$$

for some constant  $k > 0$ .  $\diamond$

With Assumption 7.2, we can state the following proposition.

**Proposition 7.4.** Consider the algorithm

$$\ddot{\hat{\mathbf{a}}} + \left( \beta \mathcal{N} - \frac{\dot{\mathcal{N}}}{\mathcal{N}} \right) \dot{\hat{\mathbf{a}}} + \gamma \beta \mathcal{N} \left[ \nabla^2 \psi \left( \hat{\mathbf{a}} + \frac{\dot{\hat{\mathbf{a}}}{\beta \mathcal{N}}}{\mathcal{N}} \right) \right]^{-1} \nabla_{\hat{\mathbf{a}}} R(\mathbf{x}, \hat{\mathbf{a}}, t) = 0$$

or its equivalent first-order form

$$\begin{aligned}\dot{\hat{\mathbf{v}}} &= -\gamma [\nabla^2 \psi(\hat{\mathbf{v}})]^{-1} \nabla_{\hat{\mathbf{a}}} R(\mathbf{x}, \hat{\mathbf{a}}, t), \\ \dot{\hat{\mathbf{a}}} &= \beta \mathcal{N}(\hat{\mathbf{v}} - \hat{\mathbf{a}}),\end{aligned}$$

along with Assumptions 5.3 & 7.2. Let  $T_x$  denote the maximal interval of existence of  $\mathbf{x}(t)$ . Then,  $\hat{\mathbf{v}}$  and  $\hat{\mathbf{a}}$  remain bounded for  $t \in [0, T_x]$ ,  $(\hat{\mathbf{a}} - \hat{\mathbf{v}}) \in \mathcal{L}_2$  over this interval, and  $\int_0^{T_x} R(\mathbf{x}(t'), \hat{\mathbf{a}}(t'), t') dt' < \infty$ . Furthermore, for any bounded solution  $\mathbf{x}$ , these conclusions hold for all  $t$  and  $R(\mathbf{x}(t), \hat{\mathbf{a}}(t), t) \rightarrow 0$ .

*Proof.* Consider the Lyapunov-like function

$$V = \frac{1}{\gamma} d_\psi(\mathbf{a} \parallel \hat{\mathbf{v}}) + \frac{1}{2\gamma} (\hat{\mathbf{a}} - \hat{\mathbf{v}})^\top (\hat{\mathbf{a}} - \hat{\mathbf{v}}). \quad (103)$$

Equation (103) implies that, with  $\mathcal{N}(t) = 1 + \mu N(t)$ ,

$$\begin{aligned}\dot{V} &= -\tilde{\mathbf{a}}^\top \nabla_{\hat{\mathbf{a}}} R(\mathbf{x}, \hat{\mathbf{a}}, t) - \frac{\beta}{\gamma} \|\hat{\mathbf{a}} - \hat{\mathbf{v}}\|^2 - \frac{\beta\mu}{\gamma} N(t) \|\hat{\mathbf{a}} - \hat{\mathbf{v}}\|^2 + (\hat{\mathbf{a}} - \hat{\mathbf{v}})^\top \left( \mathbf{I} + [\nabla^2 \psi(\hat{\mathbf{v}})]^{-1} \right) \nabla_{\hat{\mathbf{a}}} R(\mathbf{x}, \hat{\mathbf{a}}, t), \\ &\leq R(\mathbf{x}, \mathbf{a}, t) - R(\mathbf{x}, \hat{\mathbf{a}}, t) - \frac{\beta}{\gamma} \|\hat{\mathbf{a}} - \hat{\mathbf{v}}\|^2 - \frac{\beta\mu}{\gamma} N(t) \|\hat{\mathbf{a}} - \hat{\mathbf{v}}\|^2 + (\hat{\mathbf{a}} - \hat{\mathbf{v}})^\top \left( \mathbf{I} + [\nabla^2 \psi(\hat{\mathbf{v}})]^{-1} \right) \nabla_{\hat{\mathbf{a}}} R(\mathbf{x}, \hat{\mathbf{a}}, t), \\ &\leq -k R(\mathbf{x}, \hat{\mathbf{a}}, t) - \frac{\beta}{\gamma} \|\hat{\mathbf{a}} - \hat{\mathbf{v}}\|^2.\end{aligned}\tag{104}$$

The first line to the second follows by convexity of  $R(\mathbf{x}, \hat{\mathbf{a}}, t)$  in its second argument, while the second to the third follows by Assumption 7.2. The remainder of the proof is identical to Proposition 6.2.  $\square$

The general methodology captured by the proofs of Propositions 7.3 & 7.4, in combination with the results of Section 6.3, may be exploited to derive non-Euclidean variants of our non-filtered composite algorithm and our momentum algorithm for nonlinearly parameterized adaptive control. Note that the strong convexity and smoothness requirements of Propositions 7.1 & 7.2, in combination with a suitable choice of  $N(t)$ , are one way to satisfy the requirements of Assumptions 7.1 & 7.2.

**Remark 7.2.** Our implicit regularization results in Section 3 also extend to the higher-order setting captured by algorithm (93). The assumption that  $\hat{\mathbf{a}} \rightarrow \hat{\mathbf{a}}_\infty$  implies  $\dot{\hat{\mathbf{a}}} \rightarrow 0$ . As noted in Section 5.2,  $\hat{\mathbf{v}} = \hat{\mathbf{a}} + \frac{\dot{\hat{\mathbf{a}}}{\beta\mathcal{N}}}$ , and we thus conclude that under this assumption  $\hat{\mathbf{v}} \rightarrow \hat{\mathbf{a}}_\infty$ . Because  $\dot{\hat{\mathbf{v}}}$  in (94) is identical to algorithm (20), the result follows. A formal statement of this fact is provided in Appendix B.1  $\diamond$

## 8 SIMULATIONS

In this section, we perform several numerical experiments demonstrating the validity of our theory, and consider a number of applications of our non-Euclidean adaptive laws.

### 8.1 CONVERGENCE AND IMPLICIT REGULARIZATION OF A MOMENTUM ALGORITHM FOR NONLINEARLY PARAMETERIZED SYSTEMS

We first empirically verify the global convergence and implicit regularization of our momentum algorithm for nonlinearly parameterized systems (63). In particular, we consider a second order system

$$\begin{aligned}\dot{x}_1 &= x_2, \\ \dot{x}_2 &= u - f(\mathbf{x}, \mathbf{a}, t),\end{aligned}$$

with an unknown system dynamics of the form

$$f(\mathbf{x}, \mathbf{a}, t) = \sigma \left( \tanh(\mathbf{V}\mathbf{x})^\top \mathbf{a} \right).\tag{105}$$

Equation (105) represents a three-layer neural network with input layer  $\mathbf{x}$ , hidden layer weights  $\mathbf{V}$ , hidden layer nonlinearity  $\tanh(\cdot)$ , hidden layer weights  $\mathbf{a}$ , and output nonlinearity  $\sigma(x) = e^{-1}x$ . The system model (105) can clearly be seen to satisfy Assumption 2.2 with  $\alpha(\mathbf{x}) = \tanh(\mathbf{V}\mathbf{x})^{11}$ . The PI form of algorithm (63) is given by

$$\nabla \psi(\hat{\mathbf{v}}) = \bar{v} + \xi(\mathbf{x}, t) + \rho(\mathbf{x}, t),\tag{106}$$

$$\xi(\mathbf{x}, t) = -\gamma s(\mathbf{x}, t) \tanh(\mathbf{V}\mathbf{x}),\tag{107}$$

$$\rho(\mathbf{x}, t) = \gamma [\tanh(\mathbf{V}\mathbf{x}) x_2 - \log(\cosh(\mathbf{V}\mathbf{x})) \odot \mathbf{V}_2 + (\lambda \tilde{x} - x_{2,d}(t)) \tanh(\mathbf{V}\mathbf{x})],\tag{108}$$

$$\dot{\bar{v}} = \gamma (\dot{x}_{2,d}(t) - \lambda (x_2 - x_{2,d}(t)) - \eta s) \tanh(\mathbf{V}\mathbf{x}) + \gamma x_2 \tanh(\mathbf{V}\mathbf{x}) \circ \mathbf{V}_1 \odot \mathbf{V}_2,\tag{109}$$

$$\dot{\hat{\mathbf{a}}} = \beta (1 + \mu \|\tanh(\mathbf{V}\mathbf{x})\|^2) (\hat{\mathbf{v}} - \hat{\mathbf{a}}),\tag{110}$$

<sup>11</sup>While the exponential is not globally Lipschitz continuous, it is locally.

where  $\circ$  and  $\oslash$  denote elementwise multiplication and division respectively, where  $\mathbf{V}_i$  is the  $i^{\text{th}}$  column of  $\mathbf{V}$ , and where  $\hat{\mathbf{v}}$  is obtained from  $\nabla\psi(\hat{\mathbf{v}})$  by inverting  $\nabla\psi$ . For the squared  $p$  norm  $\psi(\cdot) = \frac{1}{2}\|\cdot\|_p^2$ , the inverse function can be analytically computed as

$$(\nabla\psi^{-1})(\mathbf{y}) = \|\mathbf{y}\|_q^{2-q}|\mathbf{y}|^{q-1}\text{sign}(\mathbf{y}) \quad (111)$$

where  $\frac{1}{q} + \frac{1}{p} = 1$ ,  $|\cdot|$  denotes elementwise absolute value and  $\text{sign}(\cdot)$  denotes elementwise sign (Gentile, 2003). We consider the  $l_1, l_2, l_4, l_6$ , and  $l_{10}$  norms for  $\psi$ . To approximate the  $l_1$  norm, (111) is used with  $p = 1.1$ . All other  $p$  norms can be used directly.

In all simulations we take  $\lambda = .5$  in the definition of  $s$  (4) and  $\eta = .5$  in the control input (5). For the adaptation hyperparameters, we choose  $\gamma = 1.5$  for the  $l_2, l_4$ , and  $l_6$  norms. We take  $\gamma = 50$  for the  $l_1$  norm and  $\gamma = .5$  for the  $l_{10}$  norm<sup>12</sup>. In all cases,  $\beta = 1$  and  $\mu = \frac{3\gamma}{2\eta\beta}$ . We set  $\text{dim}(\mathbf{a}) = \text{dim}(\hat{\mathbf{a}}) = 500$  and randomly initialize  $\hat{\mathbf{a}}$  and  $\hat{\mathbf{v}}$  around zero from a normal distribution with standard deviation  $10^{-3}$ . The true parameter vector  $\mathbf{a}$  is drawn from a normal distribution with mean zero and standard deviation 7.5. The matrix  $\mathbf{V}$  is set to have normally distributed elements with standard deviation  $\frac{1}{\sqrt{\text{dim } \mathbf{a}}}$ . The state vector is initialized such that  $\mathbf{x}(0) = \mathbf{x}_d(0)$ . The desired trajectory is taken to be

$$x_d(t) = \sin\left(\frac{\sqrt{2}\pi}{12}t + \cos\left(\frac{\sqrt{3}\pi}{12}t\right)\right)$$

The tracking error for each choice of  $\psi$  along with a baseline comparison to fixed  $\hat{\mathbf{a}}(t) = \hat{\mathbf{a}}(0)$  is shown in Figure 1A. Figures 1B-F show trajectories for 100 out of the 500 parameters. The timescale on each axis is set to show the trajectories approximately until the parameters converge for the given algorithm. Each case results in remarkably different dynamics and resulting converged parameter vectors  $\hat{\mathbf{a}}_\infty^\psi$ . The tracking performance is good for each algorithm.

Further insight can be gained into the structure of the parameter vector  $\hat{\mathbf{a}}_\infty^\psi$  found by each adaptation algorithm by consideration of the histograms (rug plots shown on  $x$  axis) for  $\hat{\mathbf{a}}$  at the end of the simulation in Figures 2A-F. Figure 2A shows the true parameter vector. The choice of  $\psi(\cdot) = \frac{1}{2}\|\cdot\|_{1.1}^2$  in Figure 2B leads to a sparse solution with most of the weight placed on a few parameters. This is consistent with  $l_1$  regularized solutions found by the LASSO algorithm (Tibshirani, 1996). The inset displays a closer view around zero. The choice of  $\psi(\cdot) = \frac{1}{2}\|\cdot\|_2^2$  in Figure 2C (Euclidean adaptation law) leads to a parameter vector  $\hat{\mathbf{a}}_\infty^{\frac{1}{2}\|\cdot\|_2^2} \neq \mathbf{a}$  that is roughly Gaussian distributed. This distribution highlights the implicit  $l_2$  regularization of standard adaptation laws. The progression from  $\psi(\cdot) = \frac{1}{2}\|\cdot\|_4^2$  to  $\psi(\cdot) = \frac{1}{2}\|\cdot\|_{10}^2$  displays a trend towards approximate  $l_\infty$ -norm regularization: the distribution of parameters is pushed to be bimodal and peaked around  $\pm 1$ , and the  $l_\infty$  norm of  $\hat{\mathbf{a}}_\infty$  decreases as  $p$  is increased.

Figure 3A shows the function approximation error  $\tilde{f}^2(\mathbf{x}(t), \hat{\mathbf{a}}(t), \mathbf{a})$  for each algorithm along with a reference value for fixed  $\hat{\mathbf{a}}(t) = \hat{\mathbf{a}}(0)$ . Each algorithm, as expected by our theory and seen by the low tracking error in Figure 1A, pushes  $\tilde{f}^2$  to zero despite the different forms of regularization imposed on the parameter vectors. Figures 3B-F show the control input as a function of time along with the unique “ideal” control law  $u(t) = \ddot{x}_d + f(\mathbf{x}_d(t), \mathbf{a}(t))$  valid when  $\mathbf{x}(0) = \mathbf{x}_d(0)$ . All control inputs can be seen to converge to the ideal law, though the rate of convergence depends on the choice of algorithm. The control input is of reasonable magnitude throughout adaptation for each algorithm.

## 8.2 LEARNING TO CONTROL WITH PRIMITIVES

We now demonstrate that the mirror descent-like laws of Section 3 can be used to learn convex combinations of control primitives. Our approach is analogous to the use of multiplicative

<sup>12</sup>These values of  $\gamma$  were chosen to ensure good control performance without excessively high control inputs or fast parameter adaptation. In particular, adaptation occurs very slowly with  $l_1$  regularization, as small parameters are quickly eliminated to promote sparsity. A high adaptation gain was needed to ensure adaptation on a similar timescale to the other norms.

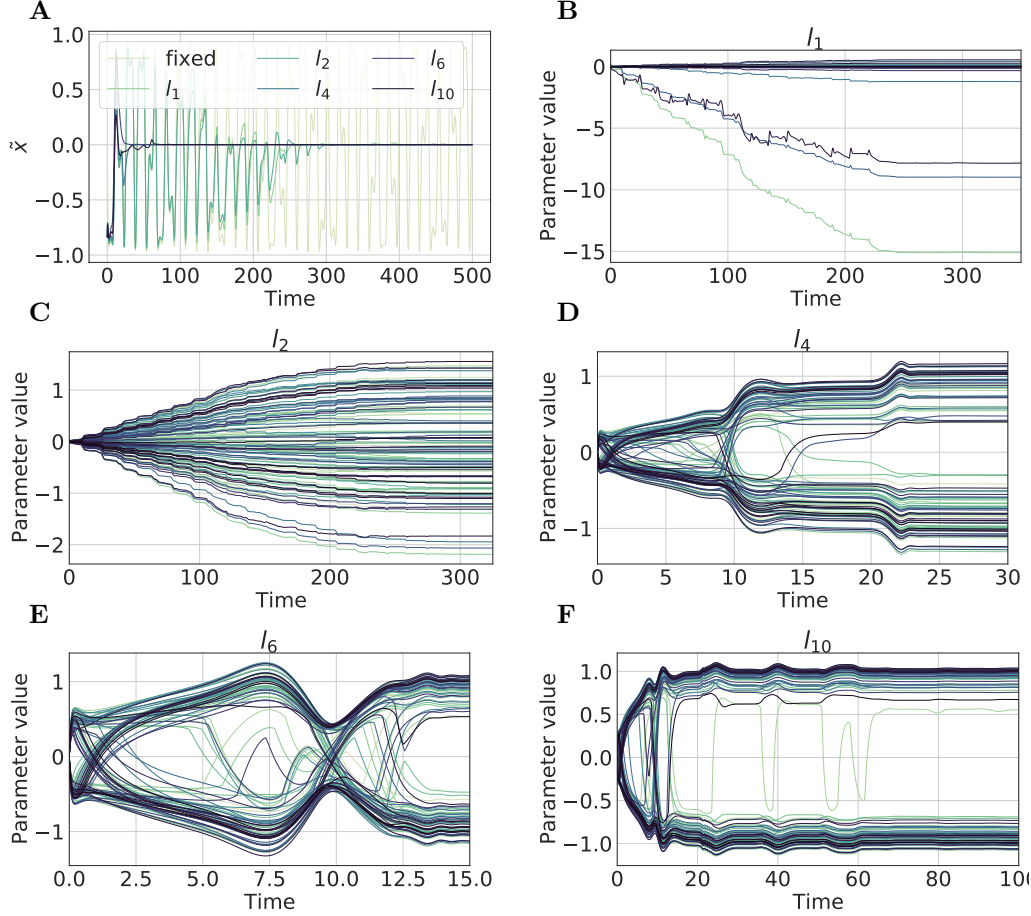


Figure 1: **Tracking error and parameter trajectories.** (A) Trajectory tracking error. All algorithms result in convergence  $\mathbf{x} \rightarrow \mathbf{x}_d$ , though transient performance differs between the algorithms. (B-F) Parameter trajectories for 100/500 of the total parameters. Each algorithm results in remarkably different parameter trajectories and final values  $\hat{\mathbf{a}}_\infty^\psi$ .

weight updates in machine learning and respects the natural  $l_1$  geometry over the probability simplex.

As a model problem for this setting, we consider the second-order system

$$\begin{aligned}\dot{x}_1 &= x_2, \\ \dot{x}_2 &= u - \tanh(\mathbf{V}\mathbf{x})^\top \mathbf{a},\end{aligned}$$

with  $\mathbf{a} \in \mathbb{R}^p$  a fixed vector of unknown parameters and  $\mathbf{V} \in \mathbb{R}^{p \times 2}$  a random matrix with  $V_{ij} \sim \mathcal{N}(0, \frac{1}{p^2})$ . To define our control primitives, we consider a distribution over tasks specified by random desired trajectories

$$x_d^{(i)}(t) = M \sin(A_i t + B_i \cos(C_i t)) + D_i$$

with  $D_i = 2i(-1)^i \times M$ ,  $A_i \sim \text{Unif}(0, 5\pi)$ ,  $B_i \sim \text{Unif}(0, 3)$ , and  $C_i \sim \text{Unif}(0, 5\pi)$ . The shift  $D_i$  ensures that the desired trajectories occupy non-overlapping regions of state space. We then learn primitives  $\{u_i\}_{i=1}^N$  to track  $\{x_d^{(i)}(t)\}_{i=1}^N$  where each  $u_i$  is given by (5) with parameter estimates  $\hat{\mathbf{a}}^{(i)}$ . The parameter estimates are found via the Slotine and Li adaptation law

$$\dot{\hat{\mathbf{a}}}^{(i)} = -\gamma \tanh(\mathbf{V}\mathbf{x})^\top s,$$

which is allowed to run until the parameter estimates converge. We set  $p = 15$ ,  $N = 300$ ,  $M = 0.1$ ,  $\gamma = 5$ , and  $\eta = \lambda = 0.5$ . Each vector of parameter estimates  $\hat{\mathbf{a}}^{(i)}$  is initialized

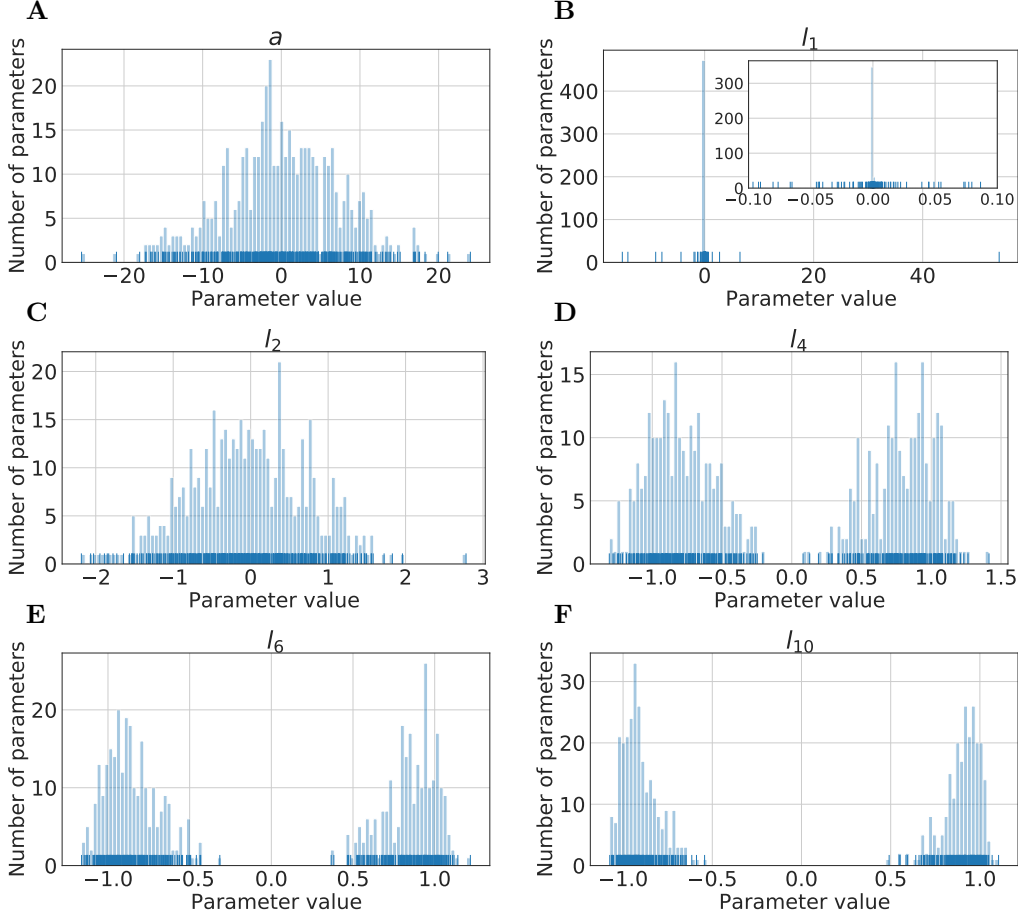


Figure 2: **Parameter histograms.** (A) True parameters  $\mathbf{a}$ . (B) Parameter vector found by the algorithm with  $\psi(\cdot) = \frac{1}{2} \|\cdot\|_{1,1}^2$ . The resulting solution is extremely sparse, and has a few parameters with large magnitude, indicative of implicit  $l_1$  regularization. (C) Parameter vector found by the standard Euclidean algorithm with  $\psi(\cdot) = \frac{1}{2} \|\cdot\|_2^2$ . The resulting parameter vector looks approximately Gaussian distributed, indicating  $l_2$  regularization. (C)-(F) Parameter vectors found by  $\psi(\cdot) = \frac{1}{2} \|\cdot\|_p^2$  with  $p = 4, 6$ , and  $10$  respectively. The transition clearly indicates a trend towards  $l_\infty$ -norm regularization, with two bimodal peaks forming around  $\pm 1$ . The  $l_\infty$  norm of the parameter vector decreases with increasing  $p$ .

randomly,  $\hat{\mathbf{a}}^{(i)}(0) \sim \mathcal{N}(0, \sigma_{\hat{\mathbf{a}}}^2)$  with  $\sigma_{\hat{\mathbf{a}}} = 10^{-3}$ . The state is initialized randomly for each task,  $\mathbf{x}_0 \sim \mathcal{N}(0, \sigma_{\mathbf{x}}^2)$  with  $\sigma_{\mathbf{x}} = 5$ . The true parameters  $\mathbf{a}$  are drawn randomly,  $\mathbf{a} \sim \mathcal{N}(0, \sigma_{\mathbf{a}}^2)$  with  $\sigma_{\mathbf{a}} = 2$ .

With control primitives  $u_i$  capable of tracking trajectories  $x_d^{(i)}$  in hand, we consider tracking a desired trajectory  $x_d(t)$  given piecewise by the previously drawn random trajectories. Concretely, we fix a time horizon  $T$  and a number of tasks  $k$ , and set

$$x_d(t) = x_d^{(i_l)}(t) \text{ if } t_{l-1} \leq t < t_l,$$

with  $l = 1, \dots, k$ ,  $i_l$  drawn uniformly from  $i = 1, \dots, N$ ,  $t_0 = 0$ , and  $t_l = \frac{lT}{k}$ . To leverage the learned control primitives, we use the input

$$u = \sum_{i=1}^N \hat{\beta}_i u_i = \mathbf{u} \hat{\beta}.$$

Above,  $\mathbf{u} \in \mathbb{R}^{1 \times N}$  is a row vector with components  $u_i$ . We require that  $\hat{\beta}_i > 0$  for all  $i$  and that  $\sum_{i=1}^N \hat{\beta}_i = 1$ . In our experiments, we fix  $T = 1000$  and set  $k = 5$ .

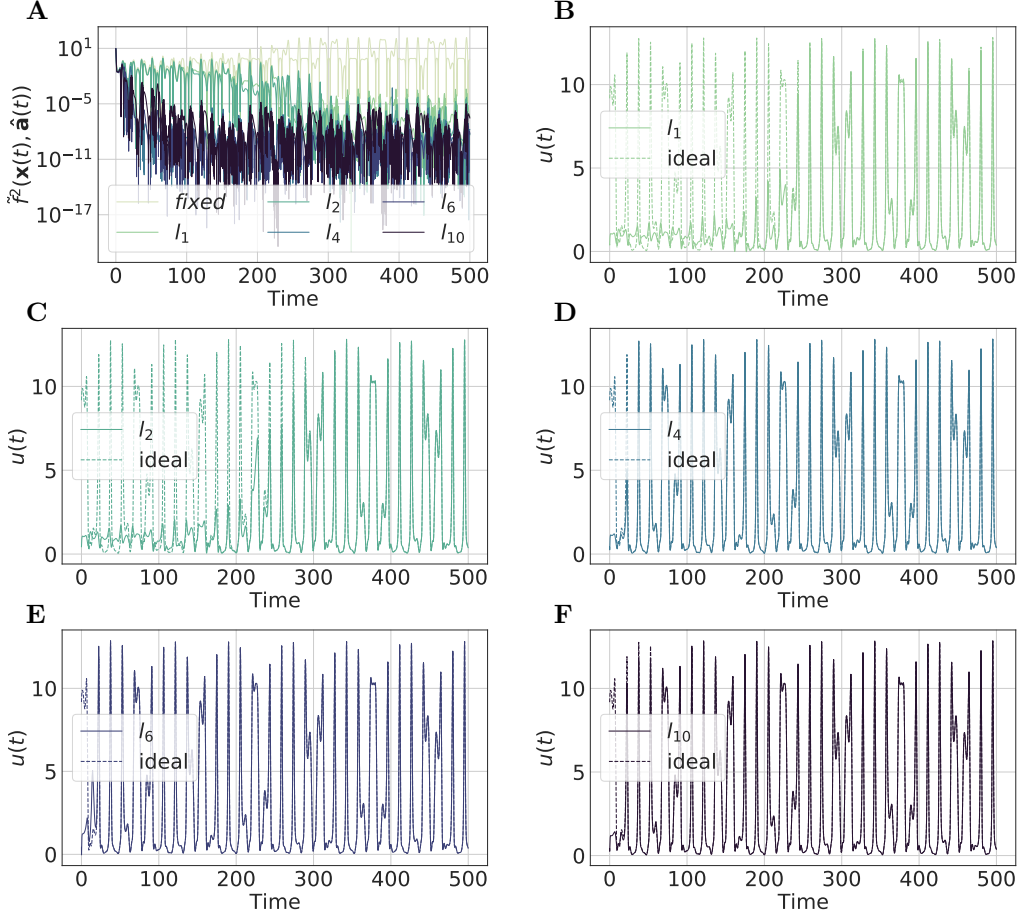


Figure 3: **Function approximation error and control inputs.** (A) The function approximation error  $\tilde{f}^2(\mathbf{x}(t), \hat{\mathbf{a}}(t))$ . All algorithms drive the error to zero. (B)-(F) Comparison of the control input  $u^\psi(t)$  to the “ideal” control  $u(t) = \ddot{x}_d(t) + f(\mathbf{x}_d(t), \mathbf{a})$ . All algorithms converge to the ideal control, though at a different rate. The control magnitude is kept to a reasonable level in every case.

It is well-known in the online convex optimization community that mirror descent with respect to the entropy  $\psi(\hat{\beta}) = \sum_i \hat{\beta}_i \log \hat{\beta}_i$  can improve the dimension dependence of convergence rates in comparison to projected gradient descent when optimizing over the simplex (Hazan, 2016). Here we demonstrate that the same phenomenon appears in adaptive control. We consider two adaptation laws,

$$\dot{\hat{\beta}} = -\gamma \mathbf{u}^T s,$$

$$\frac{d}{dt} \nabla \psi(\hat{\beta}) = -\gamma \mathbf{u}^T s,$$

with projection of  $\hat{\beta}$  onto the simplex<sup>13</sup>. In both cases, we initialize  $\hat{\beta}_i = \frac{1}{N}$  and set  $\gamma = .25$ .

Our results are shown in Figure 4. In Figure 4A, we show convergence of  $s$  for both adaptive laws.  $s$  jumps every 200 units of time as the task changes discretely. While both converge,

<sup>13</sup>We use the `lsoda` integrator in `scipy.integrate.ode`. For the Euclidean adaptation law, we zero any components if they become negative and divide by the one norm of the parameter vector. For the non-Euclidean adaptation law, we integrate the mirror descent-like dynamics directly, and update  $\nabla \psi(\hat{\beta})$  via `lsoda`. After each timestep, we compute  $\hat{\beta}$  by inverting the gradient of  $\psi$ , which ensures that each component is positive. We then project by dividing by the one norm of the parameter vector.

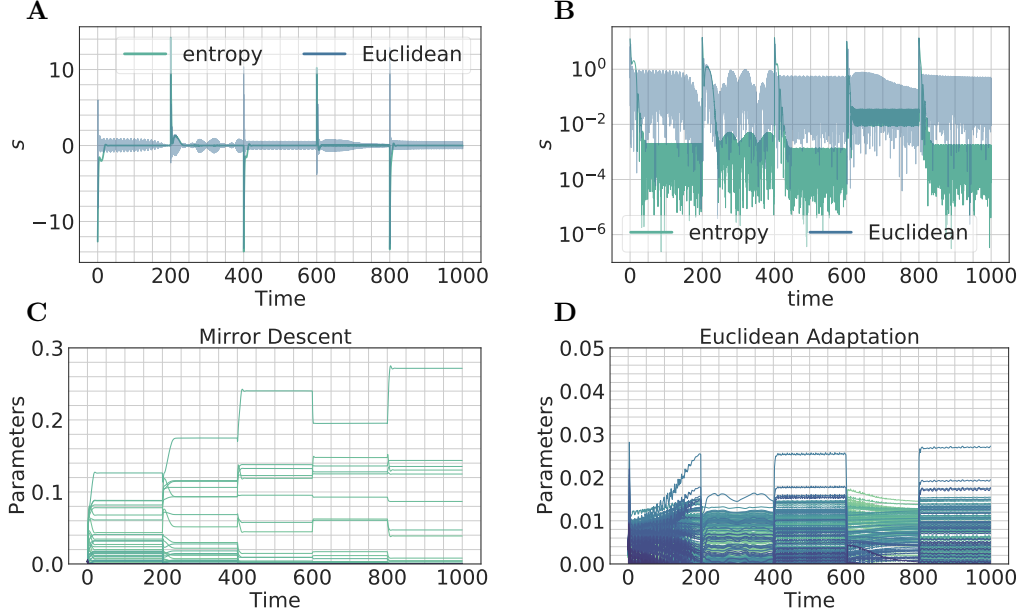


Figure 4: **Learning to control with primitives.** (A)  $s$  on a linear scale for the Euclidean and mirror descent-like adaptation laws. Mirror descent converges faster for all tasks. (B)  $s$  on a logarithmic scale for the Euclidean and mirror descent-like adaptation laws. Mirror descent converges faster and minimizes  $s$  further for all tasks. (C/D) Parameter trajectories for the mirror descent and Euclidean adaptation laws. Mirror descent leads to smoother trajectories with fewer parameters straying from 0.

adaptation with respect to the entropy converges significantly faster and minimizes  $s$  to lower values. This effect is more prominently displayed in Figure 4B, which shows convergence of  $s$  on a logarithmic scale. Figures 4C and D show the parameter trajectories for the mirror descent and Euclidean laws, respectively. The mirror descent law displays trajectories in which fewer parameters stray from zero. Those that do stray an order of magnitude further from zero than the Euclidean law. The discrete changes of the desired trajectory are more visible in the parameter trajectories for the mirror descent law.

### 8.3 DYNAMICS PREDICTION FOR HAMILTONIAN SYSTEMS

We now experimentally demonstrate the predictions of the theoretical calculations performed in Section 4.2. Similar to Chen et al. (2019), consider the Hamiltonian for three point masses interacting in  $d = 2$  dimensions via Newtonian gravitation (in units such that the gravitational constant  $G = 1$ ),

$$\mathcal{H} = \frac{1}{2m_1} \|\mathbf{p}_1\|^2 + \frac{1}{2m_2} \|\mathbf{p}_2\|^2 + \frac{1}{2m_3} \|\mathbf{p}_3\|^2 - \frac{m_1 m_2}{\|\mathbf{q}_1 - \mathbf{q}_2\|} - \frac{m_1 m_3}{\|\mathbf{q}_1 - \mathbf{q}_3\|} - \frac{m_2 m_3}{\|\mathbf{q}_2 - \mathbf{q}_3\|}, \quad (112)$$

with  $m_i$  the mass of body  $i$ ,  $\mathbf{p}_i$  the momentum of body  $i$ , and  $\mathbf{q}_i$  the position of body  $i$ . Denote by  $\mathbf{q}$  the vector  $(\mathbf{q}_1^\top, \mathbf{q}_2^\top, \mathbf{q}_3^\top)^\top$  with similar notation for  $\mathbf{p}$ .

It is well-known that physical systems can often be described by a few common mechanisms (see, e.g., Feynman et al. (1977), Section 12.7). As such, we consider estimating the Hamiltonian (112) directly with a physically motivated overparameterized basis

$$\hat{\mathcal{H}}(\hat{\mathbf{a}}) = \mathbf{Y}(\mathbf{q}, \mathbf{p}) \hat{\mathbf{a}}$$

to form the dynamics predictor (25) & (26). We define  $\mathbf{Y}(\mathbf{q}, \mathbf{p})$  to be a row vector of basis functions consisting of quadratics and quartics in  $\mathbf{p}_i$  and  $\mathbf{q}_i$ , as well as  $1/r_{ij}$ ,  $1/r_{ij}^2$ , and  $1/r_{ij}^3$  potentials with  $r_{ij} = \|\mathbf{q}_i - \mathbf{q}_j\|$  for  $i \neq j$ , comprising 21 total basis functions. These choices represent standard expressions for kinetic energy, spring potentials, central force potentials,

and higher-order terms; any basis functions can be chosen motivated by knowledge of the physical system at hand.

We set  $k = 5$ ,  $\gamma = 3.5$ , and choose  $\psi(\cdot) = \frac{1}{2} \|\cdot\|_{1.05}^2$  to identify basis functions relevant to the observed trajectory. We fix  $m_i = 1$  for all  $i$  and initialize  $\mathbf{q}$  and  $\mathbf{p}$  to lock the system in an oscillatory mode. Past  $t = 10$ , we set  $k = \gamma = 0$  and run the predictor open-loop, as well as perform shrinkage and set all coefficients with magnitude below  $10^{-3}$  formally equal to zero, leaving 13 remaining terms.

Results are shown in Figure 5. Figure 5A displays convergence of the predictor trajectory  $\hat{\mathbf{x}}$  (solid) to the true trajectory  $\mathbf{x}$  (open circles). The open-loop predictor, indicated past the vertical line at  $t = 10$ , maintains the correct oscillatory behavior. Figure 5B displays convergence of  $\hat{\mathbf{x}}$  to zero with adaptation (top) and demonstrates that adaptation is necessary for convergence (bottom). When switching to the open-loop predictor past  $t = 10$ , the system without adaptation sustains large errors, while the learned predictor maintains good performance. Figure 5C shows the qualitative structure of the predictor trajectory without learning (solid): when run closed-loop, it does not converge to the true trajectory (open circles), and when run open-loop, it spuriously converges to a fixed point. Figures 5D and E show parameter trajectories and asymptotically converged parameters, respectively. Together, the two panes demonstrate that the implicit bias of the algorithm ensures convergence to a sparsified estimate of the system Hamiltonian.

#### 8.4 SPARSE IDENTIFICATION OF CHEMICAL REACTION NETWORKS

We now demonstrate an example of regularized adaptive dynamics prediction for an unknown chemical reaction network. Consider a set of chemical reactions with  $N$  distinct chemical species. Under the continuum hypothesis and the well-mixed assumption, mass-action kinetics dictates that the system dynamics can be described exactly in a monomial basis (Liu et al., 2013),

$$\begin{aligned} \nu_j(\mathbf{x}) &= k_j \prod_{i=1}^N x_i^{a_{ji}}, \\ \dot{\mathbf{x}} &= \mathbf{\Gamma} \nu(\mathbf{x}), \end{aligned}$$

where  $x_i$  is the concentration of chemical species  $i$ ,  $\mathbf{\Gamma}$  is the stoichiometric matrix, and the  $a_{ji}$  are stoichiometric coefficients. Under the assumption that the full state of the network is measured, consider the adaptive dynamics predictor

$$\dot{\hat{\mathbf{x}}} = \hat{\mathbf{\Gamma}} \hat{\nu}(\hat{\mathbf{x}}) + k(\mathbf{x} - \hat{\mathbf{x}}), \quad (113)$$

$$\frac{d}{dt} \nabla \psi(\hat{\mathbf{\Gamma}}) = -\gamma(\hat{\mathbf{x}} - \mathbf{x}) \hat{\nu}(\hat{\mathbf{x}})^\top, \quad (114)$$

with  $\gamma > 0$  a positive learning rate,  $k > 0$  an observer gain,  $\psi$  a strictly convex function,  $\hat{\mathbf{\Gamma}}$  an estimate of the stoichiometric matrix, and  $\hat{\nu}(\hat{\mathbf{x}})$  a vector of monomial basis functions representing available knowledge of the system. Here we consider a four-species chemical reaction network (see Liu et al. (2013), supplementary information),

$$\begin{aligned} \dot{x}_1 &= -k_1 x_1 x_2, \\ \dot{x}_2 &= -k_1 x_1 x_2 - k_2 x_2 x_3^2, \\ \dot{x}_3 &= -k_1 x_1 x_2 - 2k_2 x_2 x_3^2, \\ \dot{x}_4 &= k_2 x_2 x_3^2, \end{aligned}$$

with corresponding adaptive dynamics predictor (113) & (114). We set  $\hat{\nu}$  to be a vector of all monomials up to degree three comprising a total of 140 candidate basis functions, and we set  $\psi(\hat{\mathbf{\Gamma}}) = \frac{1}{2} \|\text{vec}(\hat{\mathbf{\Gamma}})\|_{1.01}^2$  to identify a sparse, parsimonious model consistent with the data. Searching over sparse models ensures that our learned predictor selects only a few relevant terms in the approximate system dynamics. We fix  $k = 1.5$  and  $\gamma = 0.25$  for  $t < 10$ . As in Section 8.3, past  $t = 10$  we set  $k = \gamma = 0$  and run the predictor open-loop. We also perform shrinkage and set all coefficients with magnitude below  $10^{-3}$  formally equal to zero, leaving 19 remaining parameters.

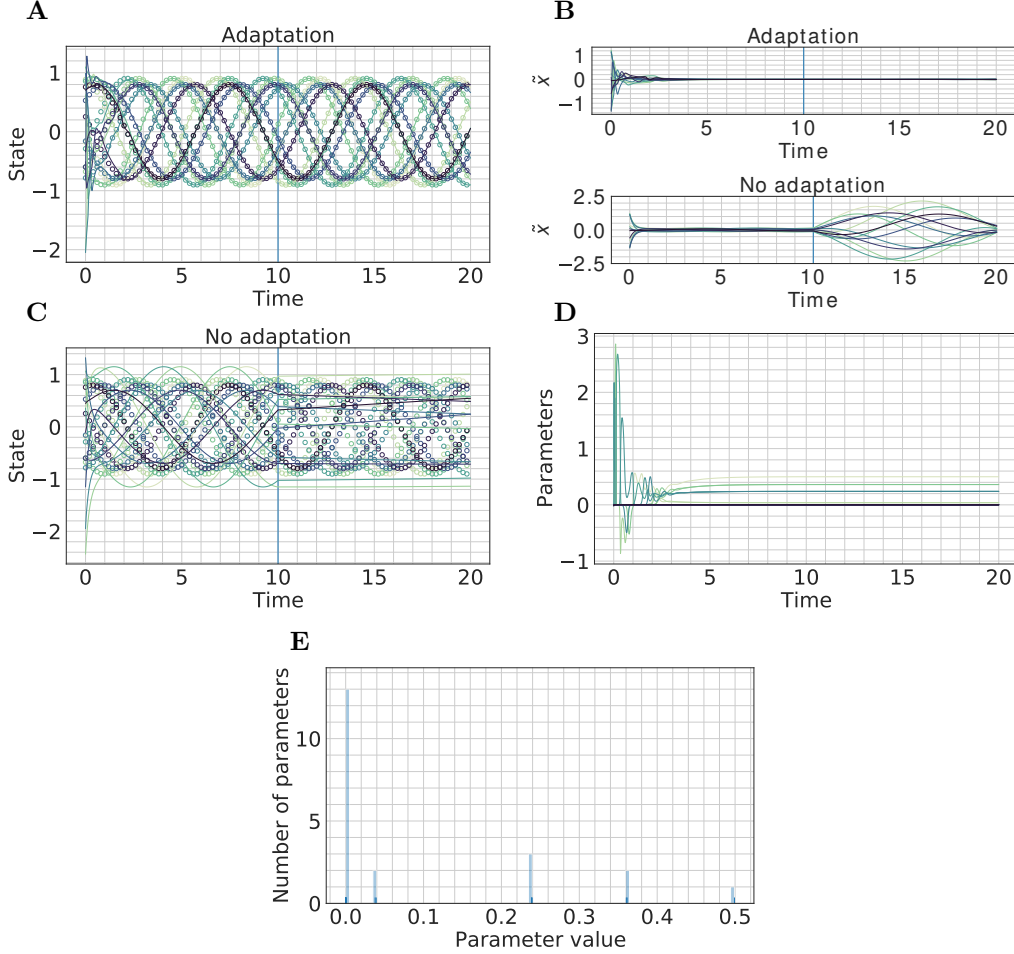


Figure 5: **Three-body system.** (A) Convergence of the predictor with adaptation (solid) to the true system trajectory (open circles). Past the vertical line at  $t = 10$ , coefficients below  $10^{-3}$  are removed and the predictor is run open-loop, demonstrating that the limit cycle is correctly learned. (B) Predictor error  $\hat{x} = \hat{x} - x$  for the adaptive dynamics predictor (25) & (26) with adaptation (top) and without adaptation (bottom). The system without adaptation is inaccurate when run open-loop, while the system with adaptation maintains accuracy. (C) Failure of the predictor trajectory without adaptation (solid) to converge to the true system trajectory (open circles). When run open-loop, the predictor without learning incorrectly tends to a fixed point. (D) Parameter trajectories for the adaptive dynamics predictor. Many parameters stay at or near zero, as predicted by Proposition 3.1. (E) Histogram of final parameter values learned by the adaptive dynamics predictor.

Results are shown in Figure 6. In Figure 6A, we show convergence of the observer error to zero with adaptation (solid) and divergence away from zero without adaptation (dashed), demonstrating that adaptation is necessary for effective prediction. The inset displays a closer look at the asymptotic behavior of the open-loop dynamics predictor after shrinkage, which shows that the fixed point of the system is correctly learned. Figure 6B shows convergence of  $\hat{x}$  (solid) to  $x$  (dashed). Figure 6C displays parameter trajectories as a function of time. Many parameters stay at or near zero as predicted by Proposition 3.1. The inset displays a finer-grained view around zero of the parameter trajectories. Figure 6D shows a histogram of the final parameter values learned by the adaptive dynamics predictor, demonstrating that only a few relevant terms are identified.

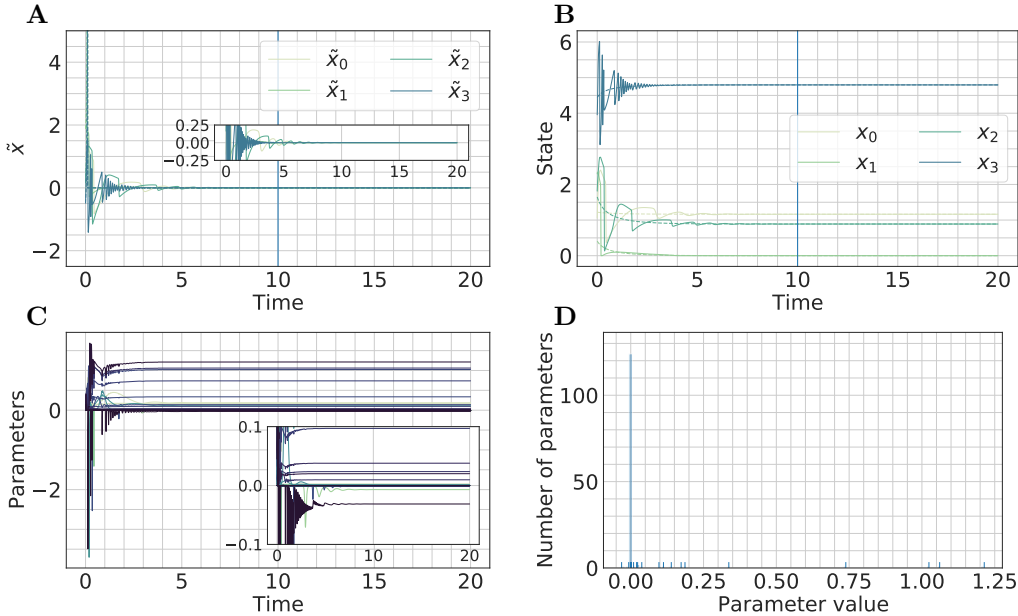


Figure 6: **Chemical reaction network.** (A) Observer error  $\tilde{x} = \hat{x} - x$  for the adaptive dynamics predictor (113) & (114) with adaptation (solid) and without adaptation (dashed). The predictor without adaptation diverges immediately. Past  $t = 10$ , shrinkage is performed, all coefficients with magnitude below  $10^{-3}$  are set to zero, and the predictor is run open-loop with  $k = \gamma = 0$ . (B) Convergence of  $\hat{x}$  to  $x$  for the adaptive dynamics predictor. The predictor accurately learns the fixed-point of the system and stays stationary when run open-loop. (C) Parameter trajectories for the adaptive dynamics predictor. Many parameters stay at or near zero, as predicted by Proposition 3.1. (D) Histogram of final parameter values learned by the adaptive dynamics predictor. Only a few relevant terms are identified.

## 9 CONCLUDING REMARKS AND FUTURE DIRECTIONS

It is somewhat unusual in nonlinear control to have a choice between a large variety of algorithms that can all be proven to globally converge. Nevertheless, in this paper, we have presented a suite of new globally convergent adaptive control algorithms. The algorithms combine the velocity gradient methodology (Fradkov, 1980; Fradkov et al., 1999) with the Bregman Lagrangian (Wibisono et al., 2016; Betancourt et al., 2018) to systematically generate velocity gradient algorithms with momentum. Based on analogies between isotonic regression (Kakade et al., 2011; Goel and Klivans, 2017; Goel et al., 2018) and algorithms for nonlinearly parameterized adaptive control (Tyukin, 2011; Tyukin et al., 2007), we extended our higher-order velocity gradient algorithms to the nonlinearly parameterized setting of generalized linear models. Using a similar parallel to distributed stochastic gradient descent algorithms (Zhang et al., 2014; Boffi and Slotine, 2020), we developed a stable modification of all of our algorithms. We subsequently fused our developments with time-dependent learning rates based on the bounded gain forgetting formalism (Slotine and Li, 1991).

By consideration of the non-Euclidean Bregman Lagrangian, we derived natural gradient (Amari, 1998) and mirror descent (Nemirovski and Yudin, 1983; Beck and Teboulle, 2003)-like algorithms with momentum. Taking the infinite friction limit of these algorithms recovers a recent algorithm for adaptive robot control (Lee et al., 2018) that respects physical Riemannian constraints on the parameters throughout adaptation. By extending recent results on the implicit bias of optimization algorithms in machine learning (Azizan et al., 2019; Azizan and Hassibi, 2019) to the continuous-time setting, we proved that these mirror descent like-algorithms – in the first-order, second-order, and nonlinearly parameterized settings – impose implicit regularization on the parameter vectors found by adaptive control.

Throughout the paper, for simplicity of exposition, we focused on the  $n^{\text{th}}$  order system (1). As discussed in Remark 2.2, our results extend to more general systems which have an error model similar to (6), in the sense that the proof technique summarized by Lemma A.2 is roughly preserved. The  $n^{\text{th}}$  order system structure makes the employed proportional-integral forms simple, as they can be written down explicitly as in (54)-(57). As summarized in Remark 6.5, a PDE needs to be solved in the general case, and solutions to this PDE may not exist. Solution of the PDE can be avoided by the dynamic scaling technique of Karagiannis et al. (2009) or a similar embedding technique of Tyukin (2011).

A significant outstanding question is whether there is an empirical advantage to using our proposed momentum algorithms. In optimization, accelerated algorithms generated by the Bregman Lagrangian provide faster convergence when properly discretized, and it is thus likely that a careful discretization is necessary to obtain optimal performance of our momentum algorithms. However, we are not aware of any available convergence rates in adaptive control, and it would be necessary to prove such rates to understand analytically if there is an advantage. Similar higher-order algorithms have appeared in the literature for linear systems of relative degree greater than one (Morse, 1992; Fradkov et al., 1999), where first-order algorithms cannot control the system. Here we have focused on feedback linearizable systems, and perhaps there exist classes of nonlinear systems that cannot be adaptively controlled with a first-order algorithm, but can with a momentum algorithm. We leave the investigation of these interesting and important questions to future work.

## A OMITTED PROOFS AND REQUIRED RESULTS

Barbalat's Lemma is a classical technique in adaptive control theory, which is used in conjunction with a Lyapunov-like analysis to prove convergence of a given signal.

**Lemma A.1** (Barbalat's Lemma, (Slotine and Li, 1991)). *Assume that  $\lim_{t \rightarrow \infty} \int_0^t |x(\tau)| d\tau < \infty$ . If  $x(t)$  is uniformly continuous, then  $\lim_{t \rightarrow \infty} x(t) = 0$ .*

Note that a sufficient condition for uniform continuity of  $x(t)$  is for  $\dot{x}(t)$  to be bounded. Hence, for any signal  $x(t) \in \mathcal{L}_2 \cap \mathcal{L}_\infty$  with  $\dot{x}(t) \in \mathcal{L}_\infty$ , we can apply Lemma A.1 to the signal  $x^2(t)$  and conclude that  $x(t) \rightarrow 0$ .

**Lemma A.2.** *Assume that  $\int_0^t \tilde{f}^2(\mathbf{x}(t'), \hat{\mathbf{a}}(t'), \mathbf{a}, t') dt' < \infty$  where  $[0, T)$  is the maximal interval of existence of  $\mathbf{x}(t)$ . Further assume that  $\hat{\mathbf{a}}(t)$  is bounded over  $[0, T)$ , that both bounds are independent of  $T$ , and that  $\tilde{f}$  is locally bounded in  $\mathbf{x}$  and  $\hat{\mathbf{a}}$  uniformly in  $t$ . Then  $\hat{\mathbf{a}} \in \mathcal{L}_\infty$ ,  $\tilde{f} \in \mathcal{L}_2$ ,  $s \in \mathcal{L}_2 \cap \mathcal{L}_\infty$ ,  $s \rightarrow 0$  and  $\mathbf{x} \rightarrow \mathbf{x}_d$ .*

*Proof.* By (6), we can write explicitly

$$s(t) = \int_0^t e^{-\eta(t-\tau)} \tilde{f}(\mathbf{x}(\tau), \hat{\mathbf{a}}(\tau), \mathbf{a}, \tau) d\tau. \quad (115)$$

By the Cauchy-Schwarz inequality,

$$\begin{aligned} s^2(T) &\leq \left( \int_0^T e^{-2\eta(T-\tau)} d\tau \right) \left( \int_0^T \tilde{f}^2(\tau) d\tau \right) \\ &\leq \frac{1}{2\eta} \left( \int_0^T \tilde{f}^2(\tau) d\tau \right) (1 - e^{-2\eta T}) \\ &\leq \frac{1}{2\eta} \left( \int_0^T \tilde{f}^2(\tau) d\tau \right) \end{aligned}$$

so that  $\sup_{t \in [0, T)} |s(t)| < \infty$ . Observe that this bound is independent of  $T$ . It immediately follows that  $\sup_{t \in [0, T)} \|\mathbf{x}(t)\| < \infty$ , and that this bound is independent of  $T$ . This observation contradicts that  $[0, T)$  is the maximal interval of existence of  $\mathbf{x}(t)$  for any  $T$ , and thus  $\mathbf{x}(t)$  must exist for all  $t$ . This shows that  $\mathbf{x} \in \mathcal{L}_\infty$ ,  $s \in \mathcal{L}_\infty$ , and that the bounds on  $\tilde{f}$  and  $\hat{\mathbf{a}}$  can be extended for all  $t$ . From this we conclude  $\tilde{f} \in \mathcal{L}_2$  and  $\hat{\mathbf{a}} \in \mathcal{L}_\infty$ . Similarly, Parseval's

theorem applied to the low-pass filter (115) shows that  $s \in \mathcal{L}_2$ . Because  $\mathbf{x} \in \mathcal{L}_\infty$  and  $\hat{\mathbf{a}} \in \mathcal{L}_\infty$ , and because  $\tilde{f}$  is locally bounded in  $\mathbf{x}$  and  $\hat{\mathbf{a}}$  uniformly in  $t$ ,  $\tilde{f} \in \mathcal{L}_\infty$ . By (6),  $\dot{s} \in \mathcal{L}_\infty$ , and hence by Barbalat's Lemma (Lemma A.1),  $s \rightarrow 0$ . By definition of  $s$ , we then conclude that  $\mathbf{x} \rightarrow \mathbf{x}_d$ .  $\square$

### A.1 PROOF OF PROPOSITION 6.3

*Proof.* Consider the Lyapunov-like function

$$V = \frac{1}{2}s^2 + \frac{1}{2\gamma}\hat{\mathbf{a}}^\top \mathbf{P}^{-1}\hat{\mathbf{a}},$$

which has time derivative

$$\dot{V} = -\eta s^2 - \frac{\kappa}{\gamma}\tilde{f}^2.$$

This immediately shows  $s \in L_\infty$  and  $\hat{\mathbf{a}} \in L_\infty$ . Because  $s \in L_\infty$ ,  $\mathbf{x} \in L_\infty$  by definition of the sliding variable (Slotine and Li, 1991). Integrating  $\dot{V}$  shows that  $s \in L_2$  and  $\tilde{f} \in L_2$ . The result follows by application of Lemma A.2 or directly by Barbalat's Lemma (Lemma A.1).  $\square$

### A.2 PROOF OF PROPOSITION 6.4

*Proof.* Consider the Lyapunov function

$$V = \frac{1}{2}s^2 + \frac{1}{2\gamma}(\|\tilde{\mathbf{v}}\|^2 + \|\hat{\mathbf{a}} - \hat{\mathbf{v}}\|^2)$$

which has time derivative

$$\begin{aligned} \dot{V} &= -\eta s^2 + s\tilde{f} + \frac{1}{\gamma}[\tilde{\mathbf{v}}^\top (-\kappa\tilde{f} - \gamma s)\mathbf{Y}^\top + (\hat{\mathbf{a}} - \hat{\mathbf{v}})^\top (\beta\mathcal{N}(\hat{\mathbf{v}} - \hat{\mathbf{a}}) + \gamma s\mathbf{Y}^\top + \kappa\tilde{f}\mathbf{Y}^\top)] \\ &= -\eta s^2 - \frac{\kappa}{\gamma}\tilde{f}^2 - \frac{\beta}{\gamma}\|\hat{\mathbf{a}} - \hat{\mathbf{v}}\|^2 - \frac{\beta\mu}{\gamma}\|\hat{\mathbf{a}} - \hat{\mathbf{v}}\|\|\mathbf{Y}\|^2 + 2s(\hat{\mathbf{a}} - \hat{\mathbf{v}})^\top \mathbf{Y}^\top + 2\frac{\kappa}{\gamma}\tilde{f}(\hat{\mathbf{a}} - \hat{\mathbf{v}})^\top \mathbf{Y}^\top \\ &\leq -\eta s^2 - \frac{\kappa}{\gamma}\tilde{f}^2 - \frac{\beta}{\gamma}\|\hat{\mathbf{a}} - \hat{\mathbf{v}}\|^2 - \frac{\beta\mu}{\gamma}\|\hat{\mathbf{a}} - \hat{\mathbf{v}}\|\|\mathbf{Y}\|^2 + 2|s|\|\hat{\mathbf{a}} - \hat{\mathbf{v}}\|\|\mathbf{Y}\| + 2\frac{\kappa}{\gamma}|\tilde{f}|\|\hat{\mathbf{a}} - \hat{\mathbf{v}}\|\|\mathbf{Y}\| \\ &\leq -\epsilon_1\eta s^2 - \epsilon_2\frac{\kappa}{\gamma}\tilde{f}^2 - \left(\sqrt{(1-\epsilon_1)\eta}|s| - \frac{1}{\sqrt{(1-\epsilon_1)\eta}}\|\hat{\mathbf{a}} - \hat{\mathbf{v}}\|\|\mathbf{Y}\|\right)^2 \\ &\quad - \left(\sqrt{\frac{(1-\epsilon_2)\kappa}{\gamma}}|\tilde{f}| - \frac{\kappa}{\gamma}\sqrt{\frac{\gamma}{(1-\epsilon_2)\kappa}}\|\hat{\mathbf{a}} - \hat{\mathbf{v}}\|\|\mathbf{Y}\|\right)^2 - \frac{\beta}{\gamma}\|\hat{\mathbf{a}} - \hat{\mathbf{v}}\|^2 \end{aligned}$$

where  $0 < \epsilon_1 < 1$  and  $0 < \epsilon_2 < 1$  are arbitrary and where we have taken  $\mu = \frac{\gamma}{\beta}\left(\frac{1}{(1-\epsilon_1)\eta} + \frac{\kappa}{(1-\epsilon_2)\gamma}\right)$ . Because  $\epsilon_1$  and  $\epsilon_2$  are arbitrary, this shows that  $\dot{V}$  is negative semi-definite for  $\mu > \frac{\gamma}{\beta}\left(\frac{1}{\eta} + \frac{\kappa}{\gamma}\right)$ . Hence  $\hat{\mathbf{v}} \in \mathcal{L}_\infty$ ,  $\hat{\mathbf{a}} \in \mathcal{L}_\infty$ , and  $s \in \mathcal{L}_\infty$ . Because  $s \in \mathcal{L}_\infty$ , we automatically have  $\mathbf{x} \in \mathcal{L}_\infty$ , which shows that  $\dot{s} \in \mathcal{L}_\infty$  by local boundedness of  $\tilde{f}$  in  $\mathbf{x}$  and  $\hat{\mathbf{a}}$  uniformly in  $t$ . Integrating  $\dot{V}$  shows that  $s \in \mathcal{L}_2$  and hence by Barbalat's Lemma (Lemma A.1)  $s \rightarrow 0$  and  $\mathbf{x} \rightarrow \mathbf{x}_d$ .  $\square$

### A.3 PROOF OF PROPOSITION 6.5

*Proof.* Defining the vector  $\hat{\mathbf{v}}^t = \sum_{i=1}^m \hat{w}_i^t \phi(\mathbf{x}_i)$ , (62) implies the iteration on  $\hat{\mathbf{v}}$ ,

$$\hat{\mathbf{v}}^{t+1} = \hat{\mathbf{v}}^t - \frac{\lambda}{m} \sum_{i=1}^m \left( \hat{f}(\hat{\mathbf{w}}^t, \mathbf{x}_i) - f(\mathbf{x}_i) \right) \phi(\mathbf{x}_i). \quad (116)$$

(116) shows that at time  $t$ ,

$$\hat{\mathbf{v}}^t = -\frac{\lambda}{m} \sum_{i=1}^m \left( \sum_{j=1}^{t-1} \tilde{f}_i^j \right) \phi(\mathbf{x}_i), \quad (117)$$

where  $\tilde{f}_i^j$  in (117) is the function approximation error on the  $i^{\text{th}}$  input example at iteration  $j$ ,  $\tilde{f}_i^j = \hat{f}(\hat{\mathbf{w}}^j, \mathbf{x}_i) - f(\mathbf{x}_i)$ .

Now, assuming that for the adaptive control problem  $f(\mathbf{x}, \mathbf{a}, t) = u(\boldsymbol{\alpha}^T(\mathbf{x}, t)\mathbf{a})$ , setting  $\mathbf{P} = \lambda \mathbf{I}$ ,  $\hat{\mathbf{a}}(0) = \mathbf{0}$ , and integrating both sides of (12), we see that at time  $t$ ,

$$\hat{\mathbf{a}}(t) = -\lambda \int_0^t \tilde{f}(\mathbf{x}(t'), \hat{\mathbf{a}}(t'), \mathbf{a}, t') \boldsymbol{\alpha}^T(\mathbf{x}(t'), t') \boldsymbol{\alpha}(\mathbf{x}(t'), t') dt'. \quad (118)$$

The current function approximation  $\hat{f}$  at time  $t$  for the parameters in (118) can then be written

$$\begin{aligned} \hat{f}(t) &= u(\boldsymbol{\alpha}^T(\mathbf{x}, t)\hat{\mathbf{a}}(t)) = u\left(\int_0^t -\lambda \tilde{f}(\mathbf{x}(t'), \hat{\mathbf{a}}(t'), \mathbf{a}, t') \boldsymbol{\alpha}^T(\mathbf{x}(t'), t) \boldsymbol{\alpha}(\mathbf{x}(t'), t') dt'\right) \\ &= u\left(\int_0^t c(t') \mathcal{K}(t, t') dt'\right) \end{aligned} \quad (119)$$

where we have defined  $c(t') = -\lambda \tilde{f}(\mathbf{x}(t'), \hat{\mathbf{a}}(t'), \mathbf{a}, t')$  and  $\mathcal{K}(t, t') = \boldsymbol{\alpha}^T(\mathbf{x}(t), t) \boldsymbol{\alpha}(\mathbf{x}(t'), t')$ . Similarly, in the case of the Alphatron, the current approximation at iteration  $t$  is given by

$$\begin{aligned} \hat{f}(\hat{\mathbf{w}}^t, \mathbf{x}) &= u(\langle \hat{\mathbf{v}}^t, \boldsymbol{\phi}(\mathbf{x}) \rangle_{\mathcal{H}}) = u\left(\sum_{i=1}^m \left(\sum_{j=1}^{t-1} -\frac{\lambda}{m} \tilde{f}_i^j\right) \langle \boldsymbol{\phi}(\mathbf{x}), \boldsymbol{\phi}(\mathbf{x}_i) \rangle\right) \\ &= u\left(\sum_{i=1}^m \hat{w}_i^t \mathcal{K}(\mathbf{x}, \mathbf{x}_i)\right), \end{aligned} \quad (120)$$

where we have noted that with  $\hat{w}_i^0 = 0$  for all  $i$ ,  $\hat{w}_i^t = \sum_{j=1}^{t-1} -\frac{\lambda}{m} \tilde{f}_i^j$ .  $\square$

#### A.4 PROOF OF PROPOSITION 6.6

*Proof.* Consider the Lyapunov function candidate

$$V = \frac{1}{2\gamma} \|\tilde{\mathbf{v}}\|^2 + \frac{1}{2\gamma} \|\hat{\mathbf{a}} - \tilde{\mathbf{v}}\|^2$$

which has time derivative

$$\begin{aligned} \dot{V} &= \frac{1}{\gamma} \tilde{\mathbf{v}}^T \left( -\gamma \tilde{f} \boldsymbol{\alpha} \right) + \frac{1}{\gamma} (\hat{\mathbf{a}} - \tilde{\mathbf{v}})^T \left( \beta \mathcal{N}(\tilde{\mathbf{v}} - \hat{\mathbf{a}}) + \gamma \tilde{f} \boldsymbol{\alpha} \right) \\ &= -(\tilde{\mathbf{a}}^T \boldsymbol{\alpha}) \tilde{f} - \frac{\beta}{\gamma} \mathcal{N} \|\hat{\mathbf{a}} - \tilde{\mathbf{v}}\|^2 + 2(\hat{\mathbf{a}} - \tilde{\mathbf{v}})^T \boldsymbol{\alpha} \tilde{f} \\ &\leq -\frac{\tilde{f}^2}{D_1} - \frac{\beta}{\gamma} \|\hat{\mathbf{a}} - \tilde{\mathbf{v}}\|^2 - \frac{\beta\mu}{\gamma} \|\hat{\mathbf{a}} - \tilde{\mathbf{v}}\|^2 \|\boldsymbol{\alpha}\|^2 + 2\|\boldsymbol{\alpha}\| \|\hat{\mathbf{a}} - \tilde{\mathbf{v}}\| |\tilde{f}| \\ &\leq -\frac{\epsilon}{D_1} \tilde{f}^2 - \beta \|\hat{\mathbf{a}} - \tilde{\mathbf{v}}\|^2 - \left( \sqrt{\frac{1-\epsilon}{D_1}} |\tilde{f}| - \sqrt{\frac{D_1}{1-\epsilon}} \|\boldsymbol{\alpha}\| \|\hat{\mathbf{a}} - \tilde{\mathbf{v}}\| \right)^2 \end{aligned}$$

where  $0 < \epsilon < 1$  is arbitrary and we have chosen  $\mu = \frac{\gamma D_1}{(1-\epsilon)\beta}$ . Because  $\epsilon$  is arbitrary, this shows that  $\tilde{\mathbf{v}}$  and  $\hat{\mathbf{a}}$  remain bounded for  $\mu > \frac{\gamma D_1}{\beta}$  over the maximal interval of existence of  $\mathbf{x}(t)$ . By integrating  $\dot{V}$ , we see that  $\tilde{f} \in \mathcal{L}_2$  over this same interval. Note that the bounds are independent of the length of the interval. Application of Lemma A.2 completes the proof.  $\square$

#### A.5 PROOF OF PROPOSITION 6.7

*Proof.* The Lyapunov-like function

$$V = \frac{1}{2} \left( \tilde{\mathbf{a}}^T \mathbf{P}^{-1} \tilde{\mathbf{a}} + \tilde{\mathbf{a}}^T \mathbf{P}^{-1} \tilde{\mathbf{a}} + s^2 \right)$$

has time derivative

$$\dot{V} = -\eta s^2 - k(\bar{\mathbf{a}} - \hat{\mathbf{a}})^\top \mathbf{P}^{-1}(\bar{\mathbf{a}} - \hat{\mathbf{a}}).$$

This shows that  $s$ ,  $\hat{\mathbf{a}}$ , and  $\bar{\mathbf{a}}$  remain bounded. The remaining conclusions of the proposition are immediately drawn by integrating  $\dot{V}$  and applying Barbalat's Lemma (Lemma A.1).  $\square$

#### A.6 PROOF OF PROPOSITION 6.8

*Proof.* The Lyapunov-like function

$$V = \frac{1}{2} \left( \tilde{\mathbf{a}}^\top \mathbf{P}^{-1} \tilde{\mathbf{a}} + \tilde{\bar{\mathbf{a}}}^\top \mathbf{P}^{-1} \tilde{\bar{\mathbf{a}}} \right)$$

has time derivative

$$\dot{V} \leq -\frac{1}{D_1} \tilde{f}^2 - k(\hat{\mathbf{a}} - \bar{\mathbf{a}})^\top \mathbf{P}^{-1}(\hat{\mathbf{a}} - \bar{\mathbf{a}}).$$

This shows that  $\hat{\mathbf{a}}$  and  $\bar{\mathbf{a}}$  remain bounded over the maximal interval of existence of  $\mathbf{x}(t)$ . Integration of  $\dot{V}$  shows  $\tilde{f} \in \mathcal{L}_2$  and  $(\hat{\mathbf{a}} - \bar{\mathbf{a}}) \in \mathcal{L}_2$  over the same interval. Note that the bounds are independent of the length of the interval. Application of Lemma A.2 completes the proof.  $\square$

#### A.7 PROOF OF PROPOSITION 6.9

*Proof.* The Lyapunov-like function

$$V = \frac{1}{2\gamma} (\|\tilde{\mathbf{v}}\|^2 + \|\hat{\mathbf{a}} - \hat{\mathbf{v}}\|^2 + \|\bar{\mathbf{a}} - \hat{\mathbf{a}}\|^2)$$

has time derivative

$$\begin{aligned} \dot{V} &= -(\tilde{\mathbf{a}}^\top \boldsymbol{\alpha}) \tilde{f} - \frac{\beta}{\gamma} \mathcal{N} \|\hat{\mathbf{a}} - \hat{\mathbf{v}}\|^2 + \frac{k\beta}{\gamma} \mathcal{N} (\hat{\mathbf{a}} - \hat{\mathbf{v}})^\top (\mathbf{a} - \hat{\mathbf{a}}) + 2\tilde{f} (\hat{\mathbf{a}} - \hat{\mathbf{v}})^\top \boldsymbol{\alpha} - 2\frac{k\beta}{\gamma} \mathcal{N} \|\hat{\mathbf{a}} - \bar{\mathbf{a}}\|^2 + \frac{\beta}{\gamma} \mathcal{N} (\hat{\mathbf{a}} - \bar{\mathbf{a}})^\top (\hat{\mathbf{v}} - \hat{\mathbf{a}}) \\ &\leq -\frac{\tilde{f}^2}{D_1} - \frac{\beta \mathcal{N}}{2\gamma} (1-k) \|\hat{\mathbf{a}} - \hat{\mathbf{v}}\|^2 - \frac{\beta \mathcal{N}}{2\gamma} \|\hat{\mathbf{a}} - \bar{\mathbf{a}}\|^2 (3k-1) + 2|\tilde{f}| \|\hat{\mathbf{a}} - \hat{\mathbf{v}}\| \|\boldsymbol{\alpha}\| \\ &\leq -\frac{\tilde{f}^2}{D_1} - \frac{\beta}{2\gamma} (1-k) \|\hat{\mathbf{a}} - \hat{\mathbf{v}}\|^2 - \frac{\beta \mu}{2\gamma} (1-k) \|\hat{\mathbf{a}} - \hat{\mathbf{v}}\|^2 \|\boldsymbol{\alpha}\|^2 - \frac{\beta \mathcal{N}}{2\gamma} \|\hat{\mathbf{a}} - \bar{\mathbf{a}}\|^2 (3k-1) + 2|\tilde{f}| \|\hat{\mathbf{a}} - \hat{\mathbf{v}}\| \|\boldsymbol{\alpha}\| \\ &\leq -\frac{\epsilon}{D_1} \tilde{f}^2 - \left( \frac{\sqrt{1-\epsilon} |\tilde{f}|}{\sqrt{D_1}} - \sqrt{\frac{D_1}{1-\epsilon}} \|\hat{\mathbf{a}} - \hat{\mathbf{v}}\| \|\boldsymbol{\alpha}\| \right)^2 - \frac{\beta}{2\gamma} (1-k) \|\hat{\mathbf{a}} - \hat{\mathbf{v}}\|^2 - \frac{\beta \mathcal{N}}{2\gamma} (3k-1) \|\hat{\mathbf{a}} - \bar{\mathbf{a}}\|^2 \end{aligned}$$

where  $0 < \epsilon < 1$  is arbitrary and we have chosen  $\mu = \frac{2\gamma D_1}{\beta(1-\epsilon)(1-k)}$ . From above, we conclude  $\hat{\mathbf{v}}$ ,  $\hat{\mathbf{a}}$ , and  $\bar{\mathbf{a}}$  remain bounded over the maximal interval of existence of  $\mathbf{x}(t)$  for  $\frac{1}{3} \leq k < 1$ . By integrating  $\dot{V}$ , we see that  $\tilde{f} \in \mathcal{L}_2$ ,  $(\hat{\mathbf{a}} - \bar{\mathbf{a}}) \in \mathcal{L}_2$ , and  $(\hat{\mathbf{a}} - \hat{\mathbf{v}}) \in \mathcal{L}_2$  over the same interval. Note that the bounds are independent of the length of the interval. Application of Lemma A.2 completes the proof.  $\square$

#### A.8 PROOF OF PROPOSITION 6.10

*Proof.* The Lyapunov-like function

$$V = \frac{1}{\gamma} (\|\tilde{\mathbf{v}}\|^2 + \|\tilde{\bar{\mathbf{v}}}\|^2 + \|\hat{\mathbf{a}} - \hat{\mathbf{v}}\|^2)$$

has time derivative

$$\begin{aligned} \dot{V} &= -(\tilde{\mathbf{a}}^\top \boldsymbol{\alpha}) \tilde{f} + 2\tilde{f} (\hat{\mathbf{a}} - \hat{\mathbf{v}})^\top \boldsymbol{\alpha} - \frac{\beta \mathcal{N}}{\gamma} \|\hat{\mathbf{a}} - \hat{\mathbf{v}}\|^2 - \frac{\rho}{\gamma} \|\hat{\mathbf{v}} - \bar{\mathbf{v}}\|^2 - \frac{\rho}{\gamma} (\hat{\mathbf{a}} - \hat{\mathbf{v}})^\top (\bar{\mathbf{v}} - \hat{\mathbf{v}}) \\ &\leq -\frac{\tilde{f}^2}{D_1} + 2|\tilde{f}| \|\hat{\mathbf{a}} - \hat{\mathbf{v}}\| \|\boldsymbol{\alpha}\| - \left( \frac{\beta}{\gamma} - \frac{\rho}{2\gamma} \right) \|\hat{\mathbf{a}} - \hat{\mathbf{v}}\|^2 - \frac{\beta \mu}{\gamma} \|\hat{\mathbf{a}} - \hat{\mathbf{v}}\|^2 \|\boldsymbol{\alpha}\|^2 - \frac{\rho}{2\gamma} \|\hat{\mathbf{v}} - \bar{\mathbf{v}}\|^2 \\ &\leq -\frac{\epsilon}{D_1} \tilde{f}^2 - \left( \sqrt{\frac{1-\epsilon}{D_1}} |\tilde{f}| - \sqrt{\frac{D_1}{1-\epsilon}} \|\hat{\mathbf{v}} - \hat{\mathbf{a}}\| \|\boldsymbol{\alpha}\| \right)^2 - \frac{\rho}{2\gamma} \|\bar{\mathbf{v}} - \hat{\mathbf{v}}\|^2 - \frac{1}{2\gamma} (2\beta - \rho) \|\hat{\mathbf{v}} - \hat{\mathbf{a}}\|^2 \end{aligned}$$

where  $0 < \epsilon < 1$  is arbitrary and we have chosen  $\mu = \frac{\gamma D_1}{\beta(1-\epsilon)}$ . From above, we conclude  $\hat{\mathbf{v}}$ ,  $\bar{\mathbf{v}}$ , and  $\hat{\mathbf{a}}$  remain bounded over the maximal interval of existence of  $\mathbf{x}(t)$  for  $\rho < 2\beta$ . Integrating  $\dot{V}$  shows that  $\tilde{f} \in \mathcal{L}_2$ ,  $(\hat{\mathbf{v}} - \bar{\mathbf{v}}) \in \mathcal{L}_2$ , and  $(\hat{\mathbf{v}} - \hat{\mathbf{a}}) \in \mathcal{L}_2$  over the same interval. Note that the bounds are independent of the length of the interval. Application of Lemma A.2 completes the proof.  $\square$

### A.9 PROOF OF PROPOSITION 6.11

*Proof.* The Lyapunov-like function

$$V = \frac{1}{2\gamma} (\|\hat{\mathbf{a}} - \hat{\mathbf{v}}\|^2 + \|\hat{\mathbf{a}} - \bar{\mathbf{a}}\|^2 + \|\tilde{\mathbf{v}}\|^2 + \|\tilde{\mathbf{v}}\|^2)$$

has time derivative

$$\begin{aligned} \dot{V} &= -(\tilde{\mathbf{a}}^\top \boldsymbol{\alpha}) \tilde{f} - \frac{\beta \mathcal{N}}{\gamma} \|\hat{\mathbf{a}} - \hat{\mathbf{v}}\|^2 - \frac{2k\beta \mathcal{N}}{\gamma} \|\bar{\mathbf{a}} - \hat{\mathbf{a}}\|^2 + 2\tilde{f} (\hat{\mathbf{a}} - \hat{\mathbf{v}})^\top \boldsymbol{\alpha} + \beta N (\hat{\mathbf{a}} - \bar{\mathbf{a}})^\top (\hat{\mathbf{v}} - \hat{\mathbf{a}}) \\ &\quad + \frac{k\beta \mathcal{N}}{\gamma} (\hat{\mathbf{a}} - \hat{\mathbf{v}})^\top (\bar{\mathbf{a}} - \hat{\mathbf{a}}) - \frac{\rho}{\gamma} \|\hat{\mathbf{v}} - \bar{\mathbf{v}}\|^2 - \frac{\rho}{\gamma} (\hat{\mathbf{a}} - \hat{\mathbf{v}})^\top (\bar{\mathbf{v}} - \hat{\mathbf{v}}) \\ &\leq -\frac{1}{D_1} \tilde{f}^2 - \frac{1}{2\gamma} (\beta(1-k) - \rho) \|\hat{\mathbf{a}} - \hat{\mathbf{v}}\|^2 - \frac{1}{2\gamma} (\beta\mu(1-k)) \|\hat{\mathbf{a}} - \hat{\mathbf{v}}\|^2 \|\boldsymbol{\alpha}\|^2 \\ &\quad - \frac{\mathcal{N}\beta}{2\gamma} (3k-1) \|\bar{\mathbf{a}} - \hat{\mathbf{a}}\|^2 - \frac{\rho}{2\gamma} \|\hat{\mathbf{v}} - \bar{\mathbf{v}}\|^2 + 2|\tilde{f}| \|\hat{\mathbf{a}} - \hat{\mathbf{v}}\| \|\mathbf{Y}\| \\ &\leq -\frac{\epsilon}{D_1} \tilde{f}^2 - \left( \sqrt{\frac{1-\epsilon}{D_1}} |\tilde{f}| - \sqrt{\frac{D_1}{1-\epsilon}} \|\hat{\mathbf{a}} - \hat{\mathbf{v}}\| \|\boldsymbol{\alpha}\| \right)^2 - \frac{\rho}{2\gamma} \|\bar{\mathbf{v}} - \hat{\mathbf{v}}\|^2 \\ &\quad - \frac{\beta \mathcal{N}}{2\gamma} (3k-1) \|\hat{\mathbf{a}} - \bar{\mathbf{a}}\|^2 - \frac{1}{2\gamma} ((1-k)\beta - \rho) \|\hat{\mathbf{a}} - \hat{\mathbf{v}}\|^2 \end{aligned}$$

where  $0 < \epsilon < 1$  is arbitrary and we have chosen  $\mu = \frac{2\gamma D_1}{\beta(1-k)(1-\epsilon)}$ . This immediately shows that  $\hat{\mathbf{a}}$ ,  $\hat{\mathbf{v}}$ ,  $\bar{\mathbf{a}}$ , and  $\bar{\mathbf{v}}$  remain bounded over the maximal interval of existence of  $\mathbf{x}(t)$  for  $\frac{1}{3} \leq k < 1$  and  $\rho < \beta(1-k)$ . Integrating  $\dot{V}$  shows that  $\tilde{f} \in \mathcal{L}_2$ ,  $(\bar{\mathbf{v}} - \hat{\mathbf{v}}) \in \mathcal{L}_2$ ,  $(\hat{\mathbf{a}} - \bar{\mathbf{a}}) \in \mathcal{L}_2$ , and  $(\hat{\mathbf{a}} - \hat{\mathbf{v}}) \in \mathcal{L}_2$  over the same interval. Note that the bounds are independent of the length of the interval. Application of Lemma A.2 completes the proof.  $\square$

### A.10 PROOF OF PROPOSITION 6.12

*Proof.* The Lyapunov-like function

$$V = \frac{1}{2} s^2 + \frac{1}{2} \tilde{\mathbf{a}}^\top \mathbf{P}^{-1} \tilde{\mathbf{a}},$$

has time derivative

$$\dot{V} = -\eta s^2 - \frac{1}{2} \tilde{f}^2 - \frac{\lambda}{2} \tilde{\mathbf{a}}^\top \mathbf{P}^{-1} \tilde{\mathbf{a}},$$

which shows that  $s$  and  $\tilde{\mathbf{a}}$  remain bounded. Because  $s$  remains bounded,  $\mathbf{x}$  remains bounded. Integrating  $\dot{V}$  shows that  $s \in \mathcal{L}_2$  and  $\tilde{f} \in \mathcal{L}_2$ . The proof is completed by application of Lemma A.2 or directly by Barbalat's Lemma (Lemma A.1).  $\square$

### A.11 PROOF OF PROPOSITION 6.13

*Proof.* Consider the Lyapunov-like function

$$V = \frac{1}{2} s^2 + \frac{1}{2} \tilde{\mathbf{v}}^\top \mathbf{P}^{-1} \tilde{\mathbf{v}} + \frac{1}{2} (\hat{\mathbf{v}} - \hat{\mathbf{a}})^\top \mathbf{P}^{-1} (\hat{\mathbf{v}} - \hat{\mathbf{a}})$$

which has time derivative

$$\begin{aligned}
\dot{V} &= -\eta s^2 + s\tilde{f} - (\hat{\mathbf{v}} - \hat{\mathbf{a}} + \tilde{\mathbf{a}})^\top (s + \tilde{f}) \mathbf{Y}^\top + \frac{1}{2} (\tilde{\mathbf{v}}^\top \mathbf{Y}^\top)^2 - \frac{\lambda(t)}{2} \tilde{\mathbf{v}}^\top \mathbf{P}^{-1} \tilde{\mathbf{v}} \\
&\quad + (\hat{\mathbf{v}} - \hat{\mathbf{a}})^\top \left( -\beta \mathcal{N}(\hat{\mathbf{v}} - \hat{\mathbf{a}}) - (s + \tilde{f}) \mathbf{Y}^\top \right) + \frac{1}{2} \left[ (\hat{\mathbf{v}} - \hat{\mathbf{a}})^\top \mathbf{Y}^\top \right]^2 - \frac{\lambda(t)}{2} (\hat{\mathbf{v}} - \hat{\mathbf{a}})^\top \mathbf{P}^{-1} (\hat{\mathbf{v}} - \hat{\mathbf{a}}) \\
&= -\eta s^2 - \tilde{f}^2 - 2(\hat{\mathbf{v}} - \hat{\mathbf{a}})^\top (s + \tilde{f}) \mathbf{Y}^\top - \beta \mathcal{N} \|\hat{\mathbf{v}} - \hat{\mathbf{a}}\|^2 + \frac{1}{2} (\tilde{\mathbf{v}}^\top \mathbf{Y}^\top)^2 + \frac{1}{2} \left[ (\hat{\mathbf{v}} - \hat{\mathbf{a}})^\top \mathbf{Y}^\top \right]^2 \\
&\quad - \frac{\lambda(t)}{2} \left( \tilde{\mathbf{v}}^\top \mathbf{P}^{-1} \tilde{\mathbf{v}} + (\hat{\mathbf{v}} - \hat{\mathbf{a}})^\top \mathbf{P}^{-1} (\hat{\mathbf{v}} - \hat{\mathbf{a}}) \right)
\end{aligned}$$

Now we use that  $\tilde{\mathbf{v}}^\top \mathbf{Y}^\top = (\hat{\mathbf{v}} - \hat{\mathbf{a}})^\top \mathbf{Y}^\top + \tilde{f}$  to say that  $\frac{1}{2} (\tilde{\mathbf{v}}^\top \mathbf{Y}^\top)^2 = \frac{1}{2} \left[ (\hat{\mathbf{v}} - \hat{\mathbf{a}})^\top \mathbf{Y}^\top \right]^2 + (\hat{\mathbf{v}} - \hat{\mathbf{a}})^\top \mathbf{Y}^\top \tilde{f} + \frac{1}{2} \tilde{f}^2$ . Hence,

$$\begin{aligned}
\dot{V} &= -\eta s^2 - \frac{1}{2} \tilde{f}^2 - 2s(\hat{\mathbf{v}} - \hat{\mathbf{a}})^\top \mathbf{Y}^\top - \tilde{f}(\hat{\mathbf{v}} - \hat{\mathbf{a}})^\top \mathbf{Y}^\top - \beta \mathcal{N} \|\hat{\mathbf{v}} - \hat{\mathbf{a}}\|^2 + \left[ (\hat{\mathbf{v}} - \hat{\mathbf{a}})^\top \mathbf{Y}^\top \right]^2 \\
&\quad - \frac{\lambda(t)}{2} \left( \tilde{\mathbf{v}}^\top \mathbf{P}^{-1} \tilde{\mathbf{v}} + (\hat{\mathbf{v}} - \hat{\mathbf{a}})^\top \mathbf{P}^{-1} (\hat{\mathbf{v}} - \hat{\mathbf{a}}) \right) \\
&= -\eta s^2 - \frac{1}{2} \tilde{f}^2 - 2s(\hat{\mathbf{v}} - \hat{\mathbf{a}})^\top \mathbf{Y}^\top - \tilde{f}(\hat{\mathbf{v}} - \hat{\mathbf{a}})^\top \mathbf{Y}^\top - \beta \|\hat{\mathbf{v}} - \hat{\mathbf{a}}\|^2 - \beta \mu \|\mathbf{Y}\|^2 \|\hat{\mathbf{v}} - \hat{\mathbf{a}}\|^2 + \left[ (\hat{\mathbf{v}} - \hat{\mathbf{a}})^\top \mathbf{Y}^\top \right]^2 \\
&\quad - \frac{\lambda(t)}{2} \left( \tilde{\mathbf{v}}^\top \mathbf{P}^{-1} \tilde{\mathbf{v}} + (\hat{\mathbf{v}} - \hat{\mathbf{a}})^\top \mathbf{P}^{-1} (\hat{\mathbf{v}} - \hat{\mathbf{a}}) \right) \\
&\leq -\eta s^2 - \frac{1}{2} \tilde{f}^2 + 2|s| \|\hat{\mathbf{v}} - \hat{\mathbf{a}}\| \|\mathbf{Y}^\top\| + |\tilde{f}| \|\hat{\mathbf{v}} - \hat{\mathbf{a}}\| \|\mathbf{Y}^\top\| - \beta \|\hat{\mathbf{v}} - \hat{\mathbf{a}}\|^2 - (\beta \mu - 1) \|\mathbf{Y}\|^2 \|\hat{\mathbf{v}} - \hat{\mathbf{a}}\|^2 \\
&\quad - \frac{\lambda(t)}{2} \left( \tilde{\mathbf{v}}^\top \mathbf{P}^{-1} \tilde{\mathbf{v}} + (\hat{\mathbf{v}} - \hat{\mathbf{a}})^\top \mathbf{P}^{-1} (\hat{\mathbf{v}} - \hat{\mathbf{a}}) \right) \\
&\leq -\eta \epsilon_1 s^2 - \frac{\epsilon_2}{2} \tilde{f}^2 - \left( \sqrt{(1 - \epsilon_1) \eta} |s| - \frac{1}{\sqrt{(1 - \epsilon_1) \eta}} \|\hat{\mathbf{v}} - \hat{\mathbf{a}}\| \|\mathbf{Y}\| \right)^2 - \left( \sqrt{\frac{1 - \epsilon_2}{2}} |\tilde{f}| - \frac{1}{2} \sqrt{\frac{2}{1 - \epsilon_2}} \|\hat{\mathbf{v}} - \hat{\mathbf{a}}\| \|\mathbf{Y}^\top\| \right)^2 \\
&\quad - \beta \|\hat{\mathbf{v}} - \hat{\mathbf{a}}\|^2 - \frac{\lambda(t)}{2} \left( \tilde{\mathbf{v}}^\top \mathbf{P}^{-1} \tilde{\mathbf{v}} + (\hat{\mathbf{v}} - \hat{\mathbf{a}})^\top \mathbf{P}^{-1} (\hat{\mathbf{v}} - \hat{\mathbf{a}}) \right)
\end{aligned}$$

where  $0 < \epsilon_1 < 1$  and  $0 < \epsilon_2 < 1$  are both arbitrary and where we have chosen  $\mu = \frac{1}{\beta} \left( 1 + \frac{1}{\eta(1 - \epsilon_1)} + \frac{1}{2(1 - \epsilon_2)} \right)$ . This shows that  $s$ ,  $\hat{\mathbf{v}}$ , and  $\hat{\mathbf{a}}$  remain bounded. Because  $s$  remains bounded,  $\mathbf{x}$  remains bounded. Integrating  $\dot{V}$  shows that  $s \in \mathcal{L}_2$  and  $\tilde{f} \in \mathcal{L}_2$ . By local boundedness of  $\tilde{f}$  in  $\mathbf{x}$  and  $\hat{\mathbf{a}}$  uniformly in  $t$ ,  $\tilde{f}$  remains bounded and hence  $\dot{s}$  remains bounded. By Barbalat's Lemma (Lemma A.1),  $s \rightarrow 0$  and  $\mathbf{x} \rightarrow \mathbf{x}_d$ .  $\square$

### A.12 PROOF OF PROPOSITION 6.14

*Proof.* Consider the Lyapunov-like function

$$V = \frac{1}{2} \tilde{\mathbf{a}}^\top \mathbf{P}^{-1} \tilde{\mathbf{a}}, \quad (121)$$

which has time derivative

$$\begin{aligned}
\dot{V} &= -\tilde{f} \boldsymbol{\alpha}^\top \tilde{\mathbf{a}} + \frac{1}{2} (\tilde{\mathbf{a}}^\top \boldsymbol{\alpha})^2 - \frac{\lambda}{2} \tilde{\mathbf{a}}^\top \mathbf{P}^{-1} \tilde{\mathbf{a}}, \\
&\leq -\frac{1}{D_1} \tilde{f}^2 + \frac{1}{2D_2^2} \tilde{f}^2 = -\left( \frac{1}{D_1} - \frac{1}{2D_2^2} \right) \tilde{f}^2.
\end{aligned}$$

For  $D_1 < 2D_2^2$ ,  $\dot{V} \leq 0$  and  $\tilde{f} \in \mathcal{L}_2$  over the maximal interval of existence of  $\mathbf{x}(t)$ . Alternatively, using the same Lyapunov function,

$$\dot{V} \leq -(\boldsymbol{\alpha}^\top \tilde{\mathbf{a}})^2 \left( D_2 - \frac{1}{2} \right).$$

For  $D_2 > \frac{1}{2}$ ,  $\dot{V} \leq 0$  and  $\alpha^\top \tilde{\mathbf{a}} \in \mathcal{L}_2$  over the maximal interval of existence of  $\mathbf{x}(t)$ . By Assumption 2.2, this implies that  $\tilde{f} \in \mathcal{L}_2$  over the same interval. Hence, both approaches demonstrate that  $\hat{\mathbf{a}}$  remains bounded over the maximal interval of existence of  $\mathbf{x}(t)$ , and that  $\tilde{f} \in \mathcal{L}_2$  over the same interval. Furthermore, these bounds are independent of the length of the interval. By Lemma A.2, the proposition is proved.  $\square$

### A.13 PROOF OF PROPOSITION 6.15

*Proof.* Consider the Lyapunov-like function

$$V = \frac{1}{2} \left( \tilde{\mathbf{v}}^\top \mathbf{P}^{-1} \tilde{\mathbf{v}} + (\hat{\mathbf{a}} - \tilde{\mathbf{v}})^\top \mathbf{P}^{-1} (\hat{\mathbf{a}} - \tilde{\mathbf{v}}) \right),$$

which has time derivative

$$\begin{aligned} \dot{V} &= -\tilde{\mathbf{v}}^\top \alpha \tilde{f} + \frac{1}{2} \tilde{\mathbf{v}}^\top (-\lambda \mathbf{P}^{-1} + \alpha \alpha^\top) \tilde{\mathbf{v}} + (\hat{\mathbf{a}} - \tilde{\mathbf{v}})^\top \left( \beta \mathcal{N} (\tilde{\mathbf{v}} - \hat{\mathbf{a}}) + \alpha \tilde{f} \right) + \frac{1}{2} (\hat{\mathbf{a}} - \tilde{\mathbf{v}})^\top (-\lambda \mathbf{P}^{-1} + \alpha \alpha^\top) (\hat{\mathbf{a}} - \tilde{\mathbf{v}}) \\ &\leq -(\tilde{\mathbf{a}}^\top \alpha) \tilde{f} + \frac{1}{2} (\tilde{\mathbf{v}}^\top \alpha)^2 + \frac{1}{2} ((\hat{\mathbf{a}} - \tilde{\mathbf{v}})^\top \alpha)^2 - \beta \mathcal{N} \|\hat{\mathbf{a}} - \tilde{\mathbf{v}}\|^2 + 2\tilde{f} (\hat{\mathbf{a}} - \tilde{\mathbf{v}})^\top \alpha \\ &\leq -D_2 (\alpha^\top \tilde{\mathbf{a}})^2 + \frac{1}{2} (\tilde{\mathbf{v}}^\top \alpha)^2 + \frac{1}{2} ((\hat{\mathbf{a}} - \tilde{\mathbf{v}})^\top \alpha)^2 - \beta \mathcal{N} \|\hat{\mathbf{a}} - \tilde{\mathbf{v}}\|^2 + 2|\tilde{f}| \|\hat{\mathbf{a}} - \tilde{\mathbf{v}}\| \|\alpha\| \end{aligned}$$

Now, we use the fact that  $\frac{1}{2} (\tilde{\mathbf{v}}^\top \alpha)^2 = \frac{1}{2} [(\tilde{\mathbf{v}} - \hat{\mathbf{a}})^\top \alpha]^2 + (\tilde{\mathbf{v}} - \hat{\mathbf{a}})^\top \alpha (\alpha^\top \tilde{\mathbf{a}}) + \frac{1}{2} (\tilde{\mathbf{a}}^\top \alpha)^2$  to rewrite

$$\begin{aligned} \dot{V} &\leq -\left( D_2 - \frac{1}{2} \right) (\alpha^\top \tilde{\mathbf{a}})^2 + [(\hat{\mathbf{a}} - \tilde{\mathbf{v}})^\top \alpha]^2 - \beta \mathcal{N} \|\hat{\mathbf{a}} - \tilde{\mathbf{v}}\|^2 + \|\tilde{\mathbf{v}} - \hat{\mathbf{a}}\| \|\alpha\| |\alpha^\top \tilde{\mathbf{a}}| (2D_1 + 1) \\ &\leq -\left( D_2 - \frac{1}{2} \right) (\alpha^\top \tilde{\mathbf{a}})^2 - \beta \|\hat{\mathbf{a}} - \tilde{\mathbf{v}}\|^2 - (\beta \mu - 1) \|\hat{\mathbf{a}} - \tilde{\mathbf{v}}\|^2 \|\alpha\|^2 + \|\tilde{\mathbf{v}} - \hat{\mathbf{a}}\| \|\alpha\| |\alpha^\top \tilde{\mathbf{a}}| (2D_1 + 1) \\ &\leq -\epsilon \left( D_2 - \frac{1}{2} \right) (\alpha^\top \tilde{\mathbf{a}})^2 - \left( \sqrt{(1 - \epsilon) \left( D_2 - \frac{1}{2} \right)} |\alpha^\top \tilde{\mathbf{a}}| - \frac{2D_1 + 1}{2\sqrt{(1 - \epsilon) (D_2 - \frac{1}{2})}} \|\tilde{\mathbf{v}} - \hat{\mathbf{a}}\| \|\alpha\| \right)^2 - \beta \|\hat{\mathbf{a}} - \tilde{\mathbf{v}}\|^2 \end{aligned}$$

where  $0 < \epsilon < 1$  is arbitrary and where we have chosen  $\mu = \frac{1}{\beta} \left( 1 + \frac{(2D_1 + 1)^2}{(1 - \epsilon)(4D_2 - 2)} \right)$ .  $\dot{V}$  is clearly negative semi-definite for  $D_2 < \frac{1}{2}$ , which shows that  $\hat{\mathbf{v}}$  and  $\hat{\mathbf{a}}$  remain bounded over the maximal interval of existence of  $\mathbf{x}(t)$ . Integrating  $\dot{V}$  shows that  $(\alpha^\top \tilde{\mathbf{a}}) \in \mathcal{L}_2$  over this interval, which implies that  $\tilde{f} \in \mathcal{L}_2$  over the same interval by Assumption 2.2. Note that the bounds are independent of the length of the interval. By Lemma A.2, the proposition is proven.  $\square$

### A.14 PROOF OF PROPOSITION 7.1

*Proof.* Consider the Lyapunov-like function candidate

$$V = \frac{1}{2} s^2 + \frac{1}{\gamma} \left( d_\psi(\mathbf{a}, \hat{\mathbf{v}}) + \frac{1}{2} \|\hat{\mathbf{a}} - \hat{\mathbf{v}}\|^2 \right)$$

This function has time derivative

$$\begin{aligned} \dot{V} &= -\eta s^2 + s \mathbf{Y} \tilde{\mathbf{a}} + \frac{1}{\gamma} \left( (\hat{\mathbf{v}} - \mathbf{a})^\top \nabla^2 \psi(\hat{\mathbf{v}}) \dot{\hat{\mathbf{v}}} + (\hat{\mathbf{a}} - \hat{\mathbf{v}})^\top (\dot{\hat{\mathbf{a}}} - \dot{\hat{\mathbf{v}}}) \right) \\ &= -\eta s^2 + s \mathbf{Y} \tilde{\mathbf{a}} + (\mathbf{a} - \hat{\mathbf{v}})^\top \mathbf{Y}^\top s + \frac{1}{\gamma} (\hat{\mathbf{a}} - \hat{\mathbf{v}})^\top \left( \beta \mathcal{N} (\hat{\mathbf{v}} - \hat{\mathbf{a}}) + \gamma \nabla^2 \psi(\hat{\mathbf{v}})^{-1} \mathbf{Y}^\top s \right) \\ &= -\eta s^2 - \frac{\beta \mathcal{N}}{\gamma} \|\hat{\mathbf{a}} - \hat{\mathbf{v}}\|^2 + (\hat{\mathbf{a}} - \hat{\mathbf{v}})^\top \left( [\nabla^2 \psi(\hat{\mathbf{v}})]^{-1} + \mathbf{I} \right) \mathbf{Y}^\top s \end{aligned}$$

By  $l$ -strong convexity of  $\psi$ ,  $(\nabla^2\psi(\hat{\mathbf{v}}))^{-1} \leq l^{-1}\mathbf{I}$ . Hence, using that  $\mathcal{N} = 1 + \mu\|\mathbf{Y}\|^2$ ,

$$\dot{V} \leq -\eta s^2 - \frac{\beta}{\gamma}\|\hat{\mathbf{a}} - \hat{\mathbf{v}}\|^2 - \frac{\beta\mu}{\gamma}\|\hat{\mathbf{a}} - \hat{\mathbf{v}}\|^2\|\mathbf{Y}\|^2 + \left(\frac{l+1}{l}\right)|s|\|\hat{\mathbf{a}} - \hat{\mathbf{v}}\|\|\mathbf{Y}\| \quad (122)$$

$$\leq -\epsilon\eta s^2 - \left(\sqrt{(1-\epsilon)\eta}|s| - \frac{l+1}{2l\sqrt{(1-\epsilon)\eta}}\|\hat{\mathbf{a}} - \hat{\mathbf{v}}\|\|\mathbf{Y}\|\right)^2 - \frac{\beta}{\gamma}\|\hat{\mathbf{a}} - \hat{\mathbf{v}}\|^2 \quad (123)$$

where  $0 < \epsilon < 1$  is arbitrary and we have chosen  $\mu = \frac{\gamma(l+1)^2}{4\beta l^2(1-\epsilon)\eta}$ . This shows that  $\dot{V}$  is negative semi-definite, so that  $\hat{\mathbf{a}}, \hat{\mathbf{v}}$ , and  $s$  remain bounded. Because  $s$  remains bounded,  $\mathbf{x}$  remains bounded. Integrating  $\dot{V}$  shows that  $s \in \mathcal{L}_2$ , so that  $s \in \mathcal{L}_2 \cap \mathcal{L}_\infty$ . By local boundedness of  $\mathbf{Y}$  in  $\mathbf{x}$ ,  $\dot{s}$  remains bounded, and hence by Barbalat's Lemma (Lemma A.1)  $s \rightarrow 0$ . Then  $\mathbf{x} \rightarrow \mathbf{x}_d$  by definition of  $s$ .  $\square$

### A.15 PROOF OF PROPOSITION 7.2

*Proof.* Consider the Lyapunov-like function candidate

$$\begin{aligned} V &= \frac{1}{2}s^2 + \frac{1}{\gamma}(d_\psi(\mathbf{a}, \hat{\mathbf{v}}) + d_\psi(\hat{\mathbf{v}}, \hat{\mathbf{a}})) \\ &= \frac{1}{2}s^2 + \frac{1}{\gamma}(\psi(\mathbf{a}) - \psi(\hat{\mathbf{v}}) - \nabla\psi(\hat{\mathbf{v}})^\top(\mathbf{a} - \hat{\mathbf{v}}) + \psi(\hat{\mathbf{v}}) - \psi(\hat{\mathbf{a}}) - \nabla\psi(\hat{\mathbf{a}})^\top(\hat{\mathbf{v}} - \hat{\mathbf{a}})) \end{aligned}$$

These individual terms satisfy

$$\begin{aligned} \frac{d}{dt}\frac{1}{2}s^2 &= -\eta s^2 + \mathbf{Y}\tilde{\mathbf{a}}s \\ \frac{1}{\gamma}\frac{d}{dt}d_\psi(\mathbf{a}, \hat{\mathbf{v}}) &= -\mathbf{Y}\tilde{\mathbf{a}}s + (\hat{\mathbf{a}} - \hat{\mathbf{v}})^\top\mathbf{Y}^\top s \\ \frac{1}{\gamma}\frac{d}{dt}d_\psi(\hat{\mathbf{v}}, \hat{\mathbf{a}}) &= -\frac{1}{\gamma}(\hat{\mathbf{v}} - \hat{\mathbf{a}})^\top\nabla^2\psi(\hat{\mathbf{a}})\dot{\mathbf{a}} - s\mathbf{Y}(\nabla^2\psi(\hat{\mathbf{v}}))^{-1}(\nabla\psi(\hat{\mathbf{v}}) - \nabla\psi(\hat{\mathbf{a}})) \end{aligned}$$

Note that, by  $l$ -strong convexity and  $L$ -smoothness, the second term in the last line above can be bounded as

$$-s\mathbf{Y}(\nabla^2\psi(\hat{\mathbf{v}}))^{-1}(\nabla\psi(\hat{\mathbf{v}}) - \nabla\psi(\hat{\mathbf{a}})) \leq \frac{\gamma L}{l}|s|\|\mathbf{Y}\|\|\hat{\mathbf{a}} - \hat{\mathbf{v}}\|.$$

First consider (97). Then, by  $l$ -strong convexity of  $\psi$ ,

$$-\frac{1}{\gamma}(\hat{\mathbf{v}} - \hat{\mathbf{a}})^\top\nabla^2\psi(\hat{\mathbf{a}})\dot{\mathbf{a}} \leq -\frac{l\beta\mathcal{N}}{\gamma}\|\hat{\mathbf{a}} - \hat{\mathbf{v}}\|^2$$

For (99) we obtain

$$-\frac{1}{\gamma}(\hat{\mathbf{v}} - \hat{\mathbf{a}})^\top\nabla^2\psi(\hat{\mathbf{a}})\dot{\mathbf{a}} \leq -\frac{\beta\mathcal{N}}{\gamma}\|\hat{\mathbf{a}} - \hat{\mathbf{v}}\|^2$$

Hence, for (96) & (97),

$$\dot{V} \leq -\eta s^2 - \frac{l\beta}{\gamma}\|\hat{\mathbf{a}} - \hat{\mathbf{v}}\|^2 - \frac{l\beta\mu}{\gamma}\|\mathbf{Y}\|^2\|\hat{\mathbf{a}} - \hat{\mathbf{v}}\|^2 + \frac{l+\gamma L}{l}|s|\|\mathbf{Y}\|\|\hat{\mathbf{a}} - \hat{\mathbf{v}}\|$$

Similarly, for (98) & (99),

$$\dot{V} \leq -\eta s^2 - \frac{\beta}{\gamma}\|\hat{\mathbf{a}} - \hat{\mathbf{v}}\|^2 - \frac{\beta\mu}{\gamma}\|\mathbf{Y}\|^2\|\hat{\mathbf{a}} - \hat{\mathbf{v}}\|^2 + \frac{l+\gamma L}{l}|s|\|\mathbf{Y}\|\|\hat{\mathbf{a}} - \hat{\mathbf{v}}\|$$

In both cases,

$$\dot{V} \leq -\epsilon\eta s^2 - \left(\sqrt{(1-\epsilon)\eta}|s| - \frac{l+\gamma L}{2l\sqrt{(1-\epsilon)\eta}}\|\mathbf{Y}\|\|\hat{\mathbf{a}} - \hat{\mathbf{v}}\|\right)^2$$

In the former case, we have chosen  $\mu = \frac{\gamma(l+\gamma L)^2}{4\beta\eta(1-\epsilon)l^3}$  and in the latter we have chosen  $\mu = \frac{\gamma(l+\gamma L)^2}{4\beta\eta(1-\epsilon)l^2}$ . This shows that  $\dot{V}$  is negative semi-definite, so that  $\hat{\mathbf{a}}, \hat{\mathbf{v}}$ , and  $s$  remain bounded. Because  $s$  remains bounded,  $\mathbf{x}$  remains bounded. Integrating  $\dot{V}$  shows that  $s \in \mathcal{L}_2$ , so that  $s \in \mathcal{L}_2 \cap \mathcal{L}_\infty$ . By local boundedness of  $\mathbf{Y}$  in  $\mathbf{x}$ ,  $\dot{s}$  remains bounded, and hence by Barbalat's Lemma (Lemma A.1)  $s \rightarrow 0$ . Then  $\mathbf{x} \rightarrow \mathbf{x}_d$  by definition of  $s$ .  $\square$

## B FURTHER RESULTS ON DYNAMICS PREDICTION FOR HAMILTONIAN SYSTEMS

We now provide some extensions to the results in Section 4.2 by exploiting the structure of separable Hamiltonians. With a separable Hamiltonian, it is natural to estimate the kinetic and potential energies separately,

$$\begin{aligned} T(\hat{\mathbf{p}}) &= \mathbf{Y}_p(\hat{\mathbf{p}})\hat{\mathbf{a}}_p, \\ U(\hat{\mathbf{q}}) &= \mathbf{Y}_q(\hat{\mathbf{q}})\hat{\mathbf{a}}_q, \end{aligned}$$

where  $\mathbf{Y}_p$  and  $\mathbf{Y}_q$  are row vectors of basis functions for the kinetic and potential energies respectively. In this case, following the same derivation as in Section 4.1, the error dynamics become

$$\begin{aligned} \dot{\tilde{\mathbf{p}}} &= -\nabla_{\hat{\mathbf{q}}}\mathbf{Y}_q(\hat{\mathbf{q}})\tilde{\mathbf{a}}_q - k_p\tilde{\mathbf{p}} - (\nabla_{\hat{\mathbf{q}}}U(\hat{\mathbf{q}}) - \nabla_{\mathbf{q}}U(\mathbf{q})), \\ \dot{\tilde{\mathbf{q}}} &= \nabla_{\hat{\mathbf{p}}}\mathbf{Y}_p(\hat{\mathbf{p}})\tilde{\mathbf{a}}_p - k_q\tilde{\mathbf{q}} + (\nabla_{\hat{\mathbf{p}}}T(\hat{\mathbf{p}}) - \nabla_{\mathbf{p}}T(\mathbf{p})). \end{aligned}$$

Consider the adaptation laws

$$\begin{aligned} \dot{\hat{\mathbf{a}}}_p &= -\gamma_p [\nabla^2\psi_p(\hat{\mathbf{a}}_p)]^{-1}(\nabla_{\hat{\mathbf{p}}}\mathbf{Y}_p(\hat{\mathbf{p}}))^T\tilde{\mathbf{q}}, \\ \dot{\hat{\mathbf{a}}}_q &= \gamma_q [\nabla^2\psi_q(\hat{\mathbf{a}}_q)]^{-1}(\nabla_{\hat{\mathbf{q}}}\mathbf{Y}_q(\hat{\mathbf{q}}))^T\tilde{\mathbf{p}}, \end{aligned}$$

where  $\psi_p(\cdot)$  and  $\psi_q(\cdot)$  are strictly convex functions, and where  $\gamma_p > 0$  and  $\gamma_q > 0$  are positive learning rates. The Lyapunov-like function

$$V = \frac{1}{2}\tilde{\mathbf{p}}^T\tilde{\mathbf{p}} + \frac{1}{2}\tilde{\mathbf{q}}^T\tilde{\mathbf{q}} + \frac{1}{\gamma_p}d_{\psi_p}(\mathbf{a}_p \parallel \hat{\mathbf{a}}_p) + \frac{1}{\gamma_q}d_{\psi_q}(\mathbf{a}_q \parallel \hat{\mathbf{a}}_q) \quad (124)$$

shows that a sufficient condition for convergence  $\tilde{\mathbf{p}} \rightarrow 0$  and  $\tilde{\mathbf{q}} \rightarrow 0$  is for the Jacobian

$$\mathbf{J} = \begin{pmatrix} -k_p\mathbf{I} & -\nabla_{\mathbf{q}}^2U(\mathbf{q}) \\ \nabla_{\mathbf{p}}^2T(\mathbf{p}) & -k_q\mathbf{I} \end{pmatrix}$$

to be uniformly negative definite. A sufficient condition for uniform negative definiteness is given by (27).

While separable Hamiltonians encompass many physical systems, some, such as robotic systems, do not have this structure. A more general form encompassing robotic systems is

$$\mathcal{H}(\mathbf{p}, \mathbf{q}) = T(\mathbf{p}, \mathbf{q}) + U(\mathbf{q}).$$

Parameterizing these terms independently,

$$\begin{aligned} T(\hat{\mathbf{p}}, \hat{\mathbf{q}}) &= \mathbf{Y}_p(\hat{\mathbf{p}}, \hat{\mathbf{q}})\hat{\mathbf{a}}_p, \\ U(\hat{\mathbf{q}}) &= \mathbf{Y}_q(\hat{\mathbf{q}})\hat{\mathbf{a}}_q, \end{aligned}$$

the error dynamics becomes

$$\begin{aligned} \dot{\tilde{\mathbf{p}}} &= -(\nabla_{\hat{\mathbf{q}}}\mathbf{Y}_p(\hat{\mathbf{p}}, \hat{\mathbf{q}}))\tilde{\mathbf{a}}_p - (\nabla_{\hat{\mathbf{q}}}\mathbf{Y}_q(\hat{\mathbf{q}}))\tilde{\mathbf{a}}_q - k_p\tilde{\mathbf{p}} - (\nabla_{\hat{\mathbf{q}}}U(\hat{\mathbf{q}}) - \nabla_{\mathbf{q}}U(\mathbf{q})) - (\nabla_{\hat{\mathbf{q}}}T(\hat{\mathbf{p}}, \hat{\mathbf{q}}) - \nabla_{\mathbf{q}}T(\mathbf{p}, \mathbf{q})), \\ \dot{\tilde{\mathbf{q}}} &= (\nabla_{\hat{\mathbf{p}}}\mathbf{Y}_p(\hat{\mathbf{p}}, \hat{\mathbf{q}}))\tilde{\mathbf{a}}_p - k_q\tilde{\mathbf{q}} + (\nabla_{\hat{\mathbf{p}}}T(\hat{\mathbf{p}}, \hat{\mathbf{q}}) - \nabla_{\mathbf{p}}T(\mathbf{p}, \mathbf{q})). \end{aligned}$$

Now consider the adaptation laws

$$\begin{aligned} \dot{\hat{\mathbf{a}}}_p &= \gamma_p [\nabla^2\psi_p(\hat{\mathbf{a}}_p)]^{-1}\left((\nabla_{\hat{\mathbf{q}}}\mathbf{Y}_p(\hat{\mathbf{p}}, \hat{\mathbf{q}}))^T\tilde{\mathbf{p}} - (\nabla_{\hat{\mathbf{p}}}\mathbf{Y}_p(\hat{\mathbf{p}}, \hat{\mathbf{q}}))^T\tilde{\mathbf{q}}\right), \\ \dot{\hat{\mathbf{a}}}_q &= \gamma_q [\nabla^2\psi_q(\hat{\mathbf{a}}_q)]^{-1}(\nabla_{\hat{\mathbf{q}}}\mathbf{Y}_q(\hat{\mathbf{q}}))^T\tilde{\mathbf{p}}, \end{aligned}$$

again where  $\psi_p(\cdot)$  and  $\psi_q(\cdot)$  are strictly convex functions, and where  $\gamma_p > 0$  and  $\gamma_q > 0$  are positive learning rates. The Lyapunov-like function (124) shows that a sufficient condition for convergence is for the Jacobian matrix

$$\mathbf{J} = \begin{pmatrix} -k_p\mathbf{I} - \nabla_{\mathbf{p}}\nabla_{\mathbf{q}}T(\mathbf{p}, \mathbf{q}) & -\nabla_{\mathbf{q}}^2U(\mathbf{q}) - \nabla_{\mathbf{q}}^2T(\mathbf{p}, \mathbf{q}) \\ \nabla_{\mathbf{p}}^2T(\mathbf{p}, \mathbf{q}) & -k_q\mathbf{I} + \nabla_{\mathbf{q}}\nabla_{\mathbf{p}}T(\mathbf{p}, \mathbf{q}) \end{pmatrix}$$

to be uniformly negative definite. Sufficient conditions for this are now given by

$$\begin{aligned} k_p &> -\frac{1}{2}\lambda_{\min}(\nabla_{\hat{\mathbf{p}}}\nabla_{\hat{\mathbf{q}}}T(\hat{\mathbf{p}}, \hat{\mathbf{q}}) + \nabla_{\hat{\mathbf{q}}}\nabla_{\hat{\mathbf{p}}}T(\hat{\mathbf{p}}, \hat{\mathbf{q}})), \\ k_q &> \frac{1}{2}\lambda_{\max}(\nabla_{\hat{\mathbf{p}}}\nabla_{\hat{\mathbf{q}}}T(\hat{\mathbf{p}}, \hat{\mathbf{q}}) + \nabla_{\hat{\mathbf{q}}}\nabla_{\hat{\mathbf{p}}}T(\hat{\mathbf{p}}, \hat{\mathbf{q}})), \\ \lambda_p\lambda_q &> \frac{1}{4}\lambda_{\max}^2[\nabla_{\hat{\mathbf{p}}}^2T(\hat{\mathbf{p}}, \hat{\mathbf{q}}) - \nabla_{\hat{\mathbf{q}}}^2T(\hat{\mathbf{p}}, \hat{\mathbf{q}}) - \nabla_{\hat{\mathbf{q}}}^2U(\hat{\mathbf{q}})], \end{aligned}$$

similar to the fully general case handled in Sec. 4.2. More general results can be obtained by using a non-Euclidean metric as a replacement for the momentum and position estimation error terms in (124).

### B.1 IMPLICIT REGULARIZATION FOR HIGHER-ORDER LAWS

For simplicity, we only consider the linearly parameterized setting. The nonlinearly parameterized setting can be handled immediately.

**Proposition B.1.** *Consider the natural gradient-like higher-order adaptation law for a linearly parameterized dynamics*

$$\begin{aligned} \dot{\hat{\mathbf{a}}} &= \beta \mathcal{N}(\hat{\mathbf{v}} - \hat{\mathbf{a}}) \\ \dot{\hat{\mathbf{v}}} &= -[\nabla^2\psi(\hat{\mathbf{v}})]^{-1}\mathbf{Y}^T s \end{aligned}$$

where  $\psi(\cdot)$  is a strictly convex function. Assume that  $\hat{\mathbf{a}}(t) \rightarrow \hat{\mathbf{a}}_\infty \in \mathcal{A}$  where  $\mathcal{A}$  is defined in (19). Then

$$\hat{\mathbf{a}}_\infty = \arg \min_{\theta \in \mathcal{A}} d_\psi(\theta \parallel \hat{\mathbf{v}}(0)).$$

In particular, if  $\hat{\mathbf{v}}(0) = \arg \min_{\theta \in \mathbb{R}^p} \psi(\theta)$ , then

$$\hat{\mathbf{a}}_\infty = \arg \min_{\theta \in \mathcal{A}} \psi(\theta).$$

*Proof.* First note that if  $\hat{\mathbf{a}} \rightarrow \hat{\mathbf{a}}_\infty$ , then  $\hat{\mathbf{v}} \rightarrow \hat{\mathbf{a}}_\infty$ . Now let  $\theta$  be any constant vector of parameters. The Bregman divergence has time derivative

$$\frac{d}{dt}d_\psi(\theta \parallel \hat{\mathbf{v}}) = -\left(\frac{d}{dt}\nabla\psi(\hat{\mathbf{a}})\right)^T(\theta - \hat{\mathbf{v}}).$$

Using that  $\frac{d}{dt}\nabla\psi(\hat{\mathbf{a}}) = -\mathbf{Y}^T s$  and integrating both sides of the above shows

$$d_\psi(\theta \parallel \hat{\mathbf{v}}(0)) = d_\psi(\theta \parallel \hat{\mathbf{a}}_\infty) + \int_0^\infty s(\tau)\mathbf{Y}(\mathbf{x}(\tau), \tau)(\hat{\mathbf{v}}(\tau) - \theta) d\tau.$$

Taking  $\theta \in \mathcal{A}$ , the integral becomes independent of  $\theta$ . The proof from here is identical to the first-order case  $\square$

## REFERENCES

Ai-Poh Loh, A. M. Annaswamy, and F. P. Skantze. Adaptation in the presence of a general nonlinear parameterization: an error model approach. *IEEE Transactions on Automatic Control*, 44(9):1634–1652, 1999. ISSN 2334-3303. doi: 10.1109/9.788531.

Alireza Alemi, Christian Machens, Sophie Deneve, and Jean-Jacques Slotine. Learning nonlinear dynamics in efficient, balanced spiking networks using local plasticity rules. *AAAI Conference on Artificial Intelligence*, 2018.

Shun-ichi Amari. Natural gradient works efficiently in learning. *Neural Computation*, 10(2): 251–276, 1998. doi: <https://doi.org/10.1162/089976698300017746>.

B. R. Andrievskii, A. A. Stotskii, and A. L. Fradkov. Velocity-gradient algorithms in control and adaptation problems. *Automation and Remote Control*, 49:1533–1564, 1988.

Anuradha M. Annaswamy, Fredrik P. Skantze, and Ai-Poh Loh. Adaptive control of continuous time systems with convex/concave parametrization. *Automatica*, 34(1):33 – 49, 1998. ISSN 0005-1098. doi: [https://doi.org/10.1016/S0005-1098\(97\)00159-3](https://doi.org/10.1016/S0005-1098(97)00159-3).

A. Astolfi and R. Ortega. Immersion and invariance: a new tool for stabilization and adaptive control of nonlinear systems. *IEEE Transactions on Automatic Control*, 48(4):590–606, 2003.

Navid Azizan and Babak Hassibi. Stochastic gradient/mirror descent: Minimax optimality and implicit regularization. In *International Conference on Learning Representations*, 2019.

Navid Azizan, Sahin Lale, and Babak Hassibi. Stochastic mirror descent on overparameterized nonlinear models: Convergence, implicit regularization, and generalization. *arXiv:1906.03830*, 2019.

Peter L. Bartlett, Philip M. Long, Gábor Lugosi, and Alexander Tsigler. Benign overfitting in linear regression. *arXiv:1906.11300*, 2019.

Amir Beck and Marc Teboulle. Mirror descent and nonlinear projected subgradient methods for convex optimization. *Operations Research Letters*, 31(3):167 – 175, 2003. ISSN 0167-6377. doi: [https://doi.org/10.1016/S0167-6377\(02\)00231-6](https://doi.org/10.1016/S0167-6377(02)00231-6).

Mikhail Belkin, Daniel Hsu, Siyuan Ma, and Soumik Mandal. Reconciling modern machine-learning practice and the classical bias–variance trade-off. *Proceedings of the National Academy of Sciences*, 116(32):15849–15854, 2019. ISSN 0027-8424. doi: 10.1073/pnas.1903070116.

Michael Betancourt, Michael I. Jordan, and Ashia C. Wilson. On symplectic optimization. *arXiv:1802.03653*, 2018.

Nicholas M. Boffi and Jean-Jacques E. Slotine. A continuous-time analysis of distributed stochastic gradient. *Neural Computation*, 32(1):36–96, 2020. doi: [https://doi.org/10.1162/neco\\_a\\_01248](https://doi.org/10.1162/neco_a_01248).

L.M. Bregman. The relaxation method of finding the common point of convex sets and its application to the solution of problems in convex programming. *USSR Computational Mathematics and Mathematical Physics*, 7(3):200 – 217, 1967. ISSN 0041-5553. doi: [https://doi.org/10.1016/0041-5553\(67\)90040-7](https://doi.org/10.1016/0041-5553(67)90040-7).

Kathleen Champion, Bethany Lusch, J. Nathan Kutz, and Steven L. Brunton. Data-driven discovery of coordinates and governing equations. *Proceedings of the National Academy of Sciences*, 116(45):22445–22451, 2019. ISSN 0027-8424. doi: 10.1073/pnas.1906995116. URL <https://www.pnas.org/content/116/45/22445>.

Yubei Chen, Dylan Paiton, and Bruno Olshausen. The sparse manifold transform. In S. Bengio, H. Wallach, H. Larochelle, K. Grauman, N. Cesa-Bianchi, and R. Garnett, editors, *Advances in Neural Information Processing Systems 31*, pages 10513–10524. Curran Associates, Inc., 2018.

Zhengdao Chen, Jianyu Zhang, Martin Arjovsky, and Léon Bottou. Symplectic recurrent neural networks, 2019.

Jelena Diakonikolas and Michael I. Jordan. Generalized momentum-based methods: A hamiltonian perspective. *arXiv:1906.00436*, 2019.

Richard P. Feynman, Robert B. Leighton, and Matthews Sands. *The Feynman Lectures on Physics*, volume II. Addison–Wesley Publishing Company, 1977.

Dylan J. Foster, Alexander Rakhlin, and Tuhin Sarkar. Learning nonlinear dynamical systems from a single trajectory. *arXiv:2004.14681*, 2020.

A. L. Fradkov. Speed-gradient scheme and its application in adaptive control problems. *Automation and Remote Control*, 40:1333–1342, 1980.

A. L. Fradkov. Integrodifferentiating velocity gradient algorithms. *Sov. Phys. Dokl.*, 31: 97–98, 1986.

A. L. Fradkov, I. V. Miroshnik, and V. O. Nikiforov. *Nonlinear and Adaptive Control of Complex Systems*. Springer Netherlands, 1999.

Guilherme França, Jeremias Sulam, Daniel P. Robinson, and René Vidal. Conformal symplectic and relativistic optimization. *arXiv:1903.04100*, 2019.

J. E. Gaudio, A. M. Annaswamy, M. A. Bolender, E. Lavretsky, and T. E. Gibson. A class of high order tuners for adaptive systems. *IEEE Control Systems Letters*, 5(2):391–396, 2021.

Joseph E. Gaudio, Travis E. Gibson, Anuradha M. Annaswamy, and Michael A. Bolender. Provably correct learning algorithms in the presence of time-varying features using a variational perspective. *arXiv:1903.04666*, 2019.

Claudio Gentile. The robustness of the p-norm algorithms. *Machine Learning*, 53(3):265–299, 2003. ISSN 1573-0565. doi: <https://doi.org/10.1023/A:1026319107706>.

Aditya Gilra and Wulfram Gerstner. Predicting non-linear dynamics by stable local learning in a recurrent spiking neural network. *eLife*, 6:e28295, 2017. ISSN 2050-084X.

Surbhi Goel and Adam Klivans. Learning neural networks with two nonlinear layers in polynomial time. *arXiv:1709.06010*, 2017.

Surbhi Goel, Adam Klivans, and Raghu Meka. Learning one convolutional layer with overlapping patches. *arXiv:1802.02547*, 2018.

Suriya Gunasekar, Jason Lee, Daniel Soudry, and Nathan Srebro. Characterizing implicit bias in terms of optimization geometry. *arXiv:1802.08246*, 2018a.

Suriya Gunasekar, Jason D Lee, Daniel Soudry, and Nati Srebro. Implicit bias of gradient descent on linear convolutional networks. In *Advances in Neural Information Processing Systems 31*, pages 9461–9471. Curran Associates, Inc., 2018b.

Elad Hazan. Introduction to online convex optimization. *Foundations and Trends in Optimization*, 2(3-4):157–325, 2016. ISSN 2167-3888. doi: 10.1561/2400000013.

Petros A. Ioannou and Jing Sun. *Robust Adaptive Control*. Dover Publications, 2012.

Sham Kakade, Adam Tauman Kalai, Varun Kanade, and Ohad Shamir. Efficient learning of generalized linear and single index models with isotonic regression. *arXiv:1104.2018*, 2011.

Dimitrios Karagiannis, Mario Sassano, and Alessandro Astolfi. Dynamic scaling and observer design with application to adaptive control. *Automatica*, 45(12):2883 – 2889, 2009. ISSN 0005-1098. doi: <https://doi.org/10.1016/j.automatica.2009.09.013>.

Aleksandar Kojić and Anuradha M. Annaswamy. Adaptive control of nonlinearly parameterized systems with a triangular structure. *Automatica*, 38(1):115 – 123, 2002. ISSN 0005-1098. doi: [https://doi.org/10.1016/S0005-1098\(01\)00173-X](https://doi.org/10.1016/S0005-1098(01)00173-X).

Walid Krichene, Alexandre Bayen, and Peter L Bartlett. Accelerated mirror descent in continuous and discrete time. In *Advances in Neural Information Processing Systems 28*, pages 2845–2853. Curran Associates, Inc., 2015.

T. Lee, J. Kwon, and F. C. Park. A natural adaptive control law for robot manipulators. In *2018 IEEE/RSJ International Conference on Intelligent Robots and Systems (IROS)*, pages 1–9, 2018. doi: 10.1109/IROS.2018.8593727.

T. Lee, P. M. Wensing, and F. C. Park. Geometric robot dynamic identification: A convex programming approach. *IEEE Transactions on Robotics*, pages 1–18, 2019. ISSN 1941-0468. doi: 10.1109/TRO.2019.2926491.

X. Liu, R. Ortega, H. Su, and J. Chu. Immersion and invariance adaptive control of nonlinearly parameterized nonlinear systems . *IEEE Transactions on Automatic Control*, 55(9):2209–2214, 2010.

Yang-Yu Liu, Jean-Jacques Slotine, and Albert-László Barabási. Observability of complex systems. *Proceedings of the National Academy of Sciences*, 110(7):2460–2465, 2013. ISSN 0027-8424. doi: 10.1073/pnas.1215508110. URL <https://www.pnas.org/content/110/7/2460>.

Winfried Lohmiller and Jean-Jacques E. Slotine. On contraction analysis for non-linear systems. *Automatica*, 34(6):683–696, 1998. ISSN 0005-1098. doi: [http://dx.doi.org/10.1016/S0005-1098\(98\)00019-3](http://dx.doi.org/10.1016/S0005-1098(98)00019-3).

Brett T. Lopez and Jean-Jacques E. Slotine. Contraction metrics in adaptive nonlinear control, 2019.

David G. Luenberger. *Introduction to Dynamic Systems*. John Wiley & Sons, 1979.

Chris J. Maddison, Daniel Paulin, Yee Whye Teh, Brendan O’Donoghue, and Arnaud Doucet. Hamiltonian descent methods. *arXiv:1809.05042*, 2018.

A. S. Morse. *High-Order Parameter Tuners for the Adaptive Control of Linear and Nonlinear Systems*, pages 339–364. Birkhäuser Boston, Boston, MA, 1992. ISBN 978-1-4757-2204-8. doi: [https://doi.org/10.1007/978-1-4757-2204-8\\_23](https://doi.org/10.1007/978-1-4757-2204-8_23).

Michael Muehlebach and Michael I. Jordan. A dynamical systems perspective on nesterov acceleration. *arXiv:1905.07436*, 2019.

Michael Muehlebach and Michael I. Jordan. Optimization with momentum: Dynamical, control-theoretic, and symplectic perspectives. *arXiv:2002.12493*, 2020.

V. Muthukumar, K. Vodrahalli, and A. Sahai. Harmless interpolation of noisy data in regression. In *2019 IEEE International Symposium on Information Theory (ISIT)*, pages 2299–2303, 2019. doi: 10.1109/ISIT.2019.8849614.

Kumpati S. Narendra and Anuradha M. Annaswamy. *Stable Adaptive Systems*. Dover Publications, 2005.

A.S. Nemirovski and D.B. Yudin. *Problem Complexity and Method Efficiency in Optimization*. Wiley, 1983. ISBN 9780471103455.

Yurii Nesterov. A Method for Solving a Convex Programming Problem with Convergence Rate  $O(1/k^2)$ . *Soviet Mathematics Doklady*, 26:367–372, 1983.

Romeo Ortega, Vladislav Gromov, Emmanuel Nuño, Anton Pyrkin, and Jose Guadalupe Romero. Parameter estimation of nonlinearly parameterized regressions without overparameterization nor persistent excitation: Application to system identification and adaptive control. *arXiv:1910.08016*, 2019.

B. T. Polyak. Gradient methods for minimizing functionals (in russian). *U.S.S.R. Comput. Math. Math. Phys.*, 3:643–653, 1963.

B. T. Polyak and A. B. Juditsky. Acceleration of stochastic approximation by averaging. *SIAM Journal on Control and Optimization*, 30(4):838–855, 1992. doi: <https://doi.org/10.1137/0330046>.

B.T. Polyak. Some methods of speeding up the convergence of iteration methods. *USSR Computational Mathematics and Mathematical Physics*, 4(5):1 – 17, 1964. ISSN 0041-5553. doi: [https://doi.org/10.1016/0041-5553\(64\)90137-5](https://doi.org/10.1016/0041-5553(64)90137-5).

R. M. Sanner and J. . E. Slotine. Gaussian networks for direct adaptive control. *IEEE Transactions on Neural Networks*, 3(6):837–863, 1992. ISSN 1941-0093. doi: 10.1109/72.165588.

Robert M. Sanner and Jean-Jacques E. Slotine. Stable adaptive control of robot manipulators using “neural” networks. *Neural Computation*, 7(4):753–790, 1995. doi: 10.1162/neco.1995.7.4.753. URL <https://doi.org/10.1162/neco.1995.7.4.753>.

Bin Shi, Simon S. Du, Weijie J. Su, and Michael I. Jordan. Acceleration via symplectic discretization of high-resolution differential equations. *arXiv:1902.03694*, 2019.

J.-J.E. Slotine and J.A. Coetsee. Adaptive sliding controller synthesis for non-linear systems. *International Journal of Control*, 43(6):1631–1651, 1986. doi: <https://doi.org/10.1080/00207178608933564>.

Jean-Jacques Slotine and Weiping Li. *Applied Nonlinear Control*. Prentice Hall, 1991.

Jean-Jacques E. Slotine. Modular stability tools for distributed computation and control. *International Journal of Adaptive Control and Signal Processing*, 17(6):397–416, 2003. doi: 10.1002/acs.754.

Jean-Jacques E. Slotine and Weiping Li. On the adaptive control of robot manipulators. *The International Journal of Robotics Research*, 6(3):49–59, 1987. doi: <https://doi.org/10.1177/027836498700600303>.

Daniel Soudry, Elad Hoffer, Mor Shpigel Nacson, Suriya Gunasekar, and Nathan Srebro. The implicit bias of gradient descent on separable data. *J. Mach. Learn. Res.*, 19(1):2822–2878, 2018. ISSN 1532-4435.

Weijie Su, Stephen Boyd, and Emmanuel J. Candès. A differential equation for modeling nesterov’s accelerated gradient method: Theory and insights. *Journal of Machine Learning Research*, 17(153):1–43, 2016.

D. Sussillo and L. F. Abbott. Generating coherent patterns of activity from chaotic neural networks. *Neuron*, 63(4):544–557, 2009.

Robert Tibshirani. Regression shrinkage and selection via the lasso. *Journal of the Royal Statistical Society: Series B (Methodological)*, 58(1):267–288, 1996. doi: 10.1111/j.2517-6161.1996.tb02080.x.

I. Y. Tyukin, D. V. Prokhorov, and C. van Leeuwen. Adaptation and parameter estimation in systems with unstable target dynamics and nonlinear parametrization. *IEEE Transactions on Automatic Control*, 52(9):1543–1559, 2007. ISSN 2334-3303. doi: 10.1109/TAC.2007.904448.

I. Yu. Tyukin. Adaptation algorithms in finite form for nonlinear dynamic objects. *Automation and Remote Control*, 64(6):951–974, 2003. ISSN 1608-3032. doi: <https://doi.org/10.1023/A:1024141700331>.

Ivan Tyukin. *Adaptation in Dynamical Systems*. Cambridge University Press, 2011.

P. M. Wensing and J. Slotine. Cooperative adaptive control for cloud-based robotics. In *2018 IEEE International Conference on Robotics and Automation (ICRA)*, pages 6401–6408, 2018. doi: 10.1109/ICRA.2018.8460856.

P. M. Wensing, S. Kim, and J. E. Slotine. Linear matrix inequalities for physically consistent inertial parameter identification: A statistical perspective on the mass distribution. *IEEE Robotics and Automation Letters*, 3(1):60–67, 2018. ISSN 2377-3774. doi: 10.1109/LRA.2017.2729659.

Patrick M. Wensing and Jean-Jacques E. Slotine. Beyond convexity – contraction and global convergence of gradient descent. *arXiv:1806.06655*, 2018.

Andre Wibisono, Ashia C. Wilson, and Michael I. Jordan. A variational perspective on accelerated methods in optimization. *Proceedings of the National Academy of Sciences*, 113(47):E7351–E7358, 2016. ISSN 0027-8424. doi: 10.1073/pnas.1614734113.

Ashia C. Wilson, Benjamin Recht, and Michael I. Jordan. A lyapunov analysis of momentum methods in optimization. *arXiv:1611.02635*, 2016.

Chiyuan Zhang, Samy Bengio, Moritz Hardt, Benjamin Recht, and Oriol Vinyals. Understanding deep learning requires rethinking generalization. *arXiv:1611.03530*, 2016.

Sixin Zhang, Anna Choromanska, and Yann LeCun. Deep learning with elastic averaging sgd. *arXiv:1412.6651*, 2014.